CONTENTS

MATHEMATICS

PHYSICS

BOTANY

ZOOLOGY

BUSINESS MATTERS

(Printed at the end of the Volume)

INDEX

(A) indicates the pages of the Business Matter printed at the end of the Volume

PROCEEDINGS

OF THE

NATIONAL ACADEMY OF SCIENCES

INDIA

Part I] February, 1936 [Volume 6

TAYLOR'S SERIES AND BOREL'S POLYGON OF SUMMABILITY

By S. P. Jain

Mathematics Department, Allahabad University

Communicated by Dr. P. L. Srivastava

Received, April 2, 1935

1. According to Borel, the series

$$u_0+u_1+u_2+\ldots \quad . \quad . \quad . \quad . \quad (1\cdot1)$$

is summable (B) if the integral

$$\int_0^\infty e^{-t}\, F(t)\, dt \quad . \quad . \quad . \quad . \quad . \quad . \quad (1\cdot2)$$

exists, where

$$F(t) = u_0 + \frac{u_1 t}{1!} + \frac{u_2 t^2}{2!} + \frac{u_3 t^3}{3!} + \ldots \quad . \quad . \quad . \quad (1\cdot3)$$

He has further defined the absolute summability of (1·1) by the absolute convergence of the integrals (1·2) and

$$\int_0^\infty e^{-t}\, F^\lambda(t)\, dt \quad . \quad . \quad . \quad . \quad . \quad . \quad (1\cdot4)$$

where the index λ, any positive integer, denotes the order of the derivative of $F(t)$.

According to these definitions, the Taylor's series

$$\sum_{0}^{\infty} c_n z^n \quad . \quad . \quad . \quad . \quad . \quad . \quad (1\cdot5)$$

which has a non-zero radius of convergence, is absolutely summable in a certain polygon of summability. In fact, Borel's integral associated with (1·5), namely,

$$\int_{0}^{\infty} e^{-t} F(xt)\, dt . \quad . \quad . \quad . \quad . \quad . \quad (1\cdot6)$$

provides the analytic continuation of $f(x)$ defined by the series (1·5) throughout the interior of the polygon of summability. Thus, according to Borel's definition, the series

$$1+x+x^2+\cdots \quad . \quad . \quad . \quad . \quad . \quad (1\cdot7)$$

is summable, and indeed absolutely, in a half-plane, $R(x) < 1$, since the integral

$$\int_{0}^{\infty} e^{-t}\, e^{xt}\, dt \qquad (t=\rho e^{i\Psi}) \quad . \quad . \quad . \quad (1\cdot8)$$

is absolutely and uniformly convergent in that region only. Hence, $f(x)$ defined by the series (1·7), is an analytic function of x in the region $R(x) < 1$.

In a subsequent section, I show that it is permissible to alter the path of integration of (1·8) to that along any ray making an angle ψ with the positive direction of x-axis. By the principle of analytic continuation, it follows that the function represented by (1·7) or (1·8) is analytic in the region

$$(1-x)\cos\psi + y\sin\psi > 0 \qquad (x=x+iy,\ 0 \leq |\psi| \leq \pi).$$

This covers the entire x-plane except the point $x=1$. This is obviously so, for the geometric series (1·7) represents the function $\frac{1}{1-z}$.

This suggests that the region, in which the function represented by the Taylor's series or the Borel's integral is analytic, can be greater than the polygon of summability. The possibility of obtaining a better region

is due to the fact that while Borel always takes his integral along the positive real axis, we wish to consider it along all directions.

2. Polya[1] has established several properties about the power series, and its associated integral function. For instance, if the series (1·5) has a finite radius of convergence $\frac{1}{k}$, then the associated integral function

$$F(z) = \sum_{0}^{\infty} \frac{c_n z^n}{n!}$$

is of order 1 and type K, and conversely.

Further, if

$$\overline{\lim_{R \to \infty}} \frac{\log | F(z) |}{R} = h(\varphi), \quad (z = Re^{i\varphi}) \quad . \quad . \quad . \quad (2·1)$$

$h(\varphi)$ is a continuous function of the real variable φ. Its first derivative $h'(\varphi)$ has at most discontinuities of the first kind only, and

$$-K \leq h(\varphi) \leq K$$

the value K being attained for at least one value of φ..

On considering the envelope of the lines

$$r \cos(\theta - \varphi) \equiv x \cos\varphi + y \sin\varphi = h(\varphi)$$

for the parameter φ, a curve is obtained, which is called the Indicator Diagram of the function $F(z)$.

This curve, from the properties of $h(\varphi)$, is a closed one, and is always concave to the origin.[2] It can have straight pieces, which correspond to the discontinuities of $h'(\varphi)$.

3. Now I wish to establish the following: –

If the Taylor's series (1·5) has a non-zero radius of convergence $\frac{1}{K}$ *then the function represented by it is analytic inside a curve C, which is the simple* inverse of the indicator diagram of the Borel's function F(z) corresponding to the series (1·5).*

$$F(z) = \sum_{0}^{\infty} \frac{c_n z^n}{n!} \quad . \quad . \quad (z = Re^{i\varphi})$$

is at least of order e^{KR}.

*By the attribute 'simple' is meant that the inverse is taken with respect to a unit circle, having its centre at the origin.

By easy steps

$$f(z)=\sum_{0}^{\infty} c_n z^n = \int_{0}^{\infty} e^{-t} F(zt)\, dt$$

$$= \frac{1}{z}\int_{0}^{\infty} e^{-u/z} F(u)du \quad . \quad . \quad . \quad . \quad (3\cdot1)$$

Now I wish to show that it is permissible to take the last integral along any ray issuing from the origin. The last integral taken along the ray making an angle ψ with the x-axis represents an analytic function of z at least in the region

$$\cos(\psi-\varphi) > KR \qquad (u=\rho e^{i\psi}) \quad . \quad . \quad . \quad (3\cdot2)$$

Choosing z to lie in the common region to (3·2) for the two values $\psi=\psi'$ and $\psi=\psi''$ taken suitably near

$$\int_{\psi'}^{\psi''} F(u) e^{-\frac{u}{z}}\, du$$

tends to zero with $\frac{1}{\rho}$.

By the principle of analytic continuation

$$\int_{0}^{\infty(\psi)} e^{-u/z} F(u)du \qquad (-\pi \leq \psi \leq \pi). \quad . \quad . \quad (3\cdot3)$$

continues the integral in (3·1) analytically.

Taking the more precise expression for the order of $F(u)$ as indicated in (2·1), we see that (3·6) represents an analytic function of z in the region

$$\cos(\psi-\varphi) \geq R[h(\psi)+\varepsilon]$$

$\varepsilon>0$, and is arbitrarily small.

This means that the series or the integral in (3·1) represents an analytic function of z inside the envelope of the lines

$$\cos(\psi-\varphi)=Rh(\psi) \qquad (-\pi\leq\psi\leq\pi). \quad . \quad . \quad (3\cdot4)$$

In order to interpret the region geometrically let us put

$$s=\frac{1}{z} \qquad (s=re^{i\theta})$$

Then the region in which $f_1(s)$ is an analytic function of s lies exterior to the envelope of the lines in the s-plane

$$r\cos(\theta+\psi)=h(\psi) \qquad (-\pi\leq\psi\leq\pi) \quad . \quad . \quad . \quad (3\cdot5)$$

This envelope is obviously the indicator diagram of $F(s)$ in the s-plane, but described in the negative sense. This curve, when transformed to the z-plane, is only the simple inverse of the indicator diagram of $f(z)$ in that plane. This proves the theorem.

It is worth while to note that Polya[3] has proved that $f_1(s)$ has at least one singularity on every tangent to the envelope of (3·5).

4. Now it remains to be shown that the region C that we have obtained in § 3 is, in general, greater than the region given by the ploygon of summability Σ, whose polar equation[4] is $R=\frac{1}{h(\varphi)}$. This is the simple inverse of the first positive pedal, *i.e.*, the simple polar reciprocal, of the indicator diagram of $f(z)$. In general, the simple inverse of any curve is the first positive pedal of the simple polar reciprocal of the curve. This can be readily seen by taking the equation of the indicator diagram in the pedal form $p=f(r)$. The equation of its simple polar reciprocal is $\frac{1}{r}=f\left(\frac{1}{p}\right)$, and that of its simple inverse is $p=r^2 f\left(\frac{1}{r}\right)$. The last equation also represents the first positive pedal of $\frac{1}{r}=f\left(\frac{1}{p}\right)$.

Now, the singularities of the function lie on the first positive pedal of the polygon of summability and this is exactly the curve inside which we prove $f(z)$ to be analytic. This establishes the result.

It will be interesting to compare the two regions obtained from C and Σ in two particular cases. It is easy to construct any number of such illustrations:

(*i*) $h(\varphi)=|\cos\varphi|$

Σ covers the area between the lines $R(z)=\pm1$ when C includes the whole plane when cuts have been made in it along the lines $(+1\ldots\infty)$ and $(-1\ldots-\infty)$.

(*ii*) $h(\varphi)=\sqrt{a^2\cos^2\varphi+b^2\sin^2\varphi}$

Σ is the ellipse $a^2x^2+b^2y^2=1$, while C is the curve $(x^2+y^2)^2=\frac{x^2}{a^2}+\frac{y^2}{b^2}$.

The curve C touches Σ at $x=\pm\frac{1}{a}$ and at $y=\pm\frac{1}{b}$ externally. This curve is the first positive pedal of Σ and is the line of singularities for $f(z)$.

5. From what has been said, it is apparent that the region in which the series (1·5) may be said to be absolutely summable (B) can be extended if we agree to define it by the existence of the integral

$$\int_0^{\infty(\psi)} | e^{-t} F(xt)\, dt | \qquad (0 \leq \psi \leq 2\pi)$$

I wish to thank Dr P. L. Srivastava for his interest in the paper.

References

1. G Polya, *Math. Zeit.*, 29, pp. 571–580
2. Titschmarsh, *Theory of Functions.*
3. *loc. cit.*, p. 585.
4. E Borel, *Lecons Sur les Series Divergentes*, (1901), p 141.

"ON THE CONVERGENCE AND THE SUMMABILITY OF THE CONJUGATE SERIES OF THE DERIVED FOURIER SERIES"

By K. L. Gupta

Mathematics Department, Allahabad University

Communicated by Dr. B. N. Prasad

Received November 8, 1935

1. Let $f(x)$ be a periodic function with period 2π and integrable in the sense of Lebesgue. Let the Fourier series associated with $f(x)$ be

$$\tfrac{1}{2}a_0 + \sum_{n=1}^{\infty} (a_n \cos nx + b_n \sin nx) \quad . \quad . \quad . \quad . \quad (1\cdot1)$$

Then the series

$$\sum_{n=1}^{\infty} n\,(a_n \cos nx + b_n \sin nx) \quad . \quad . \quad . \quad . \quad (1\cdot2)$$

is called the conjugate series of the derived Fourier series. The object of the present paper is to discuss the convergence and the summability of the series (1·2).

In §2, I establish a convergence test. In §§ 3, 4, I discuss the summability of the series and give some general criteria which include as particular cases the corresponding criteria given by Miss Sayer* and Mr. Takahashi.† These criteria include the existence of the integral,

$$g(x) = \lim_{\eta=0} \frac{-1}{\pi} \int_{\eta}^{\infty} \frac{\phi(t)}{t^2}\, dt, \quad . \quad . \quad . \quad . \quad (1\cdot3)$$

where

$$\phi(t) = f(x+t) + f(x-t) - 2f(x),$$

and some further restrictions on the nature of $\phi(t)$. In § 5, I discuss the problem as to what would be the nature of summability of the series (1·2) if we suppose only the existence of the integral (1·3) and no further restrictions on $\phi(t)$. For this, I show that the series (1·2) will be summable (c, δ) for every $\delta > 2$, when the integral (1·3) exists.

I take this opportunity of expressing my best thanks to Dr. B. N. Prasad for valuable guidance and keen interest in the preparation of the paper.

*Sayer, 4.

†Takahashi, 5.

2. **Theorem 1.**

The series (1·2) *converges to the sum*

$$\frac{-1}{\pi}\int_0^{\pi}\frac{f(x+t)+f(x-t)-2f(x)}{4\sin^2 t/2}\,dt$$

at every point x *at which this integral exists provided that,*

(i) $\frac{\phi t}{t}$ *is continuous and of bounded variation in* $(0, \pi)$,

and (ii) $\phi(t) = 0$ (t) *for small* t.

Let s_n denote the partial sum of the first n terms of the series (1·2), then we have,

$$s_n = \sum_{m=1}^{m=n} m\,(a_m \cos mx + b_m \sin mx),$$

$$= \frac{1}{\pi}\sum_{m=1}^{m=n}\int_0^{\pi}\{f(x+t)+f(x-t)\}m\cos mt\,dt,$$

$$= \frac{1}{\pi}\sum_{m=1}^{m=n}\int_0^{\pi}\{f(x+t)+f(x-t)-2f(x)\}\,m\cos mt\,dt,$$

since $\int_0^{\pi} m\cos mt\,dt = 0.$

Therefore,

$$s_n = \frac{1}{\pi}\int_0^{\pi}\phi(t)\,(\cos t + 2\cos 2t + \ldots\ldots + n\cos nt)\,dt$$

$$= \frac{1}{2\pi}\int_0^{\pi}\frac{\phi(t)}{1-\cos t}\left(-1+2n\sin\frac{2n+1}{2}t\sin t/2+\cos nt\right)dt$$

$$= \frac{-1}{4\pi}\int_0^{\pi}\phi(t)\operatorname{cosec}^2 t/2\,dt + \frac{1}{2\pi}\int_0^{\pi}\phi(t)\,n\cos nt\,dt$$

$$+\frac{1}{2\pi}\int_0^{\pi}\phi(t)\,n\sin nt\cot t/2\,dt + \frac{1}{4\pi}\int_0^{\pi}\phi(t)\cos nt\operatorname{cosec}^2 t/2\,dt$$

$$= -\frac{1}{4\pi}\int_0^{\pi}\phi(t)\operatorname{cosec}^2 t/2\,dt + I_2 + I_3 + I_4 \quad \ldots\ldots \quad (2\cdot1)$$

Now, integrating by parts we have,

$$I_2 = \frac{1}{2\pi}\left[\phi(t)\sin nt\right]_0^{\pi} - \frac{1}{2\pi}\int_0^{\pi}\phi'(t)\sin nt\,dt,$$

$$=0(1)-\frac{1}{2\pi}\int_0^{\pi}\phi'(t)\sin nt\,dt. \quad . \quad . \quad . \quad . \quad . \quad . \quad (2{\cdot}2)$$

Since $\phi(t)$ is continuous and of bounded variation, $\phi'(t)$ is integrable. We have, therefore, by Riemann-Lebesgue theorem,

$$\lim_{n=\infty}\int_0^{\pi}\phi'(t)\sin nt\,dt=0$$

Hence $$I_2=0(1) \quad . \quad . \quad . \quad . \quad . \quad (2{\cdot}3)$$

Again integrating by parts, we have,

$$I_3 = -\frac{1}{2\pi}\left[\phi(t)\cot t/2\cos nt\right]_0^{\pi} + \frac{1}{2\pi}\int_0^{\pi}\frac{d}{dt}\left\{\phi(t)\cot t/2\right\}\cos nt\,dt,$$

$$=0(1)+\frac{1}{2\pi}\int_0^{\pi}\frac{d}{dt}\left\{\phi(t)\cot t/2\right\}\cos nt\,dt,$$

since $\frac{\phi(t)}{t}\to 0$ with t.

Now

$$\frac{1}{2\pi}\int_0^{\pi}\{\phi(t)\cot t/2\}\cos nt\,dt$$

$$=\frac{1}{2\pi}\int_0^{\pi}\phi'(t)\cot t/2\cos nt\,dt-\frac{1}{4\pi}\int_0^{\pi}\phi(t)\operatorname{cosec}^2 t/2\cos nt\,dt$$

$$=\frac{1}{2\pi}\int_0^{\pi}\phi'(t)\cot t/2\cos nt\,dt-I_4 \quad . \quad . \quad . \quad . \quad . \quad . \quad (2.4)$$

Since $\left(\cot t/2-\frac{2}{t}\right)$ is bounded and measurable, we have by Riemann-Lebesgue theorem,

$$\lim_{n=\infty}\frac{1}{2\pi}\int_0^{\pi}\phi'(t)\left(\cot t/2-\frac{2}{t}\right)\cos nt\,dt=0$$

Hence

$$\lim_{n=\infty} \frac{1}{2\pi} \int_0^{\pi} \phi'(t) \cot t/2 \cos nt \, dt$$

$$= \lim_{n=\infty} \frac{1}{\pi} \int_0^{\pi} \phi'(t) \frac{\cos nt}{t} \, dt.$$

Since $\frac{\phi(t)}{t} = \frac{1}{t} \int_0^t \phi'(u) \, du$ is a function of bounded variation and approaches zero with t, applying de la Vallée Poussin's criterion, we have,

$$\lim_{n=\infty} \int_0^{\pi} \phi'(t) \frac{\cos nt}{t} \, dt = 0. \qquad (2{\cdot}5)$$

Combining (2·4) and (2·5), we have,

$$I_3 + I_4 = 0(1). \qquad (2{\cdot}6)$$

From (2·1), (2·2), and (2·6) we have,

$$\lim_{n=\infty} s_n = -\frac{1}{4\pi} \int_0^{\pi} \phi(t) \operatorname{cosec}^2 t/2 \, dt.$$

This proves the theorem.

Theorem 2.

The series (1·2) *is summable* (C, k) *for every* $k > 1$, *to the sum* $g(x)$ *at every point* x *at which the integral* (1·3) *exists as a Cauchy integral, provided that* $\phi(t) = O(t)$.

Miss Sayer has proved* the above theorem with the condition that $\phi(t) = 0(t)$, which is obviously more restrictive than our condition.

Let $C_p(t)$ denote Young's† function,

$$C_p(t) = \frac{t^p}{\Gamma(1+p)} \left(1 - \frac{t^2}{(p+1)(p+2)} + \frac{t^4}{(p+1)(p+2)(p+3)(p+4)} - \ldots\right) p \geq 0.$$

* Sayer : *Ibid.*

† Young, 6.

We shall require the undermentioned properties of this function and the following lemmas:—

$$C_q(u)=\frac{u^q}{\Gamma(q)}\int_0^1(1-t)^{q-1}\cos ut\,dt \quad (q>0) \quad . \quad . \quad (3\cdot01)$$

$$\frac{d}{du}C_p(u)=C_{p-1}(u) \quad (p\geq 1) \quad . \quad . \quad . \quad . \quad (3\cdot02)$$

$$C_{p+2}(u)=\frac{u^p}{\Gamma(1+p)}-C_p(u) \quad . \quad . \quad . \quad . \quad (3\cdot03)$$

For large values of u,

$$C_p(u)=O(1) \quad (p\leq 2) \quad . \quad . \quad . \quad . \quad (3\cdot04)$$

$$C_p(u)=O(u^{p-2}) \quad (p\geq 2) \quad . \quad . \quad . \quad (3\cdot05)$$

Lemma (*a*).* If $p>1$, the function $u^{-p}C_p(u)$ is of bounded variation in $(0, \infty)$ and tends to zero as t tends to ∞.

Lemma (*b*).† If $p>0$, the function $u^{-p}C_p(u)$ is of bounded variation in every finite interval.

For convenience we shall consider the equivalent Rieszian mean.

Let $T_k(\omega)$ denote the Rieszian mean of order k of the series (1·2). Then,

$$T_k(\omega)\ddagger=\frac{\omega}{\pi(1+k)}\int_0^\infty\phi(t)\frac{d}{dt}\left\{(\omega t)\,\gamma_{k+2}(\omega t)\right\}dt,$$

where $\gamma_{1+k}(u)=\int_0^1(1-t)^k\cos ut\,dt.$

Hence in virtue of (3·01), we have

$$T_k(\omega)=\frac{\omega\,\Gamma(1+k)}{\pi}\int_0^\infty\phi(t)\frac{d}{dt}\left\{(\omega t)^{-(1+k)}C_{2+k}(\omega t)\right\}dt$$

$$=-\frac{1}{\pi}\int_0^\infty\frac{\phi(t)}{t^2}\,dt-\frac{\omega\,\Gamma(1+k)}{\pi}\int_0^\infty\phi\left(\frac{t}{\omega}\right)\frac{d}{dt}\left\{t^{-(1+k)}C_k(t)\right\}dt$$

by (3·03)

* Young: *loc. cit.*, **163.**

† B. N. Prasad, **1.**

‡ Sayer: *loc. cit.*, p. 33

Since we are concerned here with $k > 1$, putting $k = 1+\eta$ where $\eta > 0$, we have

$$T_k(\omega) = -\frac{1}{\pi}\int_0^\infty \frac{\phi(t)}{t^2}\,dt - \frac{\omega\,\Gamma(2+\eta)}{\pi}\int_0^\infty \frac{\phi\left(\frac{t}{\omega}\right)}{t^2}\,t^{-\eta}\,C_\eta(t)\,dt$$

$$+\frac{\omega\Gamma(3+\eta)}{\pi}\int_0^\infty \frac{\phi\left(\frac{t}{\omega}\right)}{t^2}\,t^{-(1+\eta)}\,C_{1+\eta}(t)\,dt$$

$$= -\frac{1}{\pi}\int_0^\infty \frac{\phi(t)}{t^2}\,dt - J_1 + J_2 \quad . \quad . \quad . \quad . \quad (3\cdot2)$$

It has been shown by Dr. B. N. Prasad* that under the conditions of our theorem, the integrals J_1 and J_2 tend to zero as $\omega \to \infty$.

Thus, we have,

$$T_k(\omega) = \frac{-1}{\pi}\int_0^\infty \frac{\phi(t)}{t^2}\,dt + O(1).$$

This proves our theorem, which evidently includes Sayer's theorem as a special case.

Theorem 3.

The series (1·2) *is summable* (C, k) *for every* $k > 1$ *to the sum* $g(x)$ *at every point at which the integral* (1·3) *exists, provided that*

$$\text{(i)} \quad \frac{1}{t}\int_0^t \frac{\phi(u)}{u}\,du = o(1)$$

and $$\text{(ii)} \quad \frac{1}{t}\int_0^t \left|\frac{\phi(u)}{u}\right|\,du = O(1).$$

The k^{th} partial Rieszian δ mean of the series (1·2) is given by

$$T_k(\omega) = \frac{-1}{\pi}\int_0^\infty \frac{\phi(t)}{t^2}\,dt - \frac{\omega\Gamma(2+\eta)}{\pi}\int_0^\infty \frac{\phi(t/\omega)}{t^2}\,t^{-\eta}C_\eta(t)\,dt$$

$$+\frac{\omega\Gamma(3+\eta)}{\pi}\int_0^\infty \frac{\phi(t/\omega)}{t^2}\,t^{-(1+\eta)}\,C_{1+\eta}(t)\,dt$$

* B. N. Prasad: 2, p. 184 *et. seq.*

from (3·2), $(k>1)$.

Since $$\lim_{\omega=\infty} \omega\int_0^{\infty} \frac{\phi(t/\omega)}{t^2}\, t^{-(1+\eta)} C_{1+\eta}(t)=0,^*$$

it will be sufficient to show that

$$\lim_{\omega=\infty} \omega\int_0^{\infty} \frac{\phi(t/\omega)}{t^2}\, t^{-\eta} C_\eta(t)\, dt=0. \quad . \quad . \quad . \quad (3\cdot3)$$

Dividing the interval $(0, \infty)$ into three sub-intervals $(0, 1)$, $(1, \omega)$, (ω, ∞), let us consider this integral in each of them separately.

Clearly

$$\lim_{\omega=\infty} \omega\int_0^{1} \frac{\phi(t/\omega)}{t^2}\, t^{-\eta} C_\eta(t)\, dt = 0 \quad . \quad . \quad . \quad (3\cdot4)$$

in virtue of lemma (b).

Now $$\int_{\omega}^{\infty} \frac{\omega\,\phi(t/\omega)}{t^2}\, t^{-\eta} C_\eta(t)\, dt$$

$$= \int_1^{\infty} \frac{\phi(t)}{t^2}\, (\omega t)^{-\eta} C_\eta(\omega t)\, dt$$

$$= 0(1)\omega^{-\eta} \int_1^{\infty} \frac{|\phi(t)|}{t^{2+\eta}}\, dt$$

$$= 0(1)\dagger \quad . \quad . \quad . \quad . \quad . \quad . \quad (3\cdot5)$$

Now $$\int_1^{\omega} \frac{\omega\phi(t/\omega)}{t^2}\, t^{-\eta} C_\eta(t)\, dt$$

$$= \left(\int_{1/\omega}^{\lambda/\omega} + \int_{\lambda/\omega}^{1}\right) \frac{\phi(t)}{t^2}\, (\omega t)^{-\eta} C_\eta(\omega t)\, dt.$$

$$= I' + I''.$$

* B. N. Prasad, 2, p. 184.

† See Hobson, 3, p. 569.

To consider I′, let us suppose that,

$$\phi_1(t)=\frac{1}{t}\int_0^t \frac{\phi(t)}{t}dt=0(1)$$

Integrating by parts, we have

$$I'=\left[\omega^{-\eta}\frac{t\phi_1(t)}{t^{1+\eta}}\right]_{1/\omega}^{\lambda/\omega}-\int_{1/\omega}^{\lambda/\omega} t\phi_1(t)\frac{d}{dt}\left\{\frac{1}{t}(\omega t)^{-\eta}C_\eta(\omega t)\right\}dt$$

$$=0(1)+\int_{1/\omega}^{\lambda/\omega}\frac{\phi_1(t)}{t}(\omega t)^{-\eta}C_\eta(\omega t)\,dt$$

$$-\int_{1/\omega}^{\lambda/\omega}\phi_1(t)\frac{d}{dt}\left\{(\omega t)^{-\eta}C_\eta(\omega t)\right\}dt$$

$$=0(1)+0(1)\left[\frac{1}{t^\eta}\right]_{1/\omega}^{\lambda/\omega}\omega^{-\eta}-0(1)\int_{1/\omega}^{\lambda/\omega}\left|\frac{d}{dt}\left\{(\omega t)^{-\eta}C_\eta(\omega t)\right\}\right|dt$$

$$=0(1)-0(1)\int_{1/\omega}^{\lambda/\omega}\left|\frac{d}{dt}\left\{(\omega t)^{-\eta}C_\eta(\omega t)\right\}\right|dt.$$

Since by lemma (*b*), $(\omega t)^{-\eta}C_\eta(\omega t)$ is of bounded variation in every finite interval, the last integral denotes its total variation in the interval $(1/\omega, \lambda/\omega)$.

Hence

$$I'=o(1). \qquad (3\cdot6)$$

Next we shall estimate I″. Let us suppose that

$$\phi_1^*(t)=\frac{1}{t}\int_0^t\left|\frac{\phi(u)}{u}\right|du=O(1).$$

$$|I''|\leq O(1)\int_{\lambda/\omega}^{1}\left|\frac{\phi(t)}{t}\right|\frac{\omega^{-\eta}}{t^{1+\eta}}dt,$$

$$\leq O(1)\left[\omega^{-\eta}\frac{t\phi_1^*(t)}{t^{1+\eta}}\right]_{\lambda/\omega}^{1}+O(1)\,\omega^{-\eta}\int_{\lambda/\omega}^{1}\frac{\phi_1^*(t)}{t^{1+\eta}}dt,$$

$$\leq O(1)\frac{\phi_1^*(1)}{\omega^\eta}+\frac{O(1)}{\omega^\eta}\frac{\omega^\eta}{\lambda^\eta}, \quad . \quad . \quad . \quad . \quad . \quad (3\cdot7)$$

on neglecting negative terms; and this tends to zero when $\lambda \to \infty$ after $w \to \infty$.

Combining (3·4), (3·5), (3·6), and (3·7), we have the required result.

4. **Theorem 4.**

The series (1·2) *is summable* (C, k) *for every* $k>0$, *to the sum* $g(x)$ *at every point at which the integral* (1·3) *exists as a Cauchy integral, provided that,* $\frac{\phi(t)}{t}$ *is of bounded variation in* $(0, 2\pi)$.

The partial Rieszian mean of order k ($k>0$) of the series (1·2) is given by,

$$T_k\,\omega = \frac{-1}{\pi}\int_0^{\infty} \frac{\phi(t)}{t^2}\,dt - \frac{\omega\Gamma(1+k)}{\pi}\int_0^{\infty} \phi\left(\frac{t}{\omega}\right)\frac{d}{dt}\left\{t^{-(1+k)}C_k(t)\right\}dt.$$

To establish the theorem it is sufficient to show that

$$\lim_{\omega=\infty}\ \omega\int_0^{\infty} \phi\left(\frac{t}{\omega}\right)\frac{d}{dt}\left\{t^{-(1+k)}C_k(t)\right\}dt = 0$$

or that

$$\lim_{\omega=\infty}\ \omega\int_0^{\infty} \phi(t)\frac{d}{dt}\left\{(\omega t)^{-(1+k)}C_k(\omega t)\right\}dt = 0.$$

Now

$$\omega\int_0^{\infty} \phi(t)\frac{d}{dt}\left\{(\omega t)^{-(1+k)}C_k(\omega t)\right\}dt$$

$$= \omega\int_0^{2\pi} \frac{\phi(t)}{t}\,t\,\frac{d}{dt}\left\{(\omega t)^{-(1+k)}C_k(\omega t)\right\}dt.$$

$$+ \sum_{s=1}^{s=\infty}\omega\int_{2s\pi}^{2(s+1)\pi} \phi(t)\ \frac{d}{dt}\left\{(\omega t)^{-(1+k)}C_k(\omega t)\right\}dt.$$

Since $\frac{\phi t}{t}$ is of bounded variation in $(0, 2\pi)$, we can express it as $P(t)$—$Q(t)$, where $P(t)$ and $Q(t)$ are positive non-diminishing, monotonic functions. Further because $\frac{\phi(t)}{t}$ is of bounded variation, $\phi(t)$ is also of bounded variation in $(0, 2\pi)$; and since $\phi(t)$ is a periodic function it is of

bounded variation in every interval $\{2s\pi, 2(s+1)\pi\}$. Now $\phi(t)$ can be expressed as $P^1(t)-Q^1(t)$, where $P^1(t)$ and $Q^1(t)$ are also periodic, monotonic and non-diminishing. Applying the second theorem of the mean, it is easily seen that

$$\lim_{\omega\to\infty} \omega \int_0^{2\pi} \frac{\phi(t)}{t}\, t\, \frac{d}{dt}\left\{(\omega t)^{-(1+k)} C_k(\omega t)\right\} dt = 0$$

and

$$\lim_{\omega\to\infty} \sum_{s=1}^{s=\infty} \omega \int_{2s\pi}^{2(s+1)\pi} \phi(t)\, \frac{d}{dt}\left\{(\omega t)^{-(1+k)} C_k(\omega t)\right\} dt = 0$$

Therefore

$$\lim_{\omega=\infty} \omega \int_0^{\infty} \phi(t)\, \frac{d}{dt}\left\{(\omega t)^{-(1+k)} C_k(\omega t)\right\} dt = 0$$

Hence our theorem is proved.

Mr. Takahashi* has also used a similar proof in his paper, but he has unnecessarily supposed the condition that $\frac{\phi(t)}{t} = 0(1)$ for small t.

5. **Theorem 5.**

At every point at which the integral (1·3) *exists as a Cauchy integral, the series* (1·2) *is summable* (C, k) *for every* $k>2$, *and has for its sum the value of the integral.*

If $T_k^{(\omega)}$ denotes the k^{th} Rieszian mean of the series, then we have,

$$T_k^{(\omega)} = \frac{-1}{\pi}\int_0^{\infty} \frac{\phi(t)}{t^2}\, dt - \frac{\omega\Gamma(1+k)}{\pi} \int_0^{\infty} \phi(t/\omega)\, \frac{d}{dt}\left\{ t^{-(1+k)} C_k(t)\right\} dt . \quad . \quad (5{\cdot}1)$$

Since we are concerned with values of $k>2$, putting $k=2+\eta$, we get,

$$T_{2+\eta}^{(\omega)} = \frac{-1}{\pi} \int_0^{\infty} \frac{\phi(t)}{t^2}\, dt - \frac{\omega\Gamma(3+\eta)}{\pi} \int_0^{\infty} \frac{\phi(t/\omega)}{t^2}\, t^{-(1+\eta)} C_{1+\eta}(t)\, dt$$

$$+ \frac{\omega\Gamma(4+\eta)}{\pi} \int_0^{\infty} \frac{\phi(t/\omega)}{t^2}\, t^{-(2+\eta)} C_{2+\eta}(t)\, dt. \quad . \quad . \quad . \quad (5{\cdot}2)$$

*Takahashi: *Ibid.*

To prove the theorem, it will be sufficient to show that

$$\lim_{\omega=\infty} \omega \int_0^\infty \frac{\phi(t/\omega)}{t^2}\, t^{-(1+\eta)} C_{1+\eta}(t)\, dt = 0 \quad . \quad . \quad . \quad (5\cdot3)$$

and

$$\lim_{\omega=\infty} \omega \int_0^\infty \frac{\phi(t/\omega)}{t^2}\, t^{-(2+\eta)}\, C_{2+\eta}\,(t)\, dt = 0 \,. \quad . \quad . \quad (5\cdot4)$$

It has already been remarked that Dr. B. N. Prasad has proved that

$$\lim_{\omega=\infty} \omega \int_0^\infty \frac{\phi(t/\omega)}{t^2}\, t^{-(1+\eta)}\, C_{1+\eta}\,(t)\, dt = 0,$$

and (5·4) is satisfied *a fortriori*, since it is obtained from (5·3) by putting $1+\eta$ for η. Thus the theorem is established.

References

1. B. N. Prasad—"A theorem on the Cesàro Summability of the Allied Series of a Fourier Series," *Journal London Math. Soc.*, 5 (1931), 274—278.
2. ——·——·—— ——"Contribution a l'étude de la Série conjuguée d'une série de Fourier," *Journal de Math.*, 11 (1932), 153—205.
3. E. W. Hobson—"Theory of functions of a real Variable", Vol. 2, 2nd ed. (1926).
4. K. I. Sayer——"Cesàro's Summation of the Differentiated Series of Fourier-Lebesgue Series and their Allied Series," *Proc. London Math. Soc.*, (2), 31 (1930), 29—40.
5. T. Takashashi ——"Note on the Cesàro Summability of the Conjugate Series of the Derived Fourier Series," *Japanese Journal of Math.*, 10 (1931), 127—132.
6. W. H. Young——"On infinite integrals involving a generalisation of the sine and cosine functions," *Quarterly Journal of Math.*, 43 (1912), 161—177.

THE ABSORPTION SPECTRUM OF HYDROGEN CHLORIDE MOLECULE AND ITS UPPER UNSTABLE STATE

By Hrishikesha Trivedi

Physics Department, Allahabad University

Communicated by Prof. M. N. Saha

Received September 14, 1935

A photographic method was used to investigate the continuous absorption spectrum of hydrogen chloride at different temperatures. The contributions of individual vibrational levels to the total absorption were found out. With the help of the theory worked out elsewhere and assuming the Kratzer function to be approximately correct for the potential energy of the lower state, the form of the upper potential energy curve was calculated. It was found that the position representing the dissociation of the molecule in its unstable state lay 103·9 Kcals above the minimum of the lower state in the Frank-Condon diagram for HCl, the same as the atomic heat of formation of the molecule determined thermochemically (101 Kcals).

Although a large amount of experimental work has been done in this laboratory and elsewhere on the continuous absorption spectra of diatomic gases, very little of it has been quantitative. Most of our knowledge derived from such experimental results is qualitative. Absorption coefficients were measured quantitatively in the region of continuous absorption in the cases of oxygen,[1] chlorine,[2] etc., and a partial theory of continuous absorption had been worked out by Stueckelberg[3], Gibson, Rice and Bayliss.[4] Probably it was the lack of such a theory for other molecules that no quantitative measurements were done for them. Some times back, an attempt was made to work out a theory of continuous absorption by diatomic molecules[5] by the present author and the experiment, which is going to be described in the following pages, is an attempt to utilize that theory in finding out the constants of the molecule for the upper state of the molecule which indicates repulsion between the constituents and to test if the results of the theory agreed with experiment.

The continuous absorption spectrum of hydrogen-halides was studied first by Franck and his co-workers[6] who said that they were compounds having an atomic binding. It was also studied by Rollefson and Booher[7] and by Datta[8] only for HBr and HI.

This paper describes an experimental investigation of the continuous absorption of hydrogen chloride and gives a calculation of the constants involved in the potential energy function of the HCl molecule in its unstable state.

Experimental procedure

The gas was contained in a quartz tube, the two ends of which were closed by transparent quartz plates fixed by means of sealing wax. The gas was introduced into the vessel by means of a side tube. It was produced by heating under vacuum a sample of Merck's strong HCl acid and passing the vapour through a series of chambers containing anhydrous calcium chloride and phosphorus pentaoxide. The calcium chloride and phosphorus pentaoxide absorbed all the moisture present in that gas. The quartz tube could be evacuated through another side tube by means of a high vacuum pump. A manometer recorded the pressure of the gas in the quartz tube. The quartz tube could be heated by passing an electric current through a nichrome wire wound about it. A thick padding of asbestos minimised the radiation losses considerably. With a known amount of current passing in the heating coil and the inside of the tube having reached a steady state, the temperature distribution inside the tube along its length was found out by means of an iron-constantan thermocouple, calibrated for the temperatures of melting ice, boiling water, and boiling sulphur. Such a temperature distribution was determined for different currents passing in the heating coil. As the iron-constantan couple reads accurately only up to 550°C, it was used up to that temperature. It was found that the graph representing the current flowing in the heating coil and the temperature developed in the furnace at any particular point was a straight line up to 550°C. It was assumed that the same linear relation held even beyond it. Temperatures above 550°C were obtained from the current flowing in the heating coil by extrapolating from the above-mentioned relation between the heating current and the temperature developed in the furnace. Different proportions of the gas contained in the quartz tube at different temperatures were thus known.

A photographic method[9] was used to determine the absorption coefficients. The source of continuous ultra-violet radiation was a hydrogen discharge tube run by 2 K. W. transformer. Before each series of exposures it was run for about three hours in order that it might reach a steady state and during each run the intensity was kept as constant as

possible by maintaining the primary current through the transformer at a constant value. A series of diaphragms in front of the discharge tube cut out stray light which might have been reflected from the walls of the absorption cell.

Wire screens were used to diminish light intensity by known amounts. They were made of either copper or brass wires and a pair was constructed from a net of a particular mesh. Several such pairs were prepared. The screens were blackened by heating them uniformly in a flame which oxidised the brass or copper. When the screens were still hot they were placed between two hot discs of brass, fitted into the cold ring of the mounting frame and the collar was clamped down into place on their edges. When the guaze cooled the resulting contraction gave a very tight flat surface. They were mounted in a brass ring having an internal diameter of 10 cms, which was connected to a devise by which an oscillatory motion was imparted to the screen by the use of eccentrics. The oscillatory motion was given at about 120 revolutions per minute.

The screens were calibrated by means of an optical bench and a Weston copper-copperoxide photo-electric cell and a galvanometer. The source of light used in this calibration was an incandescent lamp lighted at a fixed voltage. By the help of the inverse square law, the percentage of light passing through a particular screen was found.

Exposures were timed by means of a shutter placed immediately in front of the slit of the spectrograph. The shutter was so worked that an exposure of any period could be repeated with an error not exceeding 0·2 second.

The light was analysed by a E_3 quartz spectrograph. Ilford special rapid plates were used. They were developed in a metal-hydroquinone developer, even development being obtained by lightly brushing the plates with a camel hair brush.[10]

Since the experiments were carried out so that each plate was independent of others, no particular precautions were observed with regard to time of development or strength of developer. For comparison a copper arc was used.

The copper arc was photographed on each side of the plate. In between, a number of spectra were photographed, all with the same exposure, *i.e.*, two minutes. One of these was the absorption spectrum of hydrogen chloride at a pressure of 515 mms. and the others were the photographs of the source weakened by various screens, the disposition of the apparatus being absolutely unchanged except that the hydrogen chloride

was pumped out by means of a high vacuum pump run for an hour. The absorption spectrum and the calibration spectra were thus taken under identical conditions.

The blackening on the plate was measured with a Zeiss self-recording microphotometer belonging to the Physics Department, Science College, Patna. Photometer traces were taken across each plate between identical lines of the copper spectra. The intensity of the light transmitted by HCl was thus compared directly with the intensity transmitted by the calibrated screens at the same wavelength.

Results

The absorption coefficient ε is defined by the relation

$$I = I_0 \cdot 10^{-\varepsilon c d}$$

where I_0 is the incident intensity, I the transmitted intensity, d the length of the absorbing path in cms. and c the concentration in mol litres^{-1}. The results for different experimental temperatures are given in table 1. The absorption coefficients in a particular column are the coefficients of a sample of gas kept inside the furnace when the maximum temperature within it was that given at the top of the column.

Table 1.

Wave-length Å	Absorption Coefficients						
	20°C	230°C	370°C	485°C	670°C	750°C	980°C
2247	0·2145	0·2147	0·2400	0·2765	0·3755	0·4195	0·5980
2238	0·2395	0·2497	0·2648	0·3016	0·4005	0·4445	0·6230
2218	0·2705	0·2707	0·2957	0·3320	0·4310	0·4755	0·6540
2210	0·2841	0·2844	0·3094	0·3460	0·4442	0·4891	0·6676
2200	0·3148	0·3151	0·3402	0·3769	0·4749	0·5200	0·6985
2192	0·3616	0·3620	0·3870	0·4235	0·5217	0·5666	0·7450
2180	0·3840	0·3844	0·4091	0·4460	0·5439	0·5890	0·7675
2165	0·4300	0·4305	0·4554	0·4920	0·5900	0·6350	0·8135
2136	0·4955	0·4961	0·5210	0·5575	0·6555	0·7005	0·8790

By using the Maxwell-Boltzmann distribution law, the contribution of each vibrational level to the total continuous absorption may be obtained from our experimental results.

If N_v be the fraction of the total number of molecules which exists in the state with vibration quantum number v at a temperature T, then the total absorption coefficient is given by

$$\varepsilon = N_0\varepsilon_0 + N_1\varepsilon_1 + N_2\varepsilon_2 + \quad . \quad . \quad . \quad . \quad . \quad . \quad (1)$$

where $N_0 + N_1 + \ldots = 1$

$\varepsilon_0, \varepsilon_1$ etc. are partial absorption coefficients appropriate to the various vibrational levels. If E_v represents the energy difference between the state v and the lowest state $v=0$, Eqn. (1) becomes

$$\varepsilon = [\varepsilon_0 + \varepsilon_1 e^{-E_1/\kappa T} + \varepsilon_2 e^{-E_2/\kappa T} + \ldots] \,/\, \sum_v e^{-E_v/\kappa T} \quad . \quad . \quad . \quad (2)$$

κ being Boltzmann's constant

From Colby's paper[11] we find that

$$\frac{E_v}{hc} = 2937{\cdot}8v - 51{\cdot}9v^2$$

With the help of this formula, the sum of the series in the denominator of equation (2) was evaluated at each temperature by calculating successive terms until further contributions could be neglected.

At 20°C the fraction of the molecules in the state $v=1$ is $75{\cdot}05 \times 10^{-8}$. This is a very small quantity and we may neglect it altogether, and the molecules which contribute towards the absorption of light are all in the state $v=0$. Therefore $\varepsilon_0 = \varepsilon$ at 20°C. At 230°C the fraction of molecules in the state $v=1$ is 15×10^{-5}, and that in the state $v=2$ is $30{\cdot}1 \times 10^{-9}$. This quantity is negligible in comparison to others and ε_1 can be very easily found out. The values of ε_0 and ε_1 at various wavelengths are given in table 2.

Table 2.

Wavelength Å	ε_0	ε_1	Wavelength Å	ε_0	ε_1
2247	0·2145	1·4	2192	0·3616	2·4
2238	0·2395	1·6	2180	0·3839	2·9
2218	0·2703	1·8	2165	0·4300	3·2
2210	0·2841	2·0	2136	0·4955	4·0
2200	0·3149	2·2			

Calculation of the molecular constants for the unstable state

The value of the absorption coefficient of the gas per mol litre^{-1} when all the molecules are in the state $v=0$, is

$$k_\nu^0 = \frac{{}_v\varepsilon_0 \log_e 10}{6{\cdot}06\times10^{20}} = \frac{8\pi^3\nu}{3hc}\left|D_{a''a'}\right|^2 = \frac{8\pi^3\nu}{3hc} D^2_{n'n''} \left|M_0^v\right|^2$$

where ν designates a light of particular frequency. $D_{n'n''}$ is a constant depending on the electronic transition involved in the experiment. As proved elsewhere,[12]

$$\left|M_0^v\right|^2 = \left|\left(-\frac{3}{2}\right)^m \cdot (e^{-2\pi B}-1)^{-\frac{1}{2}} \sqrt{\frac{8\pi^2\mu B}{ah^2}} \cdot \frac{(2b_0)^{m+\frac{1}{2}}}{\{\Gamma(2m+1)\}^{\frac{1}{2}}}\right.$$

$$\left[\frac{\left(\frac{1}{2}\right)^{iB}\Gamma\left(iB+\frac{b_0}{a}\right)}{(iG)^{\frac{b_0}{a}}\Gamma(iB+1)} \cdot {}_2F_1\left(\frac{iB+\frac{b_0}{a}}{2}, \frac{1-\frac{b_0}{a}+iB}{2}; 1+iB; 1\right)\right.$$

$$+\frac{m}{3}e^{2ar_0}\frac{\left(\frac{1}{2}\right)^{iB}\Gamma\left(iB+\frac{b_0}{a}+2\right)}{(iG)^{\frac{b_0}{a}+2}\cdot\Gamma(1+iB)} \cdot {}_2F_1\left(\frac{iB+\frac{b_0}{a}+2}{2}, \frac{iB-\frac{b_0}{a}-1}{2}; 1+iB; 1\right)$$

$$+\frac{m(m-1)}{18}e^{4ar_0}\frac{\left(\frac{1}{2}\right)^{iB}\Gamma\left(iB+\frac{b_0}{a}+4\right)}{(iG)^{\frac{b_0}{a}+4}\Gamma(1+iB)} \cdot {}_2F_1\left(\frac{iB+\frac{b_0}{a}+4}{2}, \frac{iB-\frac{b_0}{a}-3}{2}; 1+iB; 1\right)$$

$$\left.+\frac{m(m-1)(m-2)}{162}e^{6ar_0}\frac{\left(\frac{1}{2}\right)^{iB}\Gamma\left(iB+\frac{b_0}{a}+6\right)}{(iG)^{\frac{b_0}{a}+6}\Gamma(1+iB)} \cdot {}_2F_1\left(\frac{iB+\frac{b_0}{a}+6}{2}, \frac{iB-\frac{b_0}{a}-5}{2}; 1+iB; 1\right)\right]\Bigg|^2$$

where $G = C e^{2ar_0}$, $C = \sqrt{\frac{8\pi^2\mu D}{a^2}}$

$$B = \sqrt{\frac{8\pi^2\mu W}{a^2}}, \quad W = \nu - \nu_D;$$

ν_D being the energy of dissociation of the molecule in cms^{-1}.

The potential energy of the molecule in normal state was taken to be represented by the function

$$-\frac{\gamma}{\rho} + \frac{\beta}{\rho^2}$$

where $\rho = r - \rho_0$, and ρ_0, γ and β are constants. These constants were determined by comparing this function with the Kratzer function for the potential energy of HCl given by Colby[11]. Further $\frac{8\pi^2\mu}{h^2}\beta$ was taken to be equal to $m(m-1)$ and $\frac{8\pi^2\mu}{h^2}\cdot\frac{\gamma}{2b_v} - m = v$, where $v = 0, 1, 2 \ldots$. The values of all these constants are given below, energy being expressed in cms^{-1} and distance in cms.

$\rho_0 = 0{\cdot}2948 \times 10^{-8}$	$m = 1$
$\beta = 1{\cdot}2238 \times 10^{-10}$	$b_0 = 5{\cdot}223 \times 10^{-3}$
$\gamma = 9{\cdot}18 \times 10^{-3}$	$b_1 = 2{\cdot}61 \times 10^{-3}$

The values of h and c used in the calculations were taken to be $6{\cdot}547 \times 10^{-27}$ erg sec. and $2{\cdot}99796 \times 10^{10}$ cms/sec. respectively.[13]

With the help of the following relations[14] we are able to simplify the expression for $\left|M_o^v\right|^2$;

$${}_2F_1(x, y; z; 1) = \frac{\Gamma(z)\,\Gamma(z-x-y)}{\Gamma(z-y)\,\Gamma(z-x)}$$

$$\Gamma(1+x) = x\Gamma(x)$$

and

$$\Gamma(2x) = 2^{2x-1}\pi^{-\frac{1}{2}}\,\Gamma(x)\,\Gamma(x+\tfrac{1}{2})$$

The expression is simplified as

$$\left|\left(-\frac{3}{2}\right)^m \cdot \left(e^{-2\pi B}-1\right)^{-\frac{1}{2}} \sqrt{\frac{8\pi^2\mu B}{ah^2}} \cdot \frac{(2b_0)^{m+\frac{1}{2}}}{[\Gamma(2m+1)]^{\frac{1}{2}}}\right.$$

$$\left[\frac{2^{\frac{b_0}{a}-1}\pi^{-\frac{1}{2}}\Gamma\left(\frac{iB+\frac{b_0}{a}}{2}+1\right)}{(iG)^{\frac{b_0}{a}}\left(\frac{iB+\frac{b_0}{a}}{2}\right)\Gamma\left(\frac{iB-\frac{b_0}{a}}{2}+1\right)} + \frac{me^{2ar_0}\cdot 2^{\frac{b_0}{a}}\left(\frac{iB-\frac{b_0}{a}}{2}\right)\Gamma\left(\frac{iB+\frac{b_0}{a}}{2}+1\right)}{3(iG)^{\frac{b_0}{a}+2}\Gamma\left(\frac{iB-\frac{b_0}{a}}{2}+1\right)}\right.$$

$$+\frac{m(m-1)e^{4ar_0}\cdot 2^{\frac{b_0}{a}+3}\Gamma\left(\frac{iB+\frac{b_0}{a}+4}{2}\right)}{18(iG)^{\frac{b_0}{a}+4}\Gamma\left(\frac{iB-\frac{b_0}{a}-2}{2}\right)}$$

$$\left.\left.+\frac{m(m-1)(m-2)e^{6ar_0}\Gamma\left(\frac{iB+\frac{b_0}{a}+6}{2}\right)}{162(iG)^{\frac{b_0}{a}+6}\Gamma\left(\frac{iB-\frac{b_0}{a}-4}{2}\right)}\right]\right|^2$$

To simplify the above expression we take the help of the following relations[15]:

$$\log\Gamma(z)=\tfrac{1}{2}\log 2\pi+(z-\tfrac{1}{2})\log z-z+\mu(z)$$

$$\mu(z)=\frac{1}{12z}-\frac{1}{360z^3}+\frac{1}{1260z^5}\quad\cdots$$

As $|z|$ is in all the Gamma functions appearing in the above expression is fairly greater than unity except in $\Gamma\left(1+\frac{iB+\frac{b_0}{a}}{2}\right)$ and $\Gamma\left(1+\frac{iB-\frac{b_0}{a}}{2}\right)$, where it is only very slightly greater and very slightly smaller than unity the series $\mu(z)$ is rapidly convergent. Applying binomial theorem, we get the following equation, where $k^\circ_{\nu_1}$ be the absorption coefficient of gas per mol litre^{-1} when all the molecules are in frequency ν_1 and $k^\circ_{\nu_2}$ a similar absorption coefficient

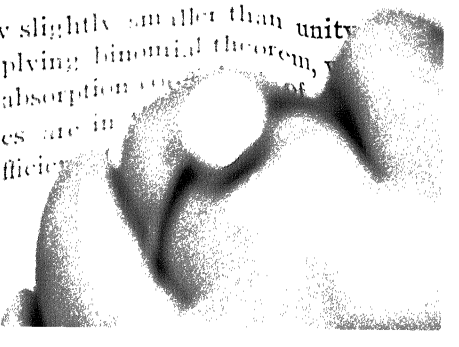

The expression is simplified as

$$\left|\left(-\frac{3}{2}\right)^m \cdot \left(e^{-2\pi B}-1\right)^{-\frac{1}{2}} \sqrt{\frac{8\pi^2\mu B}{ah^2}} \cdot \frac{(2b_0)^{m+\frac{1}{2}}}{[\Gamma(2m+1)]^{\frac{1}{2}}}\right.$$

$$\left[\frac{2^{\frac{b_0}{a}-1}\pi^{-\frac{1}{2}}\Gamma\left(\frac{iB+\frac{b_0}{a}}{2}+1\right)}{(iG)^{\frac{b_0}{a}}\left(\frac{iB+\frac{b_0}{a}}{2}\right)\Gamma\left(\frac{iB-\frac{b_0}{a}}{2}+1\right)} + \frac{me^{2ar_0}\cdot 2^{\frac{b_0}{a}}\left(\frac{iB-\frac{b_0}{a}}{2}\right)\Gamma\left(\frac{iB+\frac{b_0}{a}}{2}+1\right)}{3(iG)^{\frac{b_0}{a}+2}\Gamma\left(\frac{iB-\frac{b_0}{a}}{2}+1\right)}\right.$$

$$+\frac{m(m-1)e^{4ar_0}\cdot 2^{\frac{b_0}{a}+3}\Gamma\left(\frac{iB+\frac{b_0}{a}+4}{2}\right)}{18(iG)^{\frac{b_0}{a}+4}\Gamma\left(\frac{iB-\frac{b_0}{a}-2}{2}\right)}$$

$$\left.\left.+\frac{m(m-1)(m-2)e^{6ar_0}\Gamma\left(\frac{iB+\frac{b_0}{a}+6}{2}\right)}{162(iG)^{\frac{b_0}{a}+6}\Gamma\left(\frac{iB-\frac{b_0}{a}-4}{2}\right)}\right]\right|^2$$

To simplify the above expression we take the help of the following relations[15]:

$$\log\Gamma(z)=\tfrac{1}{2}\log 2\pi+(z-\tfrac{1}{2})\log z-z+\mu(z)$$

$$\mu(z)=\frac{1}{12z}-\frac{1}{360z^3}+\frac{1}{1260z^5}\quad\ldots$$

As $|z|$ is in all the Gamma functions appearing in the above expression is fairly greater than unity except in $\Gamma\left(1+\frac{iB+\frac{b_0}{a}}{2}\right)$ and $\Gamma\left(1+\frac{iB-\frac{b_0}{a}}{2}\right)$, where it is only very slightly greater and very slightly smaller than unity the series $\mu(z)$ is rapidly convergent. Applying binomial theorem, we get the following equation, where $k^\circ_{\nu_1}$ be the absorption coefficient of the gas per mol litre^{-1} when all the molecules are in the state $v=0$ at a frequency ν_1 and $k^\circ_{\nu_2}$ a similar absorption coefficient at the frequency ν_2.

$$k^{\circ}_{\nu_1}.\,\nu_2.\left[\frac{2^{\frac{2b_0}{a}}.\,e^{\frac{-13b_0}{6a}}.\left\{1+\frac{2b_0}{a}\left(1+B_2^{\,2}+\frac{b_0^{\,2}}{4a^2}\right)\right\}}{\pi\left(\frac{b_0^{\,2}}{a^2}+B_2^{\,2}\right)}\right.$$

$$-0{\cdot}03133\,\frac{2^{\left(\frac{2b_0}{a}-2\right)\left(\frac{b_0^{\,2}}{a^2}+B_2^{\,2}\right)}}{C^4}\cdot$$

$$\left\{1+2\,\frac{b_0}{a}\left(1+B_2^{\,2}+\frac{b_0^{\,2}}{4a^2}\right)\right\}.\,e^{-\frac{13}{6}.\frac{b_0}{a}}+0{\cdot}003446\,\frac{2^{\frac{4b_0}{a}+14}}{C^8}\cdot$$

$$\left\{1+\frac{9}{2}\,\frac{b_0}{a}+\frac{5}{4}\,\frac{b_0}{a}\,B_2^{\,2}+\frac{49}{16}\,\frac{b_0^{\,2}}{a^2}-\frac{1}{4}\,\frac{b_0^{\,2}}{a^2}\,B_2^{\,2}\right.$$

$$\left.+\frac{9}{4}\,B_2^{\,2}+\frac{5}{16}\,\frac{b_0^{\,3}}{a^3}\right\}e^{-\left(\frac{49}{24}.\frac{b_0}{a}+6\right)}$$

$$\left.-0{\cdot}09986\cdot\,2^{\frac{2b_0}{a}}.\,e^{\frac{-13}{6}.\frac{b_0}{a}}\left\{1+\frac{4b_0}{a}+2B_2^{\,2}.\,\frac{b_0}{a}+\frac{b_0^{\,3}}{a^3}\right\}\right|$$

$$=k^{\circ}_{\nu_2}.\,\nu_1.\left[\frac{2^{\frac{2b_0}{a}}.\,e^{\frac{-13b_0}{6a}}.\left\{1+\frac{2b_0}{a}\left(1+B_1^{\,2}+\frac{b_0^{\,2}}{4a^2}\right)\right\}}{\pi\left(\frac{b_0^{\,2}}{a^2}+B_1^{\,2}\right)}\right.$$

$$-0{\cdot}03133\,\frac{2^{\left(\frac{2b_0}{a}-2\right)\left(\frac{b_0^{\,2}}{a^2}+B_1^{\,2}\right)}}{C^4}\left\{1+\frac{2b_0}{a}\left(1+B_1^{\,2}+\frac{b_0^{\,2}}{4a^2}\right)\right\}.\,e^{\frac{-13}{6}.\frac{b_0}{a}}$$

$$+0{\cdot}003446\,\frac{2^{\frac{4b_0}{a}+14}}{C^8}\left\{1+\frac{9}{2}\,\frac{b_0}{a}+\frac{5}{4}\,\frac{b_0}{a}\,B_1^{\,2}+\frac{49}{16}\,\frac{b_0^{\,2}}{a^2}-\frac{1}{4}\,\frac{b_0^{\,2}}{a^2}\,B_1^{\,2}\right.$$

$$\left.+\frac{9}{4}\,B_1^{\,2}+\frac{5}{16}\,\frac{b_0^{\,3}}{a^3}\right\}e^{-\left(\frac{49}{24}.\frac{b_0}{a}+6\right)}$$

$$\left.-0{\cdot}09986\cdot\,2^{\frac{2b_0}{a}}.\,e^{\frac{-13}{6}.\frac{b_0}{a}}\left\{1+4\,\frac{b_0}{a}+2B_1^{\,2}.\frac{b_0}{a}+\frac{b_0^{\,3}}{a^3}\right\}\right|$$

where $B_1=9{\cdot}0112/a\times10^{-4}\sqrt{\nu_1-\nu_0}$ and $B_2=9{\cdot}0112/a\times10^{-4}\sqrt{\nu_2-\nu_0}$

We get the values of the constants involved in the potential function of the HCl molecule in its unstable state from the values of k_ν° at four different wavelengths appearing in equations similar to the above

one. The constants derived from the values of k°_{ν} at λλ 2247, 2238, 2218 and 2210 are as follows

$$D = 423735 \text{ cms}^{-1}$$
$$\nu_D = 37563 \text{ cms}^{-1} \qquad (I)$$
$$a = 1{\cdot}6002.$$

The same constants derived from the values of k°_{ν} at λλ 2200, 2192, 2180 and 2165 are as follows

$$D = 404089 \text{ cms}^{-1}$$
$$\nu_D = 35497 \text{ cms}^{-1} \qquad (II)$$
$$a = 1{\cdot}6012$$

The average of these constants is as below

$$D = 413912 \text{ cms}^{-1}$$
$$\nu_D = 36530 \text{ cms}^{-1} \qquad (III)$$
$$a = 1{\cdot}6007$$

Taking into consideration all the errors of the experiment, the agreement between the sets of values for the constants is remarkable.

With the help of these values the ratios between $k_{\nu}{}^{1}$ for different values of ν was calculated and it was found that they agreed well with the experimental value. HCl dissociates to a very small degree at higher temperatures[16]. The number of HCl molecules per c.c. is not the same as when there was no dissociation, and the correct number was obtained by multiplying it with the fraction of undissociated molecules.

This agreement between the values of these constants calculated from observational data taken at absolutely different sets of wavelengths shows that the choice of the potential function of a diatomic molecule[5] in its unstable state was correct as well as the theory of continuous absorption[12] of diatomic molecules.

The value of ν_D is interesting. The thermo-chemical energy of dissociation[17] is 101 Kcals whereas the value as obtained here is 103·9 Kcals.

Acknowledgment

My best thanks are due to Prof. M. N. Saha, F.R.S., who has been bestowing great kindness on the author. My thanks are also due to Prof. Kamta Prasad and Principal Ashutosh Mukerji of Science College, Patna, for having kindly lent me the use of Zeiss Microphotometer belonging to the Science College, Patna.

References

1. Ladenburg, Van Voorhis and Boyce, *Phy. Rev.*, **40**, 1018, 1932.
2. Halban and Siedentopf, *Zeits. f. Phys. Chem.*, **103**, 71, 1922; Ribaud, *Ann. de Phy.*, **12**, 107, 1919; Gibson and Bayliss, *Phy. Rev.*, **44**, 188, 1933.
3. Stueckelberg, *Phy. Rev.*, **42**, 522, 1932.
4. Gibson, Rice and Bayliss, *Phy. Rev.*, **44**, 193, 1933.
5. Trivedi, *Proc. Acad. Sc. U. P.*, **4**, 59, 1934; *Proc. Acad. Sc. U. P.*, **5**, 171 1935.
6. Franck and Kuhn, *Zeits. f. Phys.*, **44**, 607, 1927.
7. Rollefson and Booher, *Jour. Amer. Chem. Soc.*, **53**, 1728, 1933.
8. Datta, *Zeits. f. Phys.* **77**, 404, 1932.
9. Harrison, *Jour. Opt. Soc. Amer.*, **19**, 267, 1929.
10. Dobson, Griffiths and Harrison, *Photographic Photometry*, p. 76, 1926.
11. Colby, *Phy. Rev.*, **34**, 53, 1929.
12. Trivedi, *Proc. Acad. Sc., U. P.*, **5**, 171, 1935.
13. Saha and Saha, *Treatise on Modern Physics*, 831, 1935.
14. Milne-Thomson, *The Calculus of Finite Differences*, pp. 249, 257, 261, 1933.
15. Ginzel, *Acta Mathematica*, **56**, 273, 1931.
16. Bodenstein and Geiger, *Zeits. f. Phys.*, **49**, 72, 1904.
17. Dutta and Deb, *Zeits. f. Phys*,, **93**, 131, 1934 ; Grimm and Wolff, *Handbuch der Physik*, **24/2**, 1003, 1933.

THE ABSORPTION SPECTRUM OF HYDROGEN BROMIDE MOLECULE AND ITS UPPER UNSTABLE STATE

By Hrishikesha Trivedi

Physics Department, Allahabad University

Communicated by Prof. M. N. Saha

Received November 5, 1935

The continuous absorption spectrum of hydrogen bromide was studied at different temperatures. The form of the upper potential energy curve was calculated just as in the case of HCl. It was found that the position representing the dissociation of the molecule in its unstable state lay 92 Kcals. above the minimum of the lower state in the Franck-Condon diagram for HBr, the same as the atomic heat of formation of the molecule determined thermochemically (86 Kcals).

In a previous paper of mine[1] I had communicated the results of an experiment on the absorption of light by hydrogen chloride gas in the quartz region. It was shown there that the constants of the potential function of the unstable state of the hydrogen chloride molecule could be determined from the measurements of the absorption coefficients of the gas with the help of a theory of continuous absorption of diatomic molecules worked out by the present author.[2]

The aim of the present paper is to report the result of an experiment on the measurement of the absorption of light by hydrogen bromide gas in the ultra-violet region, an experiment in continuation with the previous one.

The experimental procedure was exactly similar to the one employed in the case of hydrogen chloride.[1] The gas was produced by heating under vacuum a sample of Merck's strong hydrobromic acid and passing the vapour through a series of chambers containing broken glass smeared with moist red phosphorus, anhydrous calcium bromide and phosphorus pentaoxide. It then passed through a short length of thin capillary tube through a mercury manometer to the absorption chamber.

Results

The absorption coefficient ε, is defined by the relation

$$I = I_0 \cdot 10^{-\epsilon c d}$$

where I_0 is the incident intensity, I the transmitted intensity, d the length

of the absorbing path in cms. and c the concentration in mol litres^{-1}. The results for different experimental temperatures are given in table 1. The absorption coefficients in a particular column are the coefficients of a sample of gas kept inside the furnace when the maximum temperature within it was that given at the top of the column.

Table 1

Wavelength Å	Absorption Coefficient						
	20°C	230°C	370°C	485°C	670°C	750°C	980°C
2492	1·118	1·120	1·321	1·530	1·971	2·349	3·444
2468	1·313	1·316	1·511	1·725	2·153	2·550	3·639
2442	1·421	1·424	1·622	1·833	2·266	2·659	3·748
2415	1·521	1·525	1·713	1·943	2·359	2·759	3·853
2407	1·671	1·673	1·874	2·081	2·514	2·900	4·003
2393	2·221	2·223	2·416	2·630	3·061	3·452	4·551
2370	2·729	2·730	2·924	3·138	3·572	3·942	5·052
2345	3·335	3·338	3·527	3·740	4·191	4·531	5·699

By using the Maxwell-Boltzmann distribution law, the contribution of each vibrational level to the total continuous absorption may be obtained from our experimental results.

If N_v be the fraction of the total number of molecules which exists in the state with vibration quantum number v at a temperature T, the total absorption coefficient is given by

$$\varepsilon = N_0 \varepsilon_0 + N_1 \varepsilon_1 + N_2 \varepsilon_2 + \ldots \quad (1)$$

where $N_0 + N_1 + \ldots = 1$

ε_0, ε_1, etc., are partial absorption coefficients appropriate to the various vibrational levels. If E_v represents the energy difference between the state v and the lowest state $v=0$, the equation (1) becomes

$$\varepsilon = [\varepsilon_0 + \varepsilon_1 e^{-E_1/\kappa T} + \varepsilon_2 e^{-E_2/\kappa T} + \ldots] / \sum_v e^{-E_v/\kappa T} \quad (2)$$

where κ is the Boltzmann's constant.

Unfortunately no measurement has been made on the 'harmonic' band of HBr and, therefore, we cannot find out the value of Ev/hc for any value of v. The series in the denominator of (2) and, therefore, the values of $\varepsilon_0, \varepsilon_1$, etc., cannot be evaluated. We may say, however, from analogy with the case of HCl that the fraction of molecules in the state $v=1$ at 20°C would be a negligibly small quantity. Neglecting this fraction altogether, we can assume that the molecules which contribute towards the absorption of light are all in the state $v=0$ at that temperature. Therefore $\varepsilon_0=\varepsilon$ at 20°C. ε_1 cannot be found out in the case of HBr.

Calculation of the molecular constants for the unstable state

The value of the absorption coefficient of the gas per mole litre^{-1} when all the molecules are in the state $v=0$, is

$$k^0_\nu = \frac{\nu \varepsilon_0 \log_e 10}{6{\cdot}06\times 10^{20}} = \frac{8\pi^3\nu}{3hc}\left| D_{\alpha''\alpha'} \right|^2$$
$$= \frac{8\pi^3\nu}{3hc} D^2_{n'n''} \left| M^v_0 \right|^2$$

where ν designates a light of any particular frequency. $D_{n'n''}$ is a constant depending on the electronic transitions involved in the experiment. The value of $\left| M^v_0 \right|^2$ has been found elsewhere[12], in terms of the constants of the potential energy curves of the upper and lower states of the molecule.

The potential energy of the molecule in the normal state was taken to be represented by the function

$$-\frac{\gamma}{\rho} + \frac{\beta}{\rho^2}$$

where $\rho=r-\rho_0$; ρ_0, γ, β being constants. These constants can be determined by comparing this function with the Kratzer's function for the potential energy of HBr.

Nobody has calculated the constants of the Kratzer's function for HBr. They were, however, calculated in this paper as follows. Fues[3] has discussed the case of a rotating vibrating dipole and has obtained an energy expression in the form given below.

$$E = A + h\nu_0 (n+\tfrac{1}{2})[1-B(j+\tfrac{1}{2})^2] + \left(\frac{h^2}{8\pi^2 J}\right)(j+\tfrac{1}{2})^2[1-k^2(j+\tfrac{1}{2})^2]$$
$$-\left(\frac{h^2}{8\pi^2 J}\right)(n+\tfrac{1}{2})^2 \quad . \quad . \quad . \quad . \quad . \qquad (3)$$

where n is the vibrational quantum number and j the rotational B,C, ν_0 and k^2 contain constants of the force function but are independent of j and

n. J is the moment of inertia of the molecule about an axis normal to the nuclear line. The transitions involved in the fundamental bands of HBr are for n, $0 \longrightarrow 1$ and for j, $j \longrightarrow j+1$. The initial values of j in the positive branch begin with zero and for the negative with 1. If, however, we do not use the initial values of j in numbering the lines, but, rather, on both sides starting with 1, as is done by Imes[4] and Czerny,[5] we can write a single formula for both the branches.

$$\nu = \nu_0 - 1\nu_0 B - \left(\frac{h}{8\pi^2 J}\right)^2 C + \left(\frac{2h}{8\pi^2 J} - 2\nu_0 B - \frac{hk^2}{8\pi^2 J}\right) j$$

$$- \nu_0 B j^2 - \frac{h}{8\pi^2 J} \cdot 4k^2 j^3 \quad . \quad . \quad . \quad . \quad . \quad . \quad (4)$$

where j is the number of the line from the centre of the band, positive for the positive branch and negative for the negative branch. Czerny[6] has found that the wave numbers of these lines fit in the following cubic formula

$$\nu = 2559{\cdot}151 + 16{\cdot}4788\, j - 0{\cdot}23044 j^2 - 0{\cdot}001457 j^3.$$

In the energy equations (3) and (4) the constants B, C and k^2 have been used to replace somewhat inconvenient combinations of the constants of force function which we are now in a position to evaluate from the empirical data for this band. In Kratzer's original paper[7] the potential energy of the molecule was developed in the form

$$\varphi = \varphi_0 - (2\pi\nu_0)^2 J \left(\frac{1}{\sigma} - \frac{1}{(2\sigma^2)} + C_3 \xi^3 + C_4 \xi^4 + \ldots\right)$$

where $\sigma = \frac{r}{r_0}$, the ratio of the distance between the nuclei to the equilibrium distance, $\xi = \sigma - 1$, and ν_0 is the frequency of vibration for infinitesimal amplitude. In terms of the above constants

$$k = \left(\frac{h}{4\pi^2 \nu_0 J}\right), \quad B = \frac{3}{2} k^2 (1 + 2C_3)$$

$$C = 3 + 15C_3 + \frac{15}{2} C_3^2 + 3C_4$$

The constant J is easily found from the band data. To determine ν_0 both the fundamental and harmonic bands must be used. It is not possible to do so in the present case, as the harmonic band is not properly measured. The value of k, (and, therefore, that of ν_0) can be found directly from the coefficient of j^3. This, however, is the least reliable of the coefficients. The value of C_3 is then calculated. The

value of C_4 was not calculated as it, itself, would be determined from the value of C, a constant appearing in the term determined only by the vibration of this molecule. As the value of ν_0 was a little uncertain, and as C is known only with the help of ν_0, its value was liable to great error. The term ξ^4 in the potential energy function was taken to be vanishingly small

The various constants are given below

$$(h/8\pi^2 J)\ (1/3 \cdot 10^{10}) = 16{\cdot}939$$
$$k^2 \cdot 10^5 = 4{\cdot}4425$$
$$\nu_0\ (1/3 \cdot 10^{10}) = 2512{\cdot}3$$
$$C_3 = 0{\cdot}18825$$
$$J_0 = 3{\cdot}267 \times 10^{-40}$$

Further $\frac{8\pi^2\mu\beta}{h^2}$ was taken to be equal to $m\ (m-1)$ and $\frac{8\pi^2\mu}{h^2} \cdot \frac{\gamma}{2b_v} - m = v$, where $v = 0, 1, 2 \ldots$. The values of all these constants are given below (energy being expressed in cms.$^{-1}$ and distance in cms.)

$$\rho_0 = 1{\cdot}8805 \times 10^{-8}$$
$$\beta = 5{\cdot}5752 \times 10^{-12}$$
$$\gamma = 5{\cdot}929 \times 10^{-4}$$
$$m = 1{\cdot}00004$$
$$b_0 = 7{\cdot}2083 \times 10^{-5}$$
$$b_1 = 3{\cdot}6041 \times 10^{-5}$$

The values[8] of h and c used in the calculations were taken to be $6{\cdot}547 \times 10^{-27}$ erg sec. and $2{\cdot}99796 \times 10^{10}$ cms/sec.

In the previous paper[1] we have obtained simplified expressions for $|M_0^v|^2$ and have obtained equations for calculating the constants of the potential function of the unstable state of the molecule. Such equations were found out for all the wavelengths at which the measurement was made in this case also.

We get the values of the constants involved in the potential function of HBr molecule in its unstable state from the values of k_v^0 at four different wavelengths. The constants derived from the values of k_v^0 at λλ 2492, 2468 2442, and 2415 are as follows.

$$D = 604206 \text{ cms.}^{-1}$$
$$\nu_D = 33398 \text{ cms}^{-1} \quad \ldots\ldots\ldots\ldots\ldots\ldots \quad (I)$$
$$a = 0{\cdot}812$$

The same constants derived from the values k_ν^0 at λλ 2407, 2393, 2370, 2345 are as follows

$$\begin{aligned} D &= 580020 \text{ cms}^{-1} \\ \nu_D &= 31318 \text{ cms}^{-1} \\ a &= 0{\cdot}788 \end{aligned} \qquad \text{(II)}$$

The average of these constants is as below

$$\begin{aligned} D &= 592133 \text{ cms}^{-1} \\ \nu_D &= 32348 \text{ cms}^{-1} \\ a &= 0{\cdot}800 \end{aligned} \qquad \text{(III)}$$

Taking into consideration all the errors of the experiment, the agreement between the sets of values for the constants is remarkable.

HBr dissociates to a very small degree at high temperatures.[9] The number of HBr molecules per c.c. is not the same as when there was no dissociation and the correct result was obtained by multiplying it with the fraction of undissociated molecules.

The value of ν_D is interesting. The thermochemical energy of dissociation of the HBr molecule[10] is 86 Kcals, whereas the value as obtained here is 92 Kcals. In view of the uncertainty in the calculation of constants for the lowest state of HBr, the agreement is very good.

Acknowledgment

My best thanks are due to Prof. M. N. Saha, F.R.S., who has been bestowing great kindness on the author. My thanks are also due to Prof. Kamta Prasad and Principal Ashutosh Mukerji of Science College, Patna, for having kindly lent me the use of Zeiss Microphotometer belonging to their College.

References

1. Trivedi, *Proc. Nat. Acad. Sc.*, (*India*), **6**, 18, 1936.
2. Trivedi, *Proc. Acad. Sc.*, U. P., **5**, 171, 1935.
3. Fues, *Ann. d. Phy.*, **80**, 367, 1926.
4. Imes, *Astr. Jour.*, **50**, 251, 1919.
5. Czerny, *Zeits. f. Phy.*, **44**, 235, 1927.
6. Czerny, *ibid.*, **45**, 476, 1927.
7. Kratzer, *ibid.*, **3**, 289, 1920.
8. Saha and Saha, *Treatise on Modern Physics*, 831, 1935.
9. Von Falckenstein, *Zeit. f. Phy.*, **68**, 270, 1910; **72**, 113, 1910.
   Bodenstein and Geiger, *Zeit. f. Phy.*, **49**, 72, 1904.
10. Dutta and Deb, *Zeit. f. Phy.*, **98**, 131, 1934.
    Grimm and Wolff, *Handbuch der Physik*, 24/2, 1003, 1933.

INFLUENCE OF TEMPERATURE ON NITROGEN FIXATION BY AZOTOBACTER

By N. R. Dhar and S. P. Tandon

Chemistry Department, Allahabad University

Received October 31, 1935

1. The fixation of atmospheric nitrogen by pure cultures of Azotobacter on mannite media has been investigated at 10°, 20°, 30°, 35°, 40°, 50°, 60° and 70°.

2. It has been observed that the maximum fixation (largest amount of ammonia formation) takes place at about 35°, which is, therefore, the optimum temperature for Azotobacter isolated from the garden soil at Allahabad as against 28° obtained in temperate countries. There is hardly any ammonia formation at 10°, on the one hand and at 60°, on the other.

3. The results obtained in this investigation show that Azotobacter requires more heat than Bacillus radicicola and several other bacteria and is eminently suitable for nitrogen fixation in tropical countries except in the months of April, May and June when the soil temperature in the day time exceeds 50°, beyond which Azotobacter is unable to fix nitrogen.

4. In temperate climates Azotobacter is not suitable for nitrogen fixation, as it requires more warmth than that which is available in such countries.

In a recent communication[1] we have investigated the influence of temperature on nitrite-formers and we have observed that the optimum temperature is 35° with the bacteria available in the soils of India and at 50° there is no bacterial nitrite formation. It is interesting to note here that the nitrite-formers of temperate countries thrive best at 25°, which is the optimum temperature observed in these countries. Walton and his collaborators[2] at Pusa reported that 30° is the optimum temperature for nitrogen-fixation by Azotobacter. As this temperature appears to be rather low in view of our observations with tropical nitrite-formers and those of Panganiban[3] with the same bacteria obtained in the Philippines, we have investigated the velocity of nitrogen fixation by Azotobacter collected from the garden soil of the Allahabad University. The determinations have been carried on at temperatures varying from 10° to 70° in order to obtain the optimum temperature and the limits between which the Azotobacter available at Allahabad can work.

Experimental

A pure culture of Azotobacter was prepared by the elective method (compare Russell[4]). The following Beijerinck's mannite liquid medium

was employed throughout this investigation

Tap water	1000c. c.
Mannite	20 grams.
$K_2H\ PO_4$	0·2 gram

In order to obtain a solid medium for plating 2·0 per cent of agar was added to the above liquid medium.

The medium was sterilized in an autoclave at 20 pounds pressure for 15 minutes. Forty cubic centimeters of the sterile medium were taken in a 100 c. c. conical Jena glass flask and plugged with sterile cotton. A gram of the garden soil was added to the flask which was then incubated at a temperature of 30° to 32°. After two days a pellicle was formed on the surface of the liquid. A portion of the pellicle when examined under the microscope showed abundant typical Azotobacter cells. By means of a platinum loop, a portion of the pellicle was transferred to another flask containing the sterile medium. In this way on repeated transfers to fresh lots of sterile media, the organism was gradually purified from the majority of the contaminating organisms. For final isolation, a loop full of the above purified culture after dilution was streaked out by means of a platinum loop on solid mannite-agar. Azotobacter colonies developed in two days on the streaks. A portion of the colony from the streak was then put by means of a sterile platinum loop on a fresh lot of sterile medium. This then gave the pure culture of Azotobacter, which was employed in this investigation The purity of the above culture was further tested by plating it on a fresh agar medium when it was found to be practically pure, forming, as far as we could judge, only Azotobacter colonies belonging to different species, but mostly to two species - Azotobacter chroococcum and Azotobacter vinelandii.

The following procedure was adopted for the study of nitrogen fixation by Azotobacter kept at various temperatures.

A three days old pure culture of Azotobacter cells was prepared by the method previously described. Forty cubic centimeters portions of the sterile mannite medium were taken in 100 c. c. conical sterile Jena glass flasks plugged with absorbent cotton. To each of the flasks was added 0·2 c.c. of the three days old culture of Azotobacter prepared as above. Duplicate sets of flasks were kept at the following temperatures:— 10°, 20°, 30°, 35°, 40°, 50°, 60° and 70°. The control flasks containing only the medium but no bacterial culture were also placed side by side with the experimental flasks at each temperature of study. The temperatures from 30° onwards were maintained in steam ovens by regulating the size of the

flame and other mechanical devices. The temperature of 35° was regulated within ± 0·5 degree in an incubator. The other temperatures were constant within one degree. Ten and twenty degrees were regulated by mechanical devices in an ice-chamber and here the error was within ± 1·5 degrees.

In general, the growth and development of the bacteria were taken to be directly proportional to the amount of nitrogen fixed in the form of ammonia, which was estimated at various temperatures from time to time by Nessler's reagent in a Duboscq colorimeter. The results are recorded below:—

Gram of Ammoniacal Nitrogen per litre

Hours	At temperatures of							
	10°	20°	30°	35°	40°	50°	60°	70°
96	Nil	0·00086	0·00105	0·00243	0·00096	0·000782	Nil	Nil
168	„	0·002169	0·00677	0·0161	0·002749	0·001674	„	„
216	„	0·00565	0·0116	0·0254	0·0064	0·00357	„	„
264	„	0·00862	0·012	0·0296	0·00924	0·00535	„	„
312	„	0·01041	0·015	0·0354	0·01054	0·00654	„	„
360	„	0·01352	0·0167	0·0423	0·01375	0·00895	„	„
408	„	0·0152	0·0207	0·0504	0·0153	0·0094	„	„

Discussion

The foregoing results show that the maximum amount of nitrogen fixation by Azotobacter which we isolated from our garden soil is at about 35° whilst at 10°, 60° and 70° there is no nitrogen fixation. The cultures at 10° and 60° were plated on solid mannite-agar media and it was found that a few colonies developed on the plates containing the culture at 10°, while on the plates containing the culture kept at 60° practically no colony appeared. This shows that although a few Azotobacter cells may remain alive at 10°, their activity is practically nil, which is evident from the fact that no ammonia formation could be detected in the experimental flasks kept at the said temperature.

Walton and his collaborators working at Pusa (India) found that different strains of Azotobacter isolated from soils of different places in India had the power of fixing maximum nitrogen at a temperature of about 30°. We believe that because in their investigation on nitrogen fixation by Azotobacter Walton and his co-workers measured the nitrogen fixation at intervals of 10°, they were unable to determine exactly the optimum point. For instance, they tried at 30° and then at 40°. Had they studied fixation at a temperature near about 35° also, we believe that they would have got practically the same optimum point as we have observed. Since in the majority of their experiments they obtained 30° as the most suitable temperature for nitrogen fixation by Azotobacter, we think that different strains of Azotobacter isolated from tropical soils do not differ much as regards their optimum.

This is a very interesting case where the lower limit (10°) of bacterial activity is much higher than with the nitrite-formers and several other bacteria. Moreover, the upper limit for Azotobacter is also appreciably higher. For example, even at 50°, Azotobacter can fix an appreciable amount of nitrogen and the fixation at 50° is almost the same as at 20°. In the case of nitrite-formers, the bacterial activity ceases completely at 50°. Even at 40° the activity of nitrite-formers is quite small in comparison to that at the optimum at about 35°. These results show definitely that Azotobacter can stand high temperatures better than the nitrite-formers and several other bacteria. Thus it is evident that Azotobacter has adapted itself fairly well to the tropical conditions as represented by the climate at Allahabad as regards minimum, optimum and maximum temperatures of their existence.

Investigations carried on in different temperate countries show that the optimum temperature is appreciably lower for Azotobacter in colder countries, than 35°. According to Waksman the optimum temperature for Azotobacter available in temperate climates is round about 28° (25° to 30°). In this connection the following lines from Russell's *Soil Conditions and Plant Growth* are of interest.

"Azotobacter requires more warmth than many other organisms and according to Koch's experiments ceases to work at 7°. Thiele read temperatures daily for three years of arable and grass soils at different depths at Breslau and concluded that only rarely were they favourable for Azotobacter."

"In neutral soils of cool countries, Bacillus radicicola is the most active fixer of nitrogen and Azotobacter is relatively inactive; lucerne, therefore, enriches the soil in nitrogen, while wheat stubble does not.

In alkaline soils of warm climates, on the other hand, Azotobacter is greatly stimulated; Bacillus radicicola is not; wheat stubble, therefore, enriches the soil in nitrogen, while lucerne has hardly any effect."

It is clear, therefore, that Azotobacter is eminently suitable for nitrogen fixation in tropical soil where it can get more warmth for the greater part of the year than in colder countries except in the months of April, May and June, when the soil temperature exceeds 50° in the day time. It is, therefore, easy to understand why Azotobacter has not been largely utilized by the farmers in temperate climates. This is evident from the following lines from Miller:—

"Wide use is being made in systems of agriculture of the bacteria which work with legume but the nitrogen-fixing power of those which work outside the plant is as yet not utilized extensively by man, since the methods of controlling them are not well understood."

The optimum temperature for the nodule bacteria in temperate climates lies between 18° and 26° and is appreciably lower than that of Azotobacter. Moreover, Bacillus radicicola can thrive even at a temperature of 3° and that is why this bacterium has been utilized to a much greater extent in Europe and America than Azotobacter.

The foregoing results show that when Azotobacter is properly fed with energy-rich substances large amounts of nitrogen fixation should be possible in tropical countries. Further work is in progress in these laboratories as regards the effect of temperature on each species of Azotobacter and other bacteria.

References.

1. Tandon, S. P., and Dhar, N. R., 1934, Influence of Temperature on Bacterial Nitrification in Tropical Countries Soil, *Science*, Vol. 38, No. 3, pages 183—189.
2. Walton, "Azotobacter and Nitrogen-Fixation in Indian Soils" (Memoirs of Department of Agriculture in India, Bacterial Series, Vol. I, No. 4, August, 1915).
3. Panganiban, E. H., Temperature as a Factor in Nitrogen Changes in the Soil, *Jour. Amer. Soc. Agron.*, *17*: 1—31, 1925.
4. *Soil Conditions and Plant Growth*, page 346, Sixth Edition, 1932.

RECORDING THE IONOSPHERIC ECHOES AT THE TRANSMITTER

By Ram Ratan Bajpai

Physics Department, Allahabad University

Communicated by Mr. G. R. Toshniwal

Received April 20, 1935

In the year 1901, Marconi's epoch-making trans-atlantic radio communication experiments startled the physicists and the mathematicians and made them think about the mechanism that could enable radio wave to overcome the curvature of the surface of the earth. The first explanation based on diffraction was soon found inadequate when put to experimental test.

In the year 1902, Kennelly[1] in America and Heaviside[2] in England independently gave definite suggestions of the existence of ionized regions responsible for the guidance of radio waves high up in the atmosphere, though these people had already been anticipated by Balfour Stewart[3] about 25 years earlier in order to explain the diurnal variation of the magnetic field of the earth. This altered the problem to some extent and gave better agreement though still inadequate; but finally it became far too complex to be amicably solved by the mathematician.

On the other hand the practical hands after immense labour gave the well known Austin-Cohen formula afterwards modified by Watson and Eckersely. Its supremacy lasted till the advent of the short wave when a closer search into the nature of the mechanism guiding the course of radio waves was necessitated.

The real advance began when Eccles[4] and Larmor[5] applied Lorentz's theory of the propagation of electro-magnetic waves through a system of molecules to radio wave propagation through electrons. The theory has been further developed by Appleton,[6] Hartree,[7] Nichols and Schelleng, Mary Taylor[8] and others[9] taking into consideration the effect of the magnetic field of the earth on the motion of electrons and ions. This gave a great impetus to the study of the ionosphere, and in the year 1925 Appleton and Barnett[10] in England, and Breit and Tube[11] in America independently proved the existence of an ionized layer at a height of

about 80 km. experimentally. Later on in 1927 the existence of a second layer was also detected by Appleton.[12] The intermediate region was shown to exist simultaneously by English and American workers[13] and now the evidence of a fine structure is also accumulating.

In view of the fact that the ionosphere has a great influence in directing radio waves a vigorous study is being made all over the world and correlation with other natural phenomena like auroral electric discharges, magnetic storms, meteor showers, sun-spot activities, etc., are being attempted. In spite of all this very little work has been done in India; however, lately excellent work has been done in Calcutta by Prof. Mitra and his coworkers and at Allahabad by Messrs. Toshniwal and Pant. It is rather unfortunate that the study of the ionosphere started by Verman at Bangalore has come to a standstill. Such a study is all the more necessary in view of the proposed radio developments in India.

Apparatus

The transmitter used was constructed on the principle of simple Hartley circuit. The variable oil condenser of the order of '001 mfd. in the grid shunted by a fixed resistance of 10 megohms was responsible for the production of 'jabs'. The grid condenser gets charged and makes the grid highly negative with respect to the filament so that the condition of maintenance of oscillations is no longer satisfied and the valve ceases to oscillate till the charge has leaked through the shunting resistance. It is obvious that the sharpness of the peaks depends on the value of the condenser while the frequency depends on the product of the capacity and the resistance.

For synchronization a small 50 cycle A.C. voltage was injected into the grid filament circuit of the transmitter and the grid condenser varied till fifty pulses per second were emitted.

The wavelength used was 75 m. The aerial used was a half wave, horizontal, Hertzian dipole placed approximately North and South. The energy was fed by a single wire feeder as outlined by Everitt and Byrne.[14]

The receiver consisted of two stages of high frequency transformer coupled screen grid valves for amplifying the signals, followed by an anode bend triode rectifier and a D. C. low frequency one stage amplifier. We dispensed with capacities and it was possible to locate the transmitter and the receiver side by side in the same room.

In place of an aerial for the receiver we used a small coil coupled to the tank circuit of the transmitter. It should be noted that in our case the same aerial served both as a transmitting and as a receiving aerial.

The output of the low frequency amplifier was fed on to the vertically deflecting plates of a cathode ray oscillograph, the horizontally deflecting plates of which were connected to a linear thyratron time base.

The reflected echoes appeared along the time base at different distances from the ground peak depending upon their temporal retardations. The distance between the ground and the reflected echo in question and the total span were measured by means of a divider and a scale. The ratio of these lengths with the knowledge of the time taken by the electrons to sweep the full span enabled us to calculate the virtual heights.

An automatic recording arrangement was also tried. It consisted of a cylinder rotating about a horizontal axis making one complete revolution in two hours. A sensitive piece of paper was wrapped around the cylinder and an image of the desired portion of the pattern was brought to a focus on it by means of a camera arrangement. As the cylinder rotated the lines due to various peaks were traced on the paper.

Results

This paper gives a record of observations taken between the period, 3rd December, 1934, to 15th February, 1935. The work was carried out on a wavelength of 75 m. at Allahabad [Long. 81° 55′ 0″. E., Lat. 25° 25′ 55″ N.]. Echoes from F-layer were generally seen, but occasionally echoes from the E-region were also visible.

Diurnal variation in virtual height

Morning and pre-dawn period.—In the morning the peaks did not appear till about 15-20 mins. before ground sunrise due to insufficient density of electrons. First a weak echo used to appear at a virtual height of about 450—500 km. Then there used to be a rapid fall in height. At about 10 mins. after the appearance of this extraordinary component, the ordinary or the longer delay component used to appear at a virtual height of 400—450 km. The temporal separation between the two echoes decreased very rapidly. In about 10 mins, the two components were superimposed at a height of about 300 km. After this the height decreased at a slower speed. The behaviour is quite expected for at the height at which peaks used to appear sunrise takes place earlier than that at the ground. Hence ionisation in that region begins to build up before ground sunrise and soon reaches

a value sufficient to reflect the 75 metre wave used for the experiment. As the ionization increases in the lower regions, the peaks are reflected from a lower height. The ordinary component requires greater ionisation, as shown by the magneto-ionic theory, and therefore appeared at about 10 mins after the appearance of the extraordinary component. After about an hour from the first appearance, the virtual height used to become almost constant with slight fluctuations. There was, however, one anomaly that on certain occasions a sudden rise in virtual height by about 30 km. was observed even during the period when the height was decreasing rapidly.

Noon.—At this time the peaks were generally not observable and whenever they appeared they were very feeble. It appears that the frequency used was only a little above that required to penetrate the E-region which had now its maximum ion-content and hence the absorption during the double journey through this region was very marked. Thus the peaks either did not appear or were very feeble. The virtual height during this period used to be about 240 km.

Evening—The reflections from the F-region were usually again visible in the late afternoon, when the absorption in the lower regions became less. Generally the virtual height remained constant at about 220—250 km with slight fluctuations during this period till about an hour after sunset. When the ionization in the lower F-region had grown sufficiently weak to reflect the echoes, the height gradually increased and two echoes due to magneto-ionic splitting could be seen. The separation between the doublet components went on increasing and the virtual height became greater and greater and after about 3 hours from sunset first the ordinary component disappeared at a height of about 400 km. due to electron limitation followed by the extraordinary component which generally disappeared at a height of 400 to 450 km. at about 10 mins. after the disappearance of the ordinary component. One thing, however, should be noted that we have observed one behaviour, which is more or less common, that at about 19·00 (I. S. T.) the virtual height of the layer gradually fell down by about 100 km. and the two components again combined. The virtual height remained almost constant at about 225—250 km. for a period varying from ½ to 1 hour. Then again the splitting used to occur and peaks disappeared in the same order at a virtual height of about 450 km. occasionally rising to 500 km. This shows some sort of evening concentration as observed by others, and may be due to an increase in the group velocity owing to the disappearance of the lower absorbing D-layer and reduction of ionization in the E-layer.

Diurnal variation of the amplitude of the peaks

In the pre-dawn period when the peak appears at first, it is very weak due to insufficient density of electrons and consequently a less percentage of power is reflected. As the ionization in the upper region builds up, more and more power is reflected and the echo gains in strength. Then multiple echoes appear and peaks sometimes even shoot beyond the oscillograph screen. But then again as ionization in the regions below F builds up, the amplitude as seen on the oscillograph screen grows weaker and weaker obviously due to absorption in these regions. This absorption goes on increasing with increase of ionization in the E-region where it is maximum. at noon. At this time all the power is absorbed and no echoes are usually seen. This seems to be due to insufficient power of the transmitter.

In the after noon the absorption in the lower regions is less so that peaks are seen though feeble. This state of affairs continues till a little before sunset. About half an hour after sunset violent fluctuations of intensity are observed. Apart from that, general intensity of peaks begins to increase after sunset due to continual removal of ionization and its attendant absorption in the lower region. However when the ionization in the F-region has grown sufficiently less the amplitude of the peaks begins to fall along with an increase in virtual heights. As the density of electrons goes on decreasing the power reflected lessens, so much so, that only a speck is seen on the oscillograph screen. Then the speck appears intermittently before finally disappearing.

Effect of Lunar Eclipse

In order to study the influence of lunar eclipse on the ionosphere measurements of the virtual height of F-layer were carried out during the eclipse of January 19, 1935, and on days previous and subsequent to it.

From 15'37 to 18'20 the virtual height of the F-layer was 250—270 km. and during the last one hour the intensity of the peaks as seen on the oscillograph screen was very strong, there being several multiple echoes from time to time, some of which were shooting beyond the screen. At 18'23 a sudden magneto-ionic double splitting was observed and the equivalent height of the layer began to increase till at 19'00 the two components were reflected from a virtual height of 426 and 457 km. respectively. In this period the intensity was generally weak and the echoes were almost disappearing. But at this time the virtual height and the time lag between the two components began to decrease while the echo gained in strength. It appeared that it was the beginning of evening concentration. However

this decrease continued only for 15 minutes, when again a rise began to take place and a virtual height of 410 km. was recorded at 19·30.

JANUARY 19th 1935.

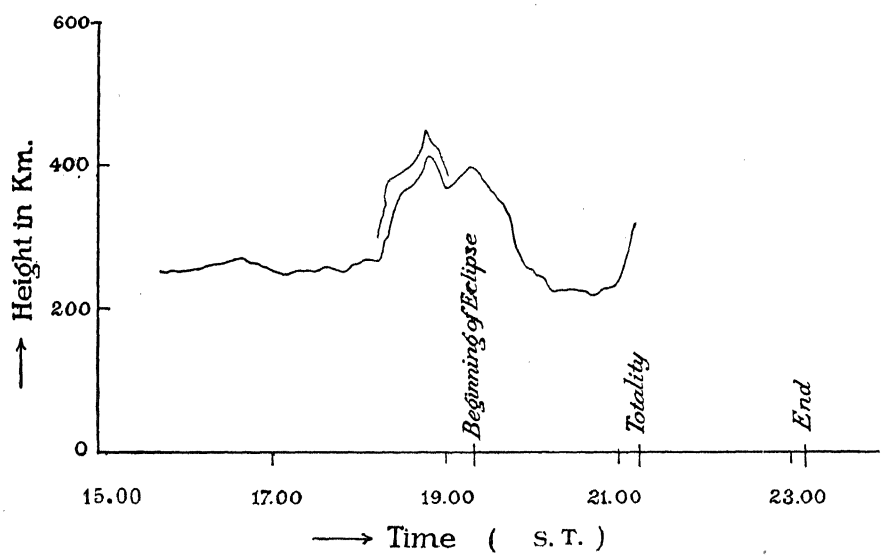

Till the beginning of the eclipse at 19·23 the behaviour was more or less normal as described above, but at 19·30 the virtual height began to decrease first slowly and then rather rapidly reaching 225 km. at 20·30 when more than half of the moon had entered the earth's shadow. During this height-decrease period of an hour the echoes gained in strength and number, several times a number of them shot beyond the screen. The virtual height remained almost constant at 225 km. till 21·17 when the moon's disc was completely invisible. For the first 30 minutes of this period of height-constancy the echoes were very weak and sometimes even appearing and disappearing possibly due to increased ionization in E-region causing heavy absorption. However, from 21·01 to 21·05 as many as eight multiple echoes were observed several of which were overshooting, but near about the time of the totality of the eclipse the echo strength grew very weak and virtual height increased at a rapid pace reaching 340 km. at 21·35 when the echo finally disappeared. The observations were continued till 23·30 but no echoes could be seen.

Superficially it may appear that it was only evening concentration phenomenon which might have occurred at a later time on this day, but the facts that this phenomenon used to occur generally between 19·00 and 20·00 whereas this day the height decrease took place after 20·00, that

during evening concentration the decrease used to be about 100 km. but this day it was about 200 km., and that the decrease in virtual height was almost in phase with the eclipse, go to show that it was not merely a chance coincidence but that the ionization had increased during the period of the eclipse, especially in view of the facts that the magnetic character for the day is reported to be quiet and that there was no thunderstorm in the locality. The variation of echo strength can also be explained on the ionization-increase theory. In spite of all this a definite statement can be made only when a large number of data are available.

It will be interesting to study the condition of the ionosphere during the next lunar eclipse of January 8, 1936, which will be under similar conditions as regards the season. It will be more useful if the maximum ion-content and the virtual height of both the layers are studied simultaneously during the period.

A number of typical graphs and their description is given below :—

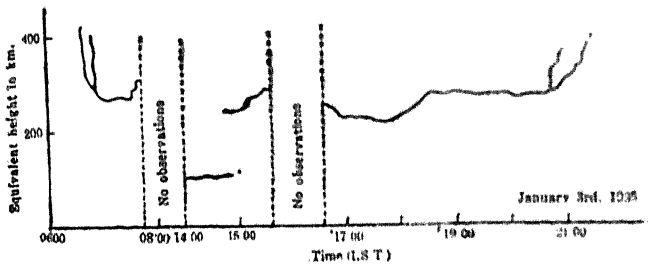

Fig. 1

Fig. 1.—In the morning the ordinary and extraordinary components are seen to appear with a difference of eleven minutes. The virtual height is decreasing very rapidly and the two components join. The increase in virtual height at 7'41 is rather unexpected. The observations were again begun at 1400 when reflections from E-layer at a virtual height of 120 km. were received. Reflections from this layer continued till 14'40, when echoes from both the layers E and F were received simultaneously for 15 minutes. After this echoes from F only appeared and the height was seen to increase. The observations were discontinued at 15'40 and restarted at 16'40. The virtual height was almost constant for about an hour after which it increased by about 60 km. within a period of 40 minutes. It then again remained constant at about 280 km. for a period

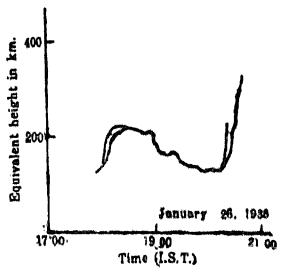

Fig. 2

of about $2\frac{1}{2}$ hours. Then the magneto ionic double splitting occurred and first the ordinary component disappeared at a height of 390 km. and then the extraordinary at 420 km.

Fig. 2.—This graph shows typically the phenomenon of evening concentration. At 1800 (I. S. T.) the double splitting occurred and the virtual height rose by 100 km. but then the doublet components joined and decrease in height by 100 km. was noted. At 20·20 the magneto ionic double splitting again occurred and the two components disappeared with a difference of 15 minutes.

Fig. 3.—This graph shows typical erratic behaviours during the incidence of a magnetic storm. On such occasions reflections from E-region are received almost invariably. The nature of the graph shows a fine structure for E-layer having three strata at virtual heights of 95, 105 and 120 km. We also noticed complete cessation of echoes on such days. These days were also marked by reflections from a virtual height of about 600—650 km., however, echoes from such heights were received on other days also. These appear to be reflected from some other higher G-layer existing at such heights. It will not be out of place to mention that sometimes, though very rarely, we received echoes from virtual heights of about 1000 km. which may be from some other layer existing at such heights.

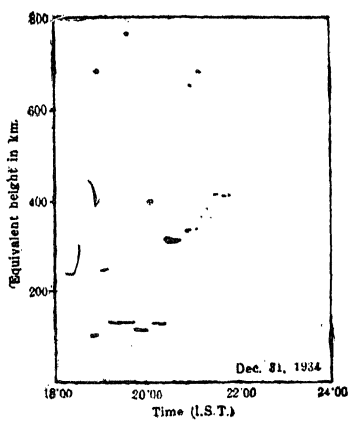

Fig. 3

Fig. 4(a) Plate I shows four multiple echoes as seen on the oscillograph screen. Note that the amplitude of the first and third is greater than that of the second, *i.e.*, odd order echoes are stronger than even ones showing the effect of some sort of interference between the two components.

Fig. 4(b) Plate I shows magneto-ionic double refraction effects. Two orders of reflections of the two components are seen. Note that ordinary component is stronger than the extraordinary in both cases. No ground ray is seen in either figure.

Fig. 5 Plate I gives an automatic record of the virtual height taken on February 9, 1935. In the beginning and occasionally two multiple reflections are seen but continuously only single echo from F is recorded.

My grateful thanks are due to Prof. M. N. Saha, F.R.S, and Mr. G. R. Toshniwal for their keen interest in the work and the facilities

they gave me. My hearty thanks are due also to Mr. B. D. Pant for his useful suggestions.

Note added in proof correction (February 10, 1936). Influence of the moon on the ionosphere has also been found by Stetson, who finds electronic tides[15] in the ionosphere caused by the moon and who observed improved radio signal strength[16] as the moon entered the earth's shadow during a lunar eclipse. Dr. Datta, at Benares, also found some influence of lunar eclipse on the ionosphere as reported by him in the *Leader*, January 14th, 1936.

As to the existence of ionized layers above F_2-region Mimno[17] reports G and H layers at 600 km. and 1100—1800 km. respectively. Kirby and Judson[18] also report to have observed a layer above F_2 which they tentatively call G-layer. It may be added that during our[19] present work also we have found evidence of the existence of two layers at the virtual heights of 600 km. and 900 km. respectively.

[Figures 1, 4 (a) and 4 (b) have been reproduced by the kind courtesy of The National Institute of Sciences of India.]

References

1. A. E. Kennelly, *Elec. World Eng.*, **39**, 473, 1902.
2. O. Heaviside, *Ency. Brit.* X Edition, **33**, 215, 1902.
3. Balfour Stewart, *Ency. Brit.* IX Edition, **16**, 181, 1878.
4. W. H. Eccless, *Pro. Roy. Soc.*, A **87**, 79, 1912.
5. J. Larmor, *Phil. Mag.*, **48**, 1025, 1924.
6. E. V. Appleton, *Jour. Inst. Elec. Eng.*, **71**, 642, 1932.
7. D. L. Hartree, *Pro. Camb. Phil. Soc.*, **27**, 143, 1930-31.
8. Mary Taylor, *Pro. Phy. Soc.*, **45**, 245, 1933.
9. S. Goldestein, *Pro. Roy. Soc.*, A **121**, 260, 1928.
10. Appleton and Barnett, *Pro. Roy. Soc.*, A **109**, 621, 1925; *Nature*, **115**, 1925.
11. Breit and Tuve, *Nature*, **116**, 357, 1925; *Phy. Rev.*, **28**, 554, 1926.
12. E. V. Appleton, *Nature*, **120**, 330, 1927.
13. Schaffer and Goodall, *Nature*, **131**, 804, 1933.
    E. V. Appleton, *Nature*, **131**, 872, 1933.
    Ratcliffe and White, *Nature*, **131**, 873, 1933.
14. Everitte and Byrne, *Pro. Inst. Rad. Eng.*, **17**, 1840, 1929.
15. Stetson, *Sc. News Letter*, **27**, 115, 1935.
16. Stetson, *Science*, Aug. 2, 10, 1935.
17. Mimno, *Nature*, **134**, 63, 1934.
18. Kirby and Judson, *Proc. I. R. E.*, **23**, 733, 1935.
19. Toshniwal, Pant, Bajpai and Verma, *Proc. Nat. Acad. Sc. India*, (in Press).

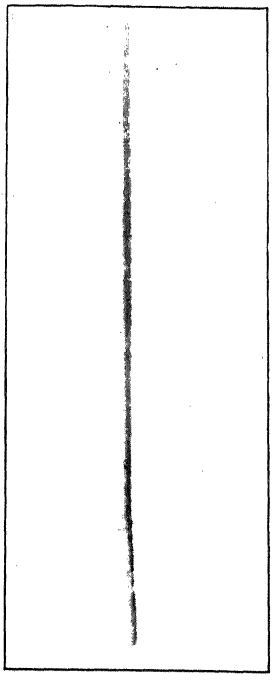

Fig. 4 (*b*)

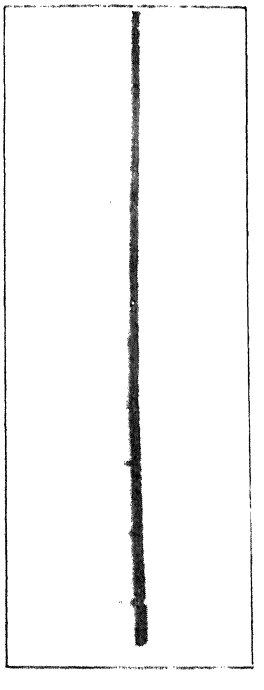

Fig. 4 (*a*)

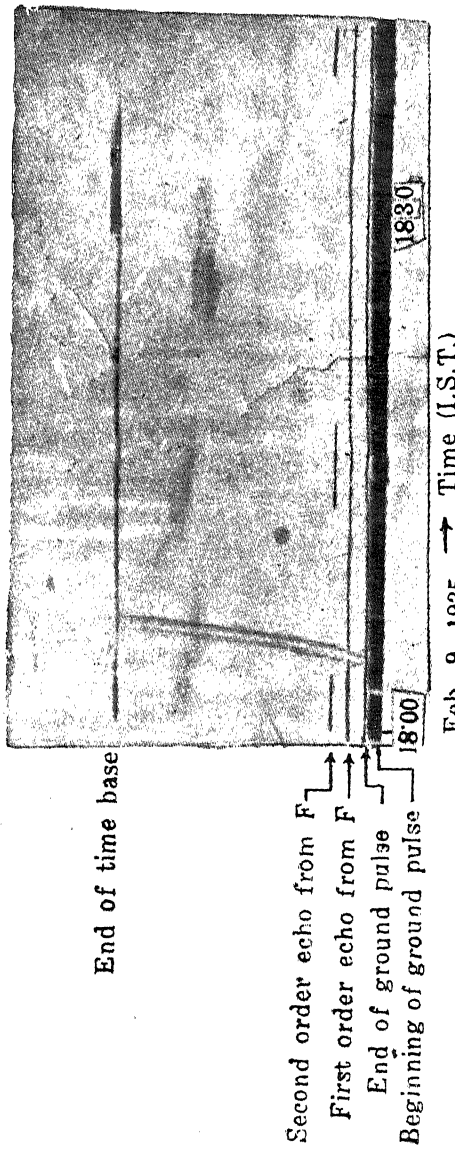

Fig. 5

A NOTE ON SIR SHAH MUHAMMAD SULAIMAN'S NEW THEORY OF RELATIVITY

By S. C. Damle

Mathematics Department, University of Allahabad

Communicated by Prof. A. C. Banerji

Received October 23, 1935

The object of the present note is to point out some inaccuracies in taking approximations that I have observed while going through Chapter I, Section V of Sir Shah Muhammad Sulaiman's Theory.

Modifications that follow from the correction of some of these inaccuracies have changed the values of (1) the deflection of light according to the calculations of Sir S. M. Sulaiman (Chapter II, Section II, equation (14·6)) and (2) the advance of the perihelion of Mercury obtained by Sir S. M. Sulaiman (4, (2) Section XII Chapter I).

It is not contended that the values obtained here are in any way nearer the experimental values.

The order of the term $\frac{1}{D}\frac{rd\theta}{dt}$ is 10^{-4} in C. G. S. units. The values of the constants quoted here are for Mercury and have been obtained by Newtonian Mechanics and stated in C. G. S. units.

$$h=2{\cdot}76\times10^{19}, \qquad \mu=6{\cdot}67\times1{\cdot}98\times10^{25}$$

$$\frac{d\theta}{dt}=8{\cdot}25\times10^{-7}, \qquad r\frac{d\theta}{dt}=4{\cdot}77\times10^{6}$$

$$\frac{dr}{dt}=1{\cdot}03\times10^{6}\sin\theta, \quad r=5{\cdot}78\times10^{12}$$

$$l=5{\cdot}41\times10^{12}, \qquad D=3\times10^{10}$$

l is the semi-latus rectum. Wherever the value of the particular quantity has been changing the average value or the mean of the maximum and minimum values has been quoted.

In equation 5·61 of Chapter I we find that the term $\frac{3}{D^2}\left(r\frac{d\theta}{dt}\right)^2$ has been retained. This makes it imperative to retain terms up to the order of 10^{-8} throughout. But in the equation

$$\frac{d}{dt}(r^2\dot{\theta}) = \frac{\mu}{D}\frac{d\theta}{dt}\left[1-\frac{3}{D}\left\{\frac{dr}{dt}-\frac{1}{D}\left(r\frac{d\theta}{dt}\right)^2\right\}\right]$$

the term $\frac{3}{D}\frac{dr}{dt}$ has been neglected. The term $\frac{3}{D}\frac{dr}{dt}$ itself is only of the order of $10^{-4}\sin\theta$ and contributes nothing to the integrated equation only when the limits of integration are 0 and 2π and the values for $\frac{dr}{dt}$ and $\frac{d\theta}{dt}$ are obtained from the equations of motion on Newtonian principles.

It should moreover be noticed that this term cannot be neglected on the ground that the orbit is nearly circular, because in the second equation, *i.e.*, in the equation 5·7 of Section V, Chapter I the terms containing $\frac{dr}{dt}$ and $\frac{d^2r}{dt^2}$ have been retained. The value of e has been considered in Section XII of Chapter I. Also the term $\frac{3}{D}\cdot\frac{dr}{dt}$ cannot be neglected on the ground that it has different signs for the two halves of the orbit and will therefore contribute nothing to the whole effect in one complete revolution; as we find that its retention considerably modifies the result. In fact, it will be shown later on that the retention of this term changes the value of the rotation of the perihelion of Mercury to $\frac{-\pi\mu^2}{D^2h^2}$, the value obtained by Sir S. M. Sulaiman on page 24, Chapter I, being $\frac{6\pi\mu^2}{D^2\mu^2}$.

Moreover in equation 5·6, cos α which is equal to $1-\frac{1}{2}\cdot\frac{1}{D^2}\left(r\frac{d\theta}{dt}\right)^2+\ldots$. has been put equal to unity neglecting the terms after and including $\frac{1}{2}\cdot\frac{1}{D^2}\left(r\frac{d\theta}{dt}\right)^2$, while the term $\frac{3}{D^2}\left(\frac{rd\theta}{dt}\right)^2$ has been retained in the other factor. Writing however $\cos\alpha = 1-\frac{1}{2}\cdot\frac{1}{D^2}\left(\frac{rd\theta}{dt}\right)^2$, equation (5·7) becomes

$$\frac{d^2r}{dt^2}-r\left(\frac{d\theta}{dt}\right)^2 = -\frac{\mu}{r^2}-\frac{5}{2}\cdot\frac{\mu}{D^2}\cdot\frac{h^2(1+k\theta)^2}{r^4}+\frac{3\mu}{D}\cdot\frac{1}{r^2}\cdot\frac{dr}{dt}$$

and again 5·9 becomes

$$\frac{d^2u}{d\theta^2}-\frac{2k}{1+k\theta}\cdot\frac{du}{d\theta}+u = \frac{\mu}{h^2(1+\theta k)^2}+\frac{5\mu u^2}{2D^2};$$

so that necessary modifications have to be made throughout, due to this change from 3 to 5/2 in the coefficient of the term $\frac{\mu u^2}{D^2}$.

As a consequence of this Einstein's value 1″·745 for the deflection of light cannot be obtained by substituting $h=\infty$. Also the value of the deflection of light by Sir S. M. Sulaiman's Theory would be at least $\frac{7}{2}\frac{\mu u^2}{c^2}$ instead of $\frac{4\mu u^2}{c^2}$ and the angle of deflection would be at least $\frac{7}{6}$ times the value obtained by Einstein, *i.e.*, at least $\frac{7}{3}$ times Newton's value

$$=\frac{7}{3}\times 0''\cdot 87=2''\cdot 03 \text{ instead of } 2''\cdot 32.$$

Similarly all formulæ in which the term $\frac{3\mu u^2}{D^2}$ is involved will be modified.

The use of approximate equations obtained on the assumption that the velocities concerned are small in comparison to D is not justified in the case of light. But the above-mentioned modifications have to be introduced even if the use of these approximate equations is taken to be valid.

There is also no justification in neglecting the term $\frac{3}{D^2}\left(\frac{dr}{dt}\right)^2$ in equation (5·61) when $\frac{3}{D^2}\left(\frac{rd\theta}{dt}\right)^2$ has been retained, since both these terms are of the same order except when θ is very small.

The modified differential equations up to the order 10^{-8} of small quantities may also be given here. They are

$$\frac{d}{dt}\left(\frac{r^2 d\theta}{dt}\right)=\frac{\mu}{D}\frac{d\theta}{dt}\left(1-\frac{3}{D}\frac{dr}{dt}\right),$$

and
$$\frac{d^2r}{dt^2}-r\left(\frac{d\theta}{dt}\right)^2=-\frac{\mu}{r^2}\left[1-\frac{3}{D}\frac{dr}{dt}+\frac{5}{2D^2}\left(\frac{rd\theta}{dt}\right)^2+\frac{3}{D^2}\left(\frac{dr}{dt}\right)^2\right]$$

The results in Section XII of Chapter I are however unaffected by considering the term $\frac{3}{D^2}\left(\frac{dr}{dt}\right)^2\left(-\frac{\mu}{r^2}\right)$ in the second of the equations above as the integral taken from 0 to 2π in each case contributes nothing in the result.

But a rather unfortunate result comes out when we consider the term $\frac{-3\mu}{D^2}\frac{d\theta}{dt}\frac{dr}{dt}$ in the first of the modified equations obtained above. The contributions to $\triangle a$ and $\triangle e$ are zero. But when we consider this

term, the total rotation of the perihelion of Mercury in one complete revolution becomes $\frac{\pi\mu^2}{D^2h^2}$. And unless this fact is explained, the theory cannot be supposed to be of much use.

Considering, therefore, the importance of this, the calculation of the term to be added to $\Delta\omega$ as obtained by Sir S. M. Sulaiman is given here in full.

Following the method adopted in Section XII of Chapter I of Sir S. M. Sulaiman's Theory, for a small transverse force

$$\delta\omega = f\,\delta t.\frac{\sin\theta}{e}\sqrt{\frac{a(1-e^2)}{\mu}}\left(\frac{2+e\cos\theta}{1+e\cos\theta}\right)$$

$$\text{Substituting } f = \frac{-3\mu}{D^2r}\cdot\frac{d\theta}{dt}\cdot\frac{dr}{dt}$$

and calling the term to be added $\Delta\omega_4$, we have

$$\delta\omega_4 = \frac{-3\mu}{D^2}\cdot\frac{1}{r}\cdot\frac{d\theta}{dt}\cdot\frac{dr}{dt}\,\delta t.\frac{\sin\theta}{e}\sqrt{\frac{a(1-e^2)}{\mu}}\left(\frac{2+e\cos\theta}{1+e\cos\theta}\right)$$

and for one complete revolution

$$\Delta\omega_4 = \int_{\theta=0}^{\theta=2\pi}\frac{-3\mu}{D^2}\cdot\frac{1}{r}\cdot\frac{d\theta}{dt}\cdot\frac{dr}{dt}\,\delta t.\frac{\sin\theta}{e}\sqrt{\frac{a(1-e^2)}{\mu}}\left(\frac{2+e\cos\theta}{1+e\cos\theta}\right)$$

$$= \frac{-3\mu}{D^2}\cdot-\frac{1}{e}\sqrt{\frac{a(1-e^2)}{\mu}}\int_0^{2\pi}\frac{1}{r}\frac{dr}{dt}\sin\theta\left(\frac{2+e\cos\theta}{1+e\cos\theta}\right)d\theta$$

Now $\frac{l}{r}=1+e\cos\theta,\ l=\frac{h^2}{\mu},\ r^2\dot{\theta}=h$

$$\therefore \frac{dr}{dt}=\frac{he\sin\theta}{l}=\frac{\mu e\sin\theta}{h}$$

and $r(1+e\cos\theta)=l=\frac{h^2}{\mu}$

$$\therefore\ \Delta\omega_4 = \frac{-3\mu}{D^2}\cdot\frac{1}{e}\cdot\sqrt{\frac{a(1-e^2)}{\mu}}\int_0^{2\pi}\frac{\mu}{h^2}\cdot\frac{\mu e\sin\theta}{h}\sin\theta(2+e\cos\theta)d\theta$$

$$= \frac{-3\mu}{D^2}\cdot\frac{1}{e}\sqrt{\frac{a(1-e^2)}{\mu}}\cdot\frac{\mu^2 e}{h^3}\int_0^{2\pi}(2+e\cos\theta)\sin^2\theta\,d\theta$$

$$= \frac{-3\mu}{D^2}\cdot\frac{\mu^2}{h^3}\sqrt{\frac{a(1-e^2)}{\mu}}\left[\int_0^{2\pi}(2\sin^2\theta)\,d\theta + e\int_0^{2\pi}\sin^2\theta\cos\theta\,d\theta\right]$$

$$= \frac{-3\mu}{D^2}\cdot\frac{\mu^2}{h^3}\sqrt{\frac{a(1-e^2)}{\mu}}\int_0^{2\pi}(1-\cos 2\theta)\,d\theta$$

$$= \frac{-3\mu^3}{D^2h^3}\sqrt{\frac{a(1-e^2)}{\mu}}\cdot 2\pi$$

$$= \frac{-6\pi\mu^3}{D^2h^3}\sqrt{\frac{h^2}{\mu.\mu}} = \frac{-6\pi\mu^2}{D^2h^2}$$

And when this is added to $\frac{5\pi\mu^2}{D^2h^2}$ we obtain $\frac{-\pi\mu^2}{D^2h^2}$.

My best thanks are due to Prof. A. C. Banerji under whose guidance the work was carried on and to Sir S. M. Sulaiman as it was a preliminary discussion with him that aroused my interest in the theory.

Reply of S. M. Sulaiman to the note of S. C. Damle

Received October 30, 1935

I am thankful to Mr. Damle for examining my equations of motion in a truly scientific spirit and I fully agree with him that for the sake of greater accuracy more terms should be retained in them, but I regret that I do not agree with all his conclusions. His objections are five in number.

I. The term $\frac{3}{D}\frac{dr}{dt}$ in (5·41) should not have been neglected.

1. As pointed out in Chapter VIII Sec. VI the equations of motion of Chapter I were really true for nearly circular orbits, *e. g.*, those of Venus, Earth and bigger planets. They do not hold to the same degree of approximation in the case of Mercury's elongated orbit, much less so for comets. For these a different set of equations have been obtained there.

2. Even for Mercury, $\frac{dr}{dt} = \frac{e\mu}{hD}\cdot\sin\theta$ is of the order $\frac{1\cdot6}{5}10^{-4}\sin\theta$ and varies from 0 to 1/5th of $\frac{rd\theta}{dt}$, and also it has different signs for the two halves of the orbit. Again, the effect of the correction for heavenly bodies is to be seen for a large number of complete revolutions and not at any single position in the orbit. For one complete orbit the net effect of $\frac{dr}{dt}$ should be very small. It was in this view that as a rough

approximation $\frac{dr}{dt}$ was neglected, which was legitimate for the purpose of integration as $h^2(1+k\theta)^2$ will be replaced by $h^2(1+k\theta+2k^2.e\cos\theta)^2$, as the next smaller term would make no practical difference to (5·7).

3. If $\frac{dr}{dt}$ were retained, the integration of the equation would become impossible.

4. If $\frac{dr}{dt}$ is retained then the orbit would cease to be nearly circular, and the angle ϕ between the tangent and the radius vector would cease to be nearly $\frac{\pi}{2}$, then for sin α also $\frac{v^1.\sin\phi}{\sqrt{1+2\frac{v^1}{D}\cos\phi+\frac{v^2}{D^2}}} = \frac{r}{D}\frac{d\theta}{dt}\left(1+\frac{1}{D}\frac{dr}{dt}\right)$ should be substituted, where v^1 is the tangential velocity.

II. Cos α should not be put equal to unity but $= 1-\frac{1}{2}\frac{1}{D^2}\left(r\frac{d\theta}{dt}\right)^2$

1. It has been known to Mr. A. N. Chatterji and myself that for a little greater accuracy $\cos\alpha = 1/\sqrt{1+\frac{1}{D^2}\left(\frac{rd\theta}{dt}\right)^2}$ for a nearly circular orbit, which would reduce the value of the advance of perihelion. (See Chapter VIII. Also Report dated August 17, 1935, in *Science and Culture*, Vol. I, No. 5, Oct. 1935, p. 289 "He has also suggested that the advance of the perihelion of Mercury should be less than what was calculated by Newcomb.")

2. The reason why this greater accuracy was not introduced was that the consideration of the question whether the magnitude of the force along the resultant is not also changed had been postponed. (See Chapter VIII.) If the magnitude also changes, then for a nearly circular orbit it is increased to $\sqrt{1+\frac{v^2}{D^2}}$ and when multiplied by $\sqrt{1-\frac{v^2}{D^2}}$ the equation (5·6) remains unaltered. But I admit that so long as the magnitude was taken to be unaltered, the correction should have been introduced.

3. For an oblique orbit $\cos\alpha = \frac{1+\frac{v^1}{D}\cos\phi}{\sqrt{1+2\frac{v^1}{D}\cos\phi+\frac{v_1^2}{D^2}}}$,

$$= 1-\frac{1}{D^2}\left(\frac{dr}{dt}\right)^2-\frac{1}{2D^2}\left(\frac{rd\theta}{dt}\right)^2.$$

III. (*a*) Mr. Damle's correction for cos α would reduce the value of the advance of the perihelion to 5/6. This would give the value of the advance as 35″·75.

Now there is a very great uncertainty as to the value of the advance and one need not be frightened by a diminution. The observed value is not reliable. So much so that von Gleich has actually asserted that the supposed excess of motion of the

perihelion of Mercury does not exist and the Newtonian theory of gravitation needs no correction by relativity. (*Astronomische Nachrichen*, 241, 105—112, 1931.) I am quite aware that if the equation obtained for a circular orbit is maintained for Mercury, then a still higher approximation will more considerably reduce the value.

(*b*) The deflection of light is also reduced to 7/4 instead of 8/3 times Newton's value, and equals 2″·03.

But the value given on page 26 was the minimum value of the deflection =2″·32. The reduced maximum value would be $\frac{1}{2}(2+\frac{2}{3}\times 4) = 8/3$ times $= 2''\cdot 32$. These values in fact tally better with Freundliche's value 2″·24.

IV. The approximate equations may not hold for light.

I have myself pointed out that the equations are true only when the tangential velocity is small. The deflection of light was calculated only on the assumption that they may hold approximately for light also. A new set of equations have been obtained for light in Chapter VIII. I have also adopted a different method of definite integrals for calculating the deflection of light.

V. $\frac{3}{D^2}\left(\frac{dr}{dt}\right)^2$ should be retained in (6·61).

But Mr. Damle himself admits that this term leaves the results in Section XII of Chapter I altogether unaffected, when the integration is taken from 0 to 2π. We are concerned only with complete revolutions, and the retention of this extra term yields no value whatsoever for a complete revolution. The proposed higher approximation is, therefore, of no utility.

In conclusion I may add that if the equations in Chapter I, which were obtained for a nearly circular orbit where $\phi = \frac{\pi}{2}$ nearly and $\left(\frac{v'}{D}\right)$ is very small, were applied to an elongated orbit, then the advance of the perihelion cannot only be reduced considerably, but even changed to a recession $= -\frac{\pi\mu^2}{D^2h^2}$. The fact is that the corrections to be introduced in Newtonian Mechanics are so numerous that until a result is obtained after taking all of them into account the values cannot be exactly known.

Postscript (*Received November 2, 1935*) 1. The last portion added to Mr. Damle's note had not been seen by me when I submitted my reply, and I myself had independently pointed out in the conclusion that if the equations were applied to the elongated orbit there would be a negative residual $= -\frac{\pi\mu^2}{D^2h^2}$. Not only is the dynamics of a changing force moving with finite velocity complex, but as shown in Chapter VIII numerous corrections have also to be introduced, and until they all are taken into account, the exact values cannot be certain.

2. If the more accurate value for sin α be substituted, the net residual is $+\frac{\pi\mu^2}{h^2D^2}$ and not $-\frac{\pi\mu^2}{h^2D^2}$. The effect of the extra term $-\frac{3}{D}\frac{dr}{dt}$ on the major axis and the eccentricity is nil. If the resistance of the medium were to act so as to reduce the

whole force along the transversal, the effect of the extra term on the advance of perihelion also can be negligible, leaving a net value $35''{\cdot}75$ nearly. Even without the resistance, the same result would follow if the second method given in Chapter VIII, Section II, p. 152 be adopted.

3. The advance of the perihelion is not a sure test as it can be easily explained by a slight change in Newton's law. Newton took h as finite even for light, but D infinite; while according to Einstein D cannot exceed c, but h is infinite for light. An empirical law of gravitation, intermediate between the two, where both D and h remain finite, h having the Newtonian value and D $= c$ is $-\frac{\mu}{r^2} - \frac{3\mu h^2}{D^2} \cdot \frac{1}{r^4}$. It gives all the required results and avoids all the difficulties.

THE QUANTUM STATISTICS AND THE INTERNAL CONSTITUTION OF THE PLANETS

By D. S. KOTHARI

PHYSICS DEPARTMENT, DELHI UNIVERSITY

AND

R. C. MAJUMDAR

PHYSICS DEPARTMENT, PUNJAB UNIVERSITY, LAHORE

Received December 12, 1935

This paper gives an account of work which has led to a relation between the radii and masses of the planets. This is arrived at by combining with the usual theory of the white dwarf stars, the theory of ionisation in *degenerate* matter (pressure ionisation). The agreement between theory and observation is reasonably good.

Is it possible from purely theoretical considerations to deduce any relation connecting the radius and mass of a planet? The present paper gives a preliminary answer to this question. The usual theory of the "white dwarf stars" is carried a stage further, and it is then found to lead to a relation between the masses and radii of the planets which agrees reasonably well with observation. The investigation owes its origin to an inspiring suggestion of Prof. H. N. Russell[1] that "somewhere between stellar and planetary masses there must be a maximum radius for a cold body. This can be estimated at about 1/10th solar radius, a value about equal to the diameter of Jupiter."

The first application of "new quantum statistics" to Astrophysics was made by Fowler[2] in a very suggestive paper dealing with the internal constitution of the white dwarf stars. This was later amplified by other workers and the recent researches of Milne,[3] which apply quantum statistics in discussing the structure of the stars in general, have been of far-reaching consequence and wide application.

So far as the white dwarf stars are concerned, the application of Fermi-Dirac statistics in accounting for their internal structure is now well-established. A white dwarf possesses much less luminosity than an ordinary star of the same mass. About half-a-dozen stars are definitely known to belong to this class—the best known example is that of the companion of Sirius which has nearly the same mass as the Sun, but has only 1/380th of its luminosity. It is believed that a white dwarf is a fairly common object in the sky, but because of its small luminosity, it escapes

observation. Kuiper has recently announced the discovery of many new white dwarfs. The radius of Sirius B as estimated both from its effective temperature (11,300°) and the shift of its spectral lines predicted by the general theory of Relativity is slightly larger than the diameter of the earth. The mean density is therefore very large: it is about 5×10^4 gms/cm.[3] A low luminosity, a high effective temperature and a very large mean density are the general features of white dwarfs.

§1. In preliminary theoretical treatment it is usual to assume the luminosity of a white dwarf to be zero, *i.e.*, to regard it as a 'black-dwarf' —a term originally due to Fowler.[2] This procedure is not as unreasonable as it may appear at first, for, as has been shown elsewhere,[4] the small luminosity of a white dwarf has very little effect on the calculated values for its radius and mean density. If we have a star of mass M and zero luminosity composed of ionised matter degenerate in the sense of Fermi-Dirac statistics, then, as has been shown by several authors, the radius R of the star is connected with its mass by the relation

$$\left.\begin{aligned} R &= \frac{5\,(\omega^0_{\frac{1}{2}})^{\frac{1}{3}}}{2^{\frac{1}{3}}\pi^{\frac{1}{3}}}\,\frac{K}{G\mu^{\frac{1}{3}}}\,\frac{1}{M^{\frac{1}{3}}} \\ &= 2{\cdot}79\times10^9\,\frac{1}{\mu^{\frac{1}{3}}}\left(\frac{\odot}{M}\right)^{\frac{1}{3}} \end{aligned}\right\} \quad . \quad . \quad . \quad . \quad (1)$$

where $\odot$ is the mass of the Sun and μ the mean molecular weight of *free-electrons* present. The above formula is quoted from Milne's[5] paper with a slight change* in notation in that the degeneracy constant K is his $K/\mu^{5/3}$ and μ here is his $\mu\, m_H$, (m_H = mass of hydrogen atom). If ρ denotes the density then $\rho/\mu m_H$ gives the number of free electrons per unit volume. Thus μ is a measure of the degree of ionisation of the stellar material.

There is a limitation of equation (1) above that may be noted. It holds so long as the *relativitistic* correction is negligible and this is so far as M is less than about $\odot$†. From (1) we can write for ρ_m the mean density of the star

$$\left.\begin{aligned} \rho_m &= \frac{96\pi}{125\,\omega^0_{\frac{1}{2}}}\left(\frac{G}{K}\right)^3\mu^5M^2 \\ &= 2{\cdot}14\times10^4\,\mu^5\left(\frac{M}{\odot}\right)^2 gms/cm.^3 \end{aligned}\right\} \quad . \quad . \quad . \quad . \quad (2)$$

* This is done to show explicitly the dependence on μ. See also Kothari, *M. N.*, **98**, 70, 1932. The pressure of degenerate gas $= \frac{8\pi h^2}{15m}\left(\frac{3\rho}{8\pi\mu m_H}\right)^{\frac{5}{3}} = \frac{K\rho^{\frac{5}{3}}}{\mu^{\frac{5}{3}}}$.

† See second footnote on p. 81, *M. N.*, **98**, 1932.

The theory[5] gives between ρ_m (mean density) and ρ_c (central density) the relation

$$\rho_m/\rho_c = 3\,\omega^{\circ}_{\frac{3}{2}}/(\sigma_{\frac{3}{2}})^{\frac{3}{2}} = 1/5{\cdot}99 \quad . \quad . \quad . \quad . \quad . \quad (3)$$

In the case of the white dwarf Sirius B for which $M \sim 0{\cdot}85\odot$, relation (2) predicts a density of $5{\cdot}0 \times 10^5$ gms/cm.^{3} *provided we take* $\mu = 2$. The observed density is about 1/10th of this value. No doubt in the above formula we assumed the luminosity to be zero, but as already remarked, even if we took account of the luminosity, the calculated value of ρ_m would not be appreciably modified.* However, we have as yet given no reason why μ is taken equal to 2 and not given any other value. The value of $\mu = 2$ has the well-known significance that it corresponds to a complete ionisation of the material, assuming of course, that there is no unduly large proportion of hydrogen. For ionised hydrogen μ is obviously unity, whereas for fully ionised atoms of any other element μ is nearly 2 (in the case of iron $\mu = 2{\cdot}15$). It is tempting to assume that in Sirius B stellar matter is fully ionised and contains a good proportion of hydrogen (about 60% by weight). The presence of hydrogen lowers the value of μ to 1·2 and ρ_m then agrees with the observed value. We now ask the question as to what will happen for masses $M \ll \odot$.

The relation (1) shows that if we assume μ to be constant (*i.e.*, independent of M), R will increase as M decreases. But such an inference stands in contradiction to observation, for in the case of planets which are cold bodies of mass much less than the sun (their cores correspond, one may say, to ideal black dwarfs), *a larger mass is associated not with a smaller but with a larger radius.* Perhaps it will seem repugnant to some that we should bring in the planets when discussing the applicability of (1), but as will appear later, we make no unreasonable demand if we require (1) to hold for planetary bodies as well. The planets, however, do not verify our inference which is based on the assumption that μ is independent of M. There is no *a priori* reason for such an assumption and further as it leads to a wrong conclusion, it must be discarded. We, therefore, enquire if theory can tell us, *how* μ *depends on* M.

* For the case of the model white dwarf ($M = \frac{1}{2}\odot$ $L = 10^{31}$ ergs/sec. $L/M = 10^{-2}$ ergs/gm. sec.) considered in *M. N.*, **93**, 70, 1932, ρ_m is found to be $2{\cdot}20 \times 10^5 \left(\frac{\mu}{2{\cdot}1}\right)^5$ gms/cm.^{3} If L be assumed zero then ρ_m will have the value $2{\cdot}25 \times 10^5 \left(\frac{\mu}{2{\cdot}1}\right)^5$ gms./cm.^{3} The effect of the luminosity in this case is to decrease ρ_m by about 2%.

§2. To answer the above question we must investigate as to why cold *degenerate* matter should be ionised at all There are two ways in which matter can be ionised:—

(*a*) *Thermal ionisation.*—This applies to *non-degenerate* matter, *i.e.*, when the density is low and the temperature high enough for the free electrons to behave as a classical perfect gas ($p = nkT$). The degree of ionisation is given by the Saha formula.

(*b*) *Pressure ionisation*[7].—This occurs in *degenerate* matter, *i.e.*, when the free electrons form a degenerate gas. When cold and initially unionised matter is so compressed (*i.e.*, its density increased) that orbits of the outermost electrons of different atoms begin to overlap, then these outermost—or as they are called, 'valence,' 'series' or 'optical'—electrons cannot be regarded as belonging to individual atoms. They are no longer bound to their own atoms (but wander, as if it were, in a 'no-atom's-land') and therefore constitute free electrons. If we continue to compress the material still further, the optical electrons of the already ionised atoms will be knocked off and the process will continue till the material is squeezed to bare nuclei and free electrons. The degree of ionisation in degenerate matter is essentially determined by its density or pressure ($p = K\rho^{\frac{5}{3}}/\mu^{\frac{5}{3}}$), for this reason it is called pressure ionisation.

The distinction between thermal and pressure ionisation may be summarised as follows:—

(*i*) Thermal ionisation occurs in non-degenerate matter: Pressure ionisation in degenerate matter.

(*ii*) If, keeping temperature constant, density be reduced, then the degree of ionisation is increased in thermal and decreased in pressure ionisation.

(*iii*) If, keeping density constant, the temperature be increased, then the degree of ionisation is increased in thermal but remains unaffected in the case of pressure ionisation (unless the increase in temperature be so much that the degeneracy of the electron gas is removed and pressure ionisation passes into thermal ionisation).

We shall now express the condition for pressure ionisation in a quantitative form. Consider matter composed of atoms of atomic weight A and atomic number Z compressed to such an extent that the (average) volume available per atom is less than the volume of $(r+1)$ times ionised atom and more than the volume of the r times ionised atom, *i.e.*,

$$\left[\begin{array}{c}\text{Number of}\\ \text{nuclei per}\\ \text{unit volume}\end{array}\right] \times \left[\begin{array}{c}\text{Volume of}\\ r-1 \text{ times}\\ \text{ionised atom}\end{array}\right] > 1 > \left[\begin{array}{c}\text{Number of}\\ \text{nuclei per}\\ \text{unit volume}\end{array}\right] \times \left[\begin{array}{c}\text{Volume of}\\ r \text{ times}\\ \text{ionised atom}\end{array}\right] \quad (4)$$

Under such conditions the material will be on an average r times ionised, for all levels which the outer r electrons can occupy, because of the closeness of packing, have been obliterated. The above is a very naive picture of a really complicated phenomenon. The problem we are discussing is essentially the same as met with in the electron theory of metals. Recently several workers and notably Slater[6] have considered this question of free electrons in metals on the basis of new quantum mechanics (the details have been worked out chiefly in the case of Lithium and Sodium). However, their discussion is too advanced and complicated to be of profit in a preliminary investigation of the astrophysical problem dealt with in this paper. For the time being we must fall back on condition (4) to give us the necessary information about the degree of ionisation in degenerate stellar matter. As has been shown elsewhere[7] this condition can be expressed in several equivalent forms. A form useful in the present case is obtained as follows.[8] Let an r times ionised atom have a series electron which describes a non-penetrating orbit under an effective nuclear charge Z_{eff}. The radius of the orbit* will approximately be a_H/Z_{eff}, where a_H is the radius of the first hydrogen orbit $\left(a_H = \frac{h^2}{4\pi^2 me^2}\right)$, and the $(r+1)$th ionisation potential—call it ψ_{r+1}—will be $\frac{1}{2}\frac{e^2 Z_{eff}^2}{a_H}$. The atomic volume of the r times ionised atom can be taken to be that of a sphere of radius $(\kappa a_H/Z_{eff})$, where κ is greater than unity. Noting that for r times ionised atoms $\mu = A/r$, (4) after a little reduction is transformed into the form

$$\frac{E^*}{\psi_r}\kappa^2\left(\frac{4\mu}{9\pi A}\right)^{\frac{2}{3}} > 1 > \frac{E^*\kappa^2}{\psi_{r+1}}\left(\frac{4\mu}{9\pi A}\right)^{\frac{2}{3}} \quad . \quad . \quad . \quad . \quad . \quad (5)$$

where E^* is the maximum energy in the degenerate Fermi-distribution,

$$E^* = \frac{h^2}{2m}\left(\frac{3\rho}{8\pi\mu m}\right)^{\frac{2}{3}} \quad . \quad . \quad . \quad . \quad . \quad . \quad (6)$$

Substituting for ρ from (2) in terms of M and μ, (5) can be expressed as

$$\frac{M}{J}\frac{A^2}{r^{\frac{5}{2}}}\frac{1}{\psi_r^{\frac{3}{2}}} > 1 > \frac{M}{J}\frac{A^2}{r^{\frac{5}{2}}}\frac{1}{\psi_{r+1}^{\frac{3}{2}}} \quad . \quad . \quad . \quad . \quad . \quad (7)$$

* We are not taking account of the excited states. For an ion in the excited state the volume will be larger than when it is in the ground state. The presence of excited states, therefore, will increase the value of κ (see later).

$$\left.\begin{aligned} \text{where } J &= \frac{10^{\frac{3}{4}}}{\kappa^{\frac{3}{2}}}\left(\frac{3\omega^{n}}{128}\right)^{\frac{1}{2}}\frac{K^{\frac{3}{2}}}{G^{\frac{3}{2}}}\frac{1}{m_H{}^{\frac{1}{2}}} \\ &= 2{\cdot}20\times10^{39}=1{\cdot}11\times10^{6}\odot. \end{aligned}\right\} \quad . \quad . \quad . \quad (8)$$

Substituting the value for J in (7) we finally obtain that when

$$0{\cdot}0202\,\frac{M}{\odot}\frac{r^{\frac{3}{2}}}{A^{2}}\frac{1}{\psi_r{}^{\frac{1}{2}}} > 1 > 0{\cdot}0202\,\frac{M}{\odot}\frac{r^{\frac{3}{2}}}{A^{2}}\frac{1}{\psi_{r+1}{}^{\frac{1}{2}}} \quad . \quad . \quad . \quad (9)$$

holds, the material is on an average r times ionised, *i.e.*, $\mu = A/r$. The ψ's in (9) are expressed in million electron volts. This relation gives the answer to the fundamental question we asked at the end of the last section. What value of μ should be taken for a given M? As follows immediately from the above criterion, for masses

$$M \leq M_z = 49{\cdot}6\,\frac{Z^{\frac{3}{2}}}{A^{2}}\odot\psi_z{}^{\frac{1}{2}} \quad . \quad . \quad . \quad . \quad . \quad (10)$$

the material will be completely ionised ($\mu = A/Z$), whereas for masses

$$M < M_1 = 49{\cdot}6\,\frac{1}{A^{2}}\odot\psi_1{}^{\frac{1}{2}} \quad . \quad . \quad . \quad . \quad . \quad (11)$$

the material will be on an average less than singly ionised ($\mu > A$). For $M = M_1$, the atoms will be just singly ionised ($\mu = A$). We may notice that

$$\frac{M_z}{M_1} = Z^{\frac{3}{2}}\left(\frac{\psi_z}{\psi_1}\right)^{\frac{1}{2}} \quad . \quad . \quad . \quad . \quad . \quad (12)^{*}$$

For values of μ intermediate between A/1 and A/Z, *i.e.*, for $\mu = \frac{A}{r}$ where r takes the values 2, 3 ... Z−1, the corresponding values for the mass (or rather mass limits) can be found from the above inequality, or, what is sufficiently accurate for our purpose, (9) may be used in the form

$$M = J\,\frac{r^{\frac{3}{2}}}{A^{2}}\,(\psi_r\,\psi_{r+1})^{\frac{1}{4}}\odot$$

For M thus calculated, the corresponding value for the radius is obtained from (1).

§3. For numerical work we have assumed the stellar matter on an average to be made of iron (A=56, Z=26). The successive ionisation

* The value of Ψ_z/Ψ_1 will be roughly about Z^2 and therefore $M_z/M_1 \sim Z^4$. Taking the case of iron (Z=26) this gives $M_z/M_1 \sim 4{\cdot}6\times10^5$. Substituting the actual values for Ψ_z and Ψ_1 for iron in (10) gives $M_z/M_1 = 6{\cdot}7\times10^5$.

potentials for iron (ψ_r's) have been calculated by Hartree from his method of self-consistent fields. Figure 1 exhibits the results of our calculations. The continuous curves represent the theoretical mass-radius

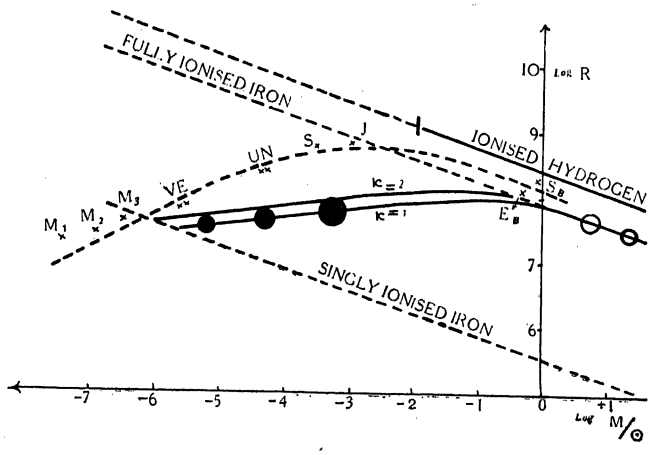

Fig. 1. -The continuous curves are theoretical. The shaded circles denote planets and the unshaded circles white dwarfs. (The radii of these circles are not drawn to scale). The dotted curve represents the observed mass-radius relation for the planets and the white dwarfs. The symbols stand for—M_1—Moon, M_2—Mercury, M_3—Mars, V—Venus, E—Earth, U—Uranus, N—Neptune, S—Saturn, J—Jupiter; S_B—Sirius B and E_B—O_2 Eridoni B.

relation calculated in the way indicated above. The upper curve* is for $\kappa=2$ and the lower one for $\kappa=1$. The dotted curve exhibits the observed relation between M and R for the planets and the white dwarfs. The straight line marked "fully ionised iron" is a plot of (1) for $\mu=56/26$ corresponding to complete ionisation. The lower parallel line corresponds to the value of μ for single ionisation, *i.e*, $\mu=56$. The uppermost straight line refers to a stellar mass consisting entirely of hydrogen and its significance is discussed later.

The run of the theoretical (M, R) curve is roughly similar to the observed curve. The theory has been too crude for us to expect a quantitative agreement, but it brings out the fundamental point that for white dwarfs a smaller mass means a larger radius, *whereas for the planetary bodies a smaller mass corresponds to a smaller radius*. The mass for maximum radius given by the theoretical curve is about $1/10\odot$ and from the observed curve about $1/100\odot$. For a given planetary mass the theory predicts a radius appreciably smaller than the observed one and the

* The reason for taking $\kappa=2$ appears later.

difference is larger for the heavier planets. There are several reasons which make the predicted radius small.—

(*i*) We have given κ the value unity, whereas κ should actually be greater. Any increase in κ will increase the predicted radius. The theoretical curve in the figure for $\kappa=1$ shows what the theory can do when placed in its worst position. It is difficult to estimate the proper value for κ. Elementary considerations of wave-mechanics suggest a value of about 2, and a curve for $\kappa=2$ has been added in the figure for comparison.*

(*ii*) In any stellar mass μ will not be constant throughout, but will decrease from centre outwards. Our taking it as constant for a given M lowers the value of the radius.

(*iii*) We now come to a third and possibly the most important reason. As already remarked at the beginning of this paper the hypothesis of hydrogen abundance appears necessary to fit the observed with the calculated M, R values for white dwarfs. The presence of hydrogen will also increase the radii of the planets For a degenerate stellar mass composed entirely of hydrogen, the (M, R) relation will be represented by the uppermost straight line in the figure. This line is a plot of (1) for $\mu=1$. The cut in the line at about $M=M_H=0{\cdot}011\odot$ corresponds to the fact that as follows from (10), for $M<M_H$, the H-atoms in the stellar mass will not be all ionised and therefore μ will no longer be unity. The radius for $M<M_H$ will not fall on the straight line but below it.

The point to be emphasised is that the observed (M, R) curve lies between the H-line on its upper side and the Fe-curve on its lower side. It appears possible that by taking a suitable proportion of H and Fe, the predicted radius could be raised near enough to the observed value. However at the present stage, it will not be very profitable to discuss the hypothesis of hydrogen-abundance in quantitative detail for as yet our theory of pressure ionisation has not been sufficiently precise to settle the most appropriate value for κ.

In conclusion it may be stressed that any satisfactory theory of the white dwarfs must combine with it the theory of *pressure ionisation* to enable the degree of ionisation in degenerate matter to be estimated. Without this the theory of the white dwarfs cannot be regarded as

* It may be recalled that in the kinetic theory of gases, treating the molecules as hard spheres, wave-mechanics gives for the collisional cross-section a value four times the classical one.

complete. We have made a preliminary attempt in this direction and this combined theory, fortunately, *also gives some insight into the essential features of the planetary structures.**

It is a pleasure to record our grateful thanks to Prof. M. N. Saha, F.R.S., for his kind interest in this work.

References

1. *Observatory*, Sept., 1935, p. 260.
2. Fowler, *M. N.*, **87**, 121, 1926.
3. Milne, *M. N.*, **91**, 1, 1930; *M. N.*, **92**, 610, 1932.
4. Kothari, *M. N.*, **93**; 70, 1932.
5. Milne, *M. N.*, **92**, 610, 1932.
6. Slater, *Rev. Mod. Phys.*, 6, 209, 1934.
7. Kothari and Mazumdar, *Astr. Nach.*, **244**, 66, 1931, where other references are also given.
8. Swirles, *Proc. Roy. Soc.*, **141**. 561, 1933.
9. Hartree, *Proc. Camb. Phil. Soc.*, **22**, 464, 1924.

*And after all the planets are in no uncongenial company with the white dwarfs. In the case of earth at any rate the works of Oldham, Gutenberg and others have shown that the interior is a core of molten iron (and therefore degenerate matter). The radius of the core is estimated at about 2/3rd the earth's radius.

STUDIES ON THE FAMILY BUCEPHALIDÆ (GASTEROSTOMATA) PART I—DESCRIPTIONS OF NEW FORMS FROM INDIAN FRESH-WATER FISHES

By S. C. Verma

Department of Zoology, University of Allahabad, India

(With 15 Figures)

Originally Received April 20, 1935; Received again November 20, 1935

Brief introduction is given indicating that there still exist some unassigned forms in the family Bucephalidæ and pointing out the existence of a *y*-shaped excretory bladder, in the majority of the Indian fresh water forms of the genus *Bucephalopsis*.

Five new species of the genus *Bucephalopsis* are described and their specific diagnoses furnished.

Two new species of the genus *Bucephalus* are established. One of these is completely described: in the other case the specific diagnosis is not yet given.

Introduction

The material which forms the subject of this communication was collected by me, from time to time, during the years 1926 onwards, in connection with the study of the parasites of Indian Fresh-water Fishes of the Families Siluridae and Ophiocephalidae which I had then undertaken, and on which a number of papers have been already published by me.

On studying these parasites and the literature concerning them, I felt that a revision of the family was called for. Therefore, instead of rushing to the press, I put myself in communication with eminent workers on the group abroad so as to obtain actual specimens of forms reported from other countries, and acquire first-hand knowledge of a number of them that had not been named and assigned their proper places. Even after Eckmann's (1933) excellent study, which was available to me only just before completing this paper, there remain quite a number of doubtful forms which he was unable to decide about, owing to lack of complete descriptions.

I am glad to place on record my deep indebtedness to Dr. Yoshimasa Ozaki who favoured me with a collection of Japanese members of the Family, last year, and to Dr. S. Yamaguti for his very kindly sending me his only specimen of *Bucephalus uranoscopi* for comparison with my species. My thanks are also due to Dr. Marie V. Lebour and Dr. W. Nicoll of England for their ready help with literature and promise of sending British representatives when available. I wish to further express my gratitude to Dr. E. Linton of the United States, who, very recently, promised to send me his preparations of Gasterostomes

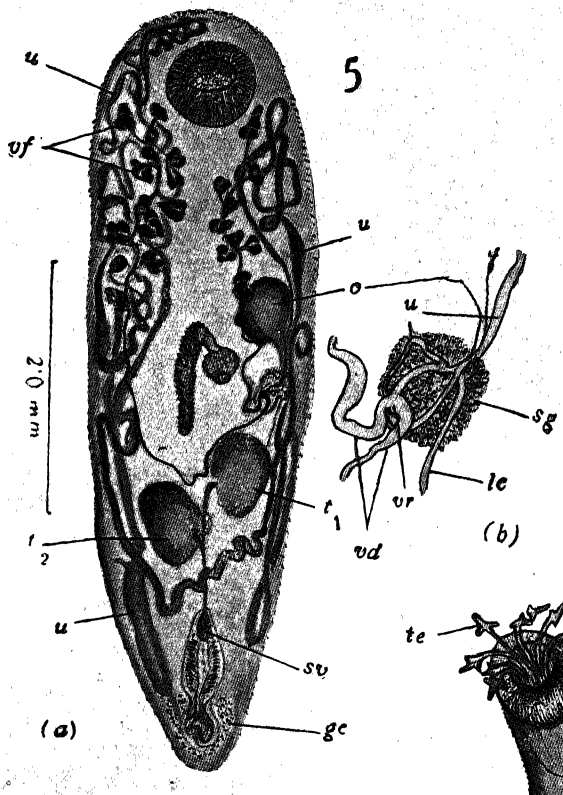

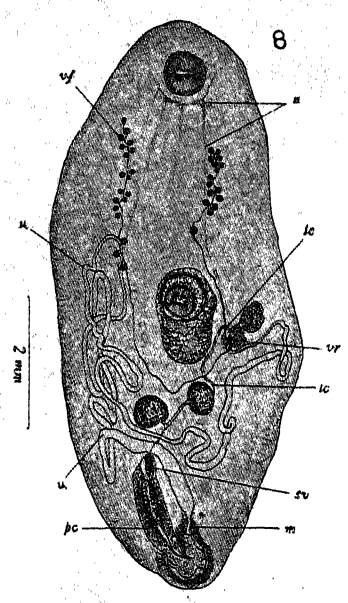

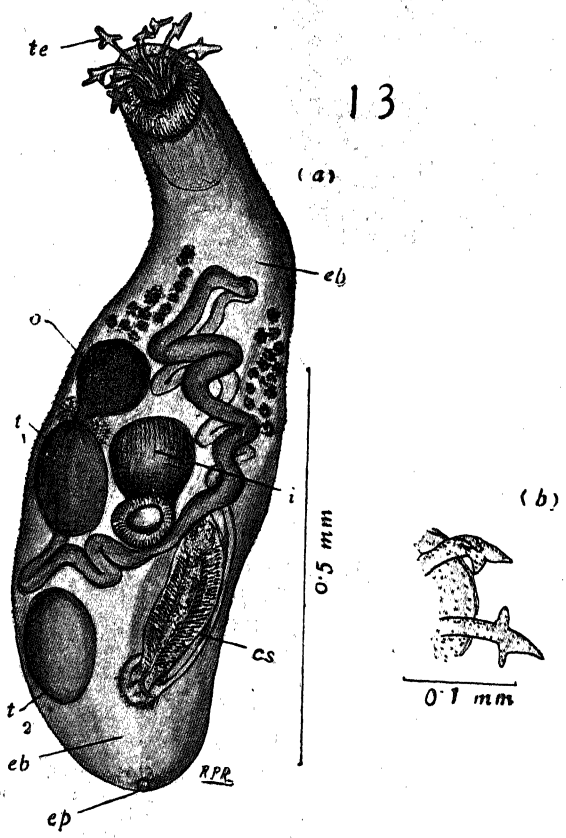

Fig. 5 a. Dorsal view of *Bucephalopsis garnai*, n. sp.; b, enlarged view of shell gland region.

Fig. 8. Dorsal view of *Bucephalopsis magnum*, n. sp.

Fig. 13. *Bucephalus tridentacularia*

a. Ventral view of entire specimen.

b. Enlarged sketch of two tentacles.

some of which, for want of full knowledge, are not yet assigned proper names or places.

The Gasterostomes are not only unique among the trematodes (Woodhead 1929) because of the peculiar position of the mouth and the

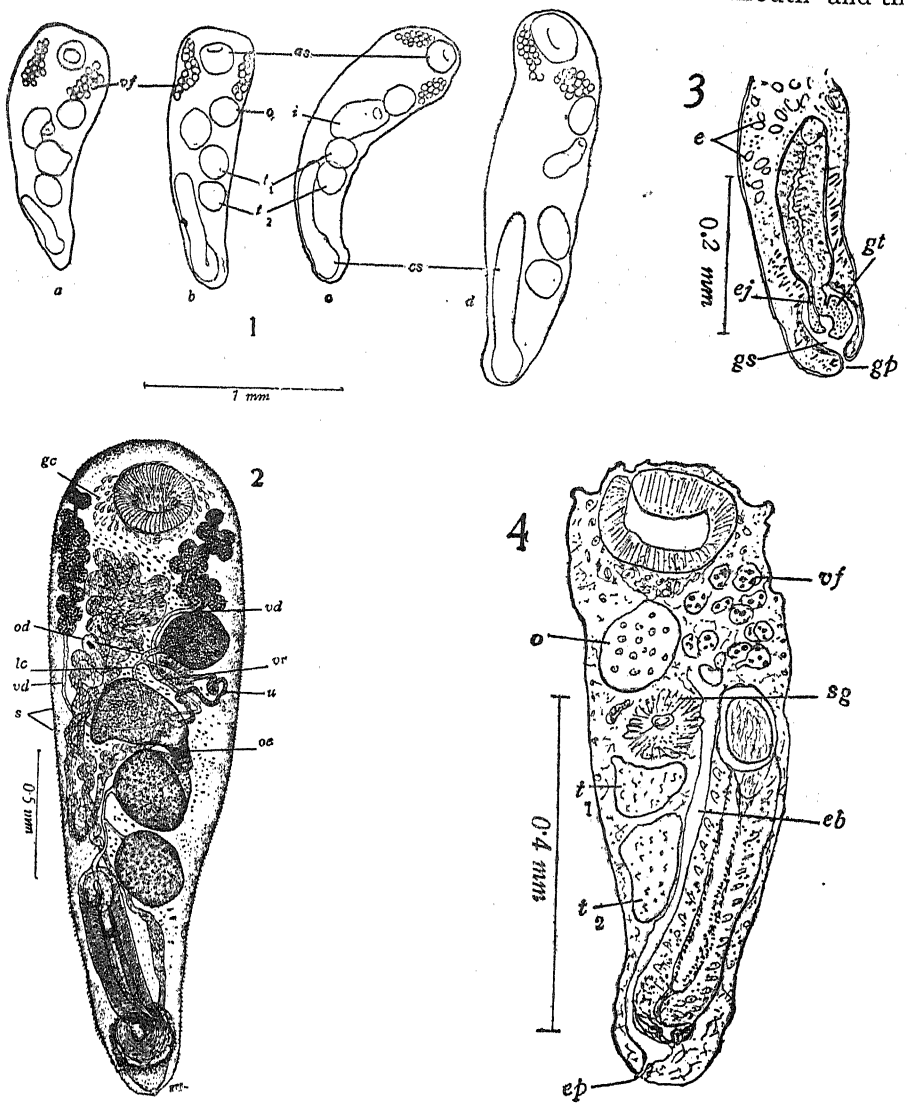

Bucephalopsis fusiformis, n. sp., Figs. 1—4.

Fig. 1, a—d. Outline sketches of four individuals showing variations *in the position* and shape of principal organs.
Fig. 2. Dorsal view of a mounted specimen.
Fig. 3. Longitudinal vertical section through genital pore.
Fig. 4. Horizontal section through excretory pore.

Key to Lettering used in Figures

as, anterior sucker: cs, cirrus sac: e, egg: ej, ejaculatory duct: eb, excretory bladder: ed, excretory duct: ep, excretory pore: gc, unicellular gland cells: gp, genital pore: gs, genital sinus: gt, genital tongue: i, intestine: lc, Laurer's canal: m, metraterm: n, nervous system: o, ovary: od, oviduct: oe, œsophagus: p, pharynx: pc, prostatic cells: s, spines: sg, shell gland: sm, sphincter muscle: sv, seminal vesicle: t_1, anterior testis: t_2, posterior testis: te, tentacle: u, uterus: vd, vitelline duct: vde, vas deferens: vf, vitelline follicles: vr, vitelline reservoir.

structure of the gut, but their taxonomic position has been of much interest and "Many of the structural characters of the order have puzzled investigators." An interesting feature, presented by some of the Indian species described here, is the existence of a peculiar *y*-shaped excretory bladder in place of the simple tubular or elongated sac-like one of the hitherto known forms. Another remarkable feature of this group of trematodes—"The great variation in the anatomical topography that may occur, even within specific limits"—first brought to notice by Nicoll 1915, was found to be true of Indian forms as well. The variations noticed by me concern the relative position of the genital glands and of the mouth opening; but I did not find any noteworthy variations in size of the excretory bladder as noted by Nicoll, in British examples. In view of this specific variability, descriptions of the new species, incorporated in this communication, have not been confined to one type specimen or even to two cotypes; but, in the majority of cases, the features representative of a fair number of similar preparations have been covered so that it may not be said of my forms, as of *Prosorhynchus crucibulum* (Rud) that "No two descriptions . . . have yet agreed as regards the position of the genital glands."

GENUS BUCEPHALOPSIS

1. **Bucephalopsis fusiformis,** n. sp.

(Figs. 1—4)

Host.—*Eutropiichthys vacha*, Day. (Butterfish.)

Habitat.—Intestine: once in stomach. Encysted larval forms on liver, kidney and mesentery round stomach and duodenum.

Locality.—Allahabad, India.

Description.—During 1927 to 1934 thirty-seven fishes were examined, from time to time. Of these 18 were found free from this parasite, 14 harboured the adult individuals and 5 only cysts; only one fish had both adult and encysted forms. The number of specimens collected from a single host varied from 6 to 37.

Measurements of selected numbers of mounted specimens are given in Table I.

The body is covered with minute spines which can only be seen, with difficulty, under the low power of a Microscope. It is slender, of elongated form, with its anterior part broad and posterior narrow. In the living condition, in physiological salt solution, measurements of the body vary a great deal, according as the condition is one of contraction or of expansion. In length the variations are from 0·9* to 2·6, rarely to 3·0; and in greatest breadth, which usually occurs in the region of the vitellaria or the posterior margin of the anterior sucker, from 0·3 to 0·7.

The anterior sucker is globular, subterminal and muscular, measuring on an average, 0·15 to 0·25, in life. Unicellar gland cells (Fig. 2, gc.) surround the sucker and, in some specimens, are seen to extend some distance behind, along the lateral margin of the body. The pharynx is rather inconspicuous, being small, and more often lies between the ovary and the first testis: only occasionally it is partly overlapped by the latter. By a short, antero-dorsally directed œsophagus it leads into a thin-walled saccular intestine, the front wall of which may reach to about one-third the body length from the anterior end.

The ovary is rounded, with just a narrow projection in the region of the origin of the oviduct. It lies close to the right margin of the body, immediately behind or just touching the yolk glands of its side. The shell gland diameter is about half to two-thirds that of the ovary, and the former lies in close contact with the latter, or even partly overlapped by it. Along the dorsal inner surface of the shell gland lies the small vitelline reservoir, formed by the union of the two conspicuous vitelline ducts (Fig. 2, vd.). The vitelline ducts are asymmetrical and their course is as indicated in the Figure. The Laurer's canal is visible in all carefully differentiated preparations of the entire worm and takes the form of a narrow, elongated tube joining the oviduct before it receives the yolk duct from the vitelline reservoir. In the fully mature flukes the uterus occupies the space between the anterior sucker and the genital sinus. Arising from the ootype, the uterus passes backwards, dorsal to the intestinal sac, besides which it hardly overlaps any other organ: after a forward course, into which it is thrown into short or long convolutions, it opens into the genital sinus from its right side. The eggs are numerous, of a light yellow colour, and densely packed together in the whole of the uterus. The vitelline follicles are of medium size, rounded in appearance, and

* All measurements are in millimeters.

arranged in two compact groups, one on each side of the body, between the ovary and the anterior sucker. In fifty per cent of the specimens examined they extend forwards a little anterior to the hind margin of the sucker. The follicles on each side number 14 to 16; those on the left exceed those on the right by one or two.

The globular testes lie one behind the other, along the line of the ovary (Fig. 1 *b, d*.), or somewhat internal to it (Fig. 2). The anterior testis is a little larger than the posterior, and separated from it by an interval varying, according to the condition of contraction of the parts, from zero to nearly half the diameter of the testis. The cirrus pouch is comparatively long. It lies on the left side of the body, nearly parallel to its margin, and extends forwards to the level of the hinder margin of the posterior testis, or a little more ahead. In 3 specimens out of 15 it is seen to approach the level of the anterior testis (Fig. 1 *d*). Enclosed within the sac, is the prominent vesicula seminalis which opens into the long pars prostatica surrounded by thick-set prostatic cells. The ejaculatory duct is short; and the cirrus of the usual type is replaced, in these forms, by the conspicuous 'genital tongue,' a muscular organ, curved upon itself. The genital sinus is full of the genital tongue, and opens to the outside by a small pore lying at a distance of about 0·6 from the posterior extremity (Fig. 3 gp). It is surrounded by gland cells on all sides.

The excretory bladder is a simple, elongated sac. It extends to near the anterior sucker and opens to the outside at the posterior extremity of the worm (Fig. 4 ep).

Relationship.—Of the eight species of the genus included by Eckmann (1933) in his diagnostic Table, the form above described is like the two known forms *B. haimeanus* (Lacaze Duthiers, 1854) and *B. ovatus* Ozaki 1928, in that it has its vitellaria closely aggregated on each side like them. But it differs from the former, among other features, in its fusiform body and, in its testes lying on the same side of the pharynx, instead of on opposite sides. From the latter, it is easily differentiated by its longer excretory bladder and by the more forward position of its ovary.

Leaving aside the character of the vitellaria, this species comes nearest the Japanese form *B. elongatus* Ozaki 1928, which has a similar excretory vessel and uterus. But the Japanese parasite has quite different body-form, a longer reach of the vitellaria and a comparatively longer cirrus sac than the species under discussion. Further, this species stands apart from all known ones in the position of its intestine, which

Table I.—Measurements of four specimens of

Bucephalus fusiformis *n. sp. from permanent mounts.*

	No. 1	No. 2	No. 3	No. 4
Length	2·5	2·52	1·6	1·24
Greatest breadth ..	0·84	0·61	0·49	0·39
Anterior Sucker, dia.* ...	0·245	0·22	0·18	0·17×0·18
Yolk glands, dis. ...	0·168	0·21	R*, 0·1: L*, 0·16	R, 0·08: L, 0·07
„ „ size ...	0·09×0·09;	0·07×0·067	0·04×0·04	...
	0·08×0·06;	0·067×0·059	...	...
	0·059×0·059	...	...	...
„ „ No. ...	R, 14: L, 16	R, 15: L, 17	R, 15: L, 16	R, 16: L. 17
Pharynx, dis.* ...	1·007	1·17	0·8	0·51
„ dia. ...	0·084	Overlapped by testis	0·08	0·07
Intestine, size ...	0·467×0·185	0·21×0·19	0·25×0·23	0·21×0·18
„ dis. ...	0·756	0·89	...	...
Ovary, dis. ...	0·547	0·547	0·42	0·34
„ size ...	0·21×0·175	0·21	0·151×0·19	0·14×0·15
Testis (1), dis. ...	1·133	1·05	0·76	0·59
„ size ...	0·252×0·252	0·294×0·26	0·2×0·18	0·18×0·17
Testis (2), dis.	1·175	1·427	0·96	0·77
„ size ...	0·252×0·193	0·25×0·21	0·19×0·17	0·16×0·15
Cirrus Sac, size ...	0·713×0·143	0·59×0·13	0·463×0·12	0·58×0·1
Seminal vesicle, size ...	0·21×0·1	0·21×0·143	0·09×0·05	0·13×0·08
Genital atrium, size ...	0·14×0·16	0·13×0·17	...	...
Ova, size ...	0·013—0·02 × 0·012—0·013	0·0168×0·0084 —0·0101	0·0226×0·0146	...

*dis.=distance from anterior end ; dia.=diameter; R=right ; L=left.

lies between the ovary and the anterior testis: it is therefore designated as a new species, *Bucephalopsis fusiformis*, and given the following diagnosis.

Specific diagnosis.—With characters of the genus. Body minute, fusiform: in balsam mounts length 1·24—2·52; greatest breadth, in region of vitellaria or anterior sucker, 0·39—0·84; anterior sucker subterminal, diameter 0·17—0·245; vitellaria compact, between ovary and anterior sucker, follicles 14 to 16 in each lateral group, on left 1 or 2 more than on right, 0·07—0·09 in diameter; pharynx, inconspicuous, about middle of body, between ovary and testis, 0·07—0·084; œsophagus short, curved; intestine wide 0·21—0·46 long; ovary near right margin, rounded, at one fourth body length from anterior end, 0·14—0·21 in diameter; testes roundish to ovoid: anterior to right side, equatorial or slightly more ahead, 0·18—0·29 × 0·17 × 0·26; posterior behind middle of body, either in same line as anterior or more internal, 0·16—0·25 × 0·15—0·21; cirrus pouch long, one third to nearly half as long as body, reaches posterior testis or more ahead, 0·46—0·7 long, 0·1—0·14 broad; genital sinus 0·13—0·16 in diameter; excretory bladder elongated, tubular or narrow, saclike; eggs vary in size, 0·013—0·0226 × 0·0084—0·0146.

Host. *Eutropiichthys vacha*, Day.

2. **Bucephalopsis garuai**, n. sp.

(Figs. 5–7)

Host—*Pseudotropius garua*, Day.

Habitat—Intestine, hinder part, and rectum: encysted larval forms in gonads, in liver and on mesentery.

Locality—Allahabad.

Description.—Thirty-six fishes were dissected from time to time between 1926 and 1934, so as to cover practically all the months of the year, except those of the rainy season when, owing to floods, these fishes are not available. Of these only 10 hosts harboured representatives of this parasite, in some cases with another distomum and, in others also with a Cestode already described by me (1928). The encysted forms were found only in 3 of the fishes examined. The number of specimens collected from one host varied from a few to 60 in one case. But unlike the previous form, in the case of this species both mature as well as immature examples were met with in the intestine, and it was also noted that the infection was heavier in winter than in summer. Detailed measurements of selected individuals are furnished in Table II.

The shape of the body is very variable, in life, as the worms are capable of considerable expansion and contraction. After fixation under gentle pressure, the anterior half to over two-thirds of the body is of a uniform width, with the sides nearly parallel; but posteriorly it narrows down towards the hind end. Minute spines, easily visible in the living state, under the low power of the Microscope, cover the whole body. The spines are not very dense, and appear to decrease in numbers behind the testes. When alive, the worm is of a beautiful, bright, flesh colour, and exhibits fairly rapid movements of expansion and contraction in normal saline. It assumes, on full expansion, a length one and a half to nearly two times as large as when contracted. The mature specimens measure 3·36 to 7·0 in length and 0·8 to 0·25 in breadth when expanded; but on contraction the length decreases from 2·18 to 3·0, while the breadth increases from 0·75 to 1·05. In the same fluke the breadth near the anterior end varies from 0·37 to 0·52, but near the posterior end it varies from 0·15 to 0·23 according as the worm is expanded or contracted. The anterior sucker is subterminal, prominent and possessed of thick muscular walls. It is globular and more often a little broader than long. Its diameter, in life, varies in the same individual, in various states of expansion and contraction between 0·335 to 0·5. The unicellular gland cells round it are clearly seen in some mounts, but are indistinguishable in others. The conspicuous pharynx is situated a short distance ahead of the equatorial line. It is rounded, with fairly developed muscular walls; the transverse muscle fibres are distinctly seen, even in entire mounts, both on the pharynx and on the anteriorly directed œsophagus into which it leads. The intestine is a rather narrow, elongated sac, bent backwards parallel to the œsophagus and the pharynx. The form and the position of the pharynx and intestine are fairly constant.

The ovary is rounded or ovoidal, with smooth outline and lies beside the anterior half of the intestine, or just ahead of it, between it and the body wall. The shell glands form a compact mass which is rounded or oval, and smaller in size than the pharynx. Its position, in relation to the ovary, varies in different preparations. In some it lies along the outer side of the ovary, in others beside its posterior, outer margin, often partly overlapped by it; or it may lie, as in Fig. 5, a short distance behind the ovary. The vitelline reservoir lies dorsal to it, and gives out a narrow duct to join the oviduct after its junction with the Laurer's canal. The latter is visible, in most of the entire mounts (Fig. 8, lc.), as a long narrow tube running bacwkards. The vitelline glands, in uniformly stretched preparations, extend from about the hinder border of the anterior sucker

to near the level of the front border of the ovary or intestine. They are not crowded together as in the first species *B. fusiformis*, and in some mounts one or two follicles may even overlap the ovary. The follicles are well developed, and larger than in all the species described here. In outline they are pear-shaped or elongated, and each one of them is either bilobed or consists of a couple attached to a common ductule. Their number varies on the left side from 12 to 14, and on the right from 16 to 18. The bilobed or double nature of the follicles is a unique feature of this species and is not reported to occur in any other Gasterostomes. The uterus arises as a narrow duct from the ootype, and forms convolutions both on the right and the left sides of the body, leaving the central area free. Its course is as depicted in Fig. 5. The metraterm is distinct and opens into the genital sinus either from its dorsal side or along the left side. Unlike the condition in *B. fusiformis* the terminal part of the uterus does not cross back to the right side before opening into the genital atrium.

Table II.—Measurements of four individuals of Bucephalopsis garuai, *n. sp., from balsam mounts*

	No. 1	No. 2	No. 3	No. 4.
Length ...	6·0	6·2	5·73	6·1
Greatest Breadth ...	1·8	1·9	1·68	1·38
Yolk glands dis.*	0·67	0·756	R,*0·7 : L,*0·84	0·67
„ „ size ...	0·182×0·1008	0·1596×0·1176	0·1596×0·1176	0·1848×0·168
	0·168×0·1344	0·1848×0·1176	0·1848×0·1176	0·210×0·151
	0·168×0·1008	0·126×0·1092	0·126×0·1092	0·262×0·210
„ „ No.* ...	R, 13 ; L, 16	R, 13 ; L, 17	R, 13 ; L, 18	R, 14 ; L, 18
Anterior sucker dis. ...	0·210	0·042	0·1428	0·042
„ „ dia.* ...	0·69×0·69	0·588×0·588	0·62×0·66	0·56×0·63
Pharynx dis. ...	2·60	2·772	2·513	2·52
„ dia. ...	0·2938	0·2938×0·336	0·26×0·25	0·252
Intestine size ...	0·88×0·168	1·22×0·50	0·756×0·21	1·26×0·335
Ovary dis. ...	2·014	2·384	2·350	2·10
„ size ...	0·58×0·39	0·547×0·42	0·463×0·378	0·67×0·29
Shell gland size ...	0·25×0·25	0·227×0·210	0·290×0·184	indistinct
Testis (1) dis. ...	3·360	3·290	3·993	3·276
„ size ...	0·86×0·48	0·756×0·660	0·756×0·463	0·713×0·380
Testis (2) dis. ...	3·70	4·147	4·30	3·61
„ size ...	0·67×0·547	0·629×0·463	0·588×0·506	0·588×0·420
Cirrus Sac size ...	0·756×0·336	0·924×0·35	0·67×0·34	0·60×0·30
Seminal vesicle size ...	0·151×0·042	0·126×0·040	indistinct	0·143×0·080
Genital atrium size ...	0·335×0·335	0·21×0·20	0·252×0·252	0·250×0·250
Ova size ...	0·0226—0·0289 × 0·0146—0·0173	faint ...	0·028—0·026 × 0·0173—0·016	0·0239—0·026 × 0·0159—0·0146

*dis. = distance from anterior end ; dia. = diameter ; R. = Right side ; L. = left side ; No. = number.

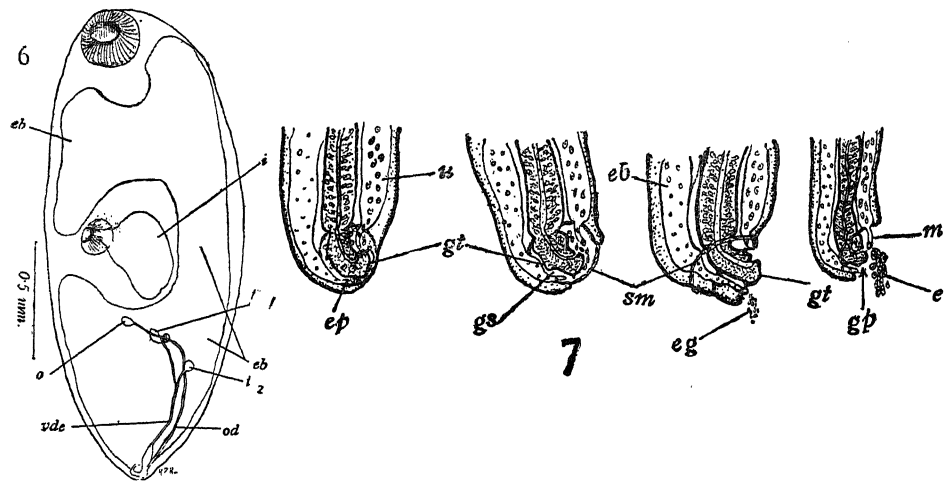

Bucephalopsis garuai, n. sp., Figs. 6-7.

Fig. 6. Ventral view of an immature worm, showing extent and nature of the excretory bladder.

Fig. 7. Sketches, from life, of terminal parts of excretory, male and female ducts, indicating the mode of their working.

The testes are roundish, oval or subglobular, sometimes even triangular. They are thus more variable in form than the female gonad. Their outline is usually regular, but it is rarely irregular or feebly lobed. The two testes are nearly of the same size though, along one diameter, the anterior testis is, in most cases, a little larger than the posterior one. The anterior testis lies just posterior to the intestine (Fig. 5, t_1) or along its postero-right margin; it is always more outwardly placed than the following testis. The gap separating the two male glands is generally shorter than that separating the first testis from the female gonad. The cirrus sac is comparatively short, in this species, and may rarely approach the vicinity of the hind border of the last testis. The seminal vesicle is short and narrow. It is often inconspicuous, but the prostatic gland cells and pars prostatica are always well developed. The genital sinus is large, rounded, and fully occupied by the prominent, curved genital tongue. It ends a little ahead of the terminal extremity (0·3 to 0·4) and is thickly surrounded by gland cells. The genital pore is surrounded by a muscular sphincter, which works more or less in the manner of Hemistomid trematodes. The working of the genital sinus and the ducts opening into it was carefully studied in living parasites, and it was noticed that the eggs are passed from the metraterm, by contraction of its muscular wall, into one

side of the atrium. There they are loosely stuck together in groups of 20 to 30 by a viscid substance, probably secreted by the genital tongue or, maybe, by the gland cells surrounding the atrium. Then, by contraction of the sphincter muscle and the atrium they are propelled out of the genital pore (Fig. 7. e). The excretory bladder opens on a narrow papilla, protruded into the genital sinus, on the side opposite to that on which the metraterm opens, and the excretory matter is voided either through the sinus, or directly to the exterior as indicated in Fig. 7. eg. The excretory bladder of this species is *y*-shaped, and differs from all other species of the genus hitherto known, both in form and extent. It is clearly seen in Fig. 6, eb.

Relationship.—In having a *y*-shaped excretory bladder this species and the following species of the genus, stand apart from all known forms. It is further distinguished from other members of the genus, in addition to its body shape and other characters, in the large size and the bilobed nature of its vitelline follicles, in its small seminal vesicle and cirrus pouch as compared with its body length, and also in the character and disposition of its uterine coils which lie laterally—mostly in ascending and descending loops—leaving the central body space free of eggs. It is therefore named *Bucephalopsis garuai*, a new species, and given the following diagnosis.

Specific diagnosis.—With characters of the genus. In balsam mounts: body medium sized, with nearly parallel lateral margins, broadly rounded anteriorly; length 5·73—6·20, greatest breadth, 1·38—1·90; anterior sucker subterminal, at times slightly broader than long, 0·56 - 0·69 in dia.; vitellaria not compact, follicles from ovary to anterior sucker, large, bilobed or paired, 12—14 groups on the right, 14—18 on left, largest roundish follicles 0·25×0·21, elongated ones 0·252×0·1008; average sized ones 0·168×0·134; pharynx, in front of middle of body, conspicuous, 0·25—0·2938×0·336; œsophagus distinct, narrow, anteriorly directed; intestine doubled upon the œsophagus and pharynx, elongated-saccular or tubular, 0·88×0·168—1·26×0·335; ovary pear-shaped, right-sided, a little behind one-third of body length from anterior end, 0·67×0·29—0·58×0·39; testis variable in form and outline, usually rounded and regular, anterior to right of median line, behind middle of body, 0·68×0·48—0·756×0·463; posterior, more centrally placed, behind anterior, 0·588×0·42—0·67×0·547; cirrus pouch short, not reaching posterior testis, about one fifth as long as body, 0·6×0·3—0·924×0·35; seminal vesicle short, narrow, 0·151×0·042; eggs 0·226—0·239×0·0146—0·173. Excretory bladder wide, filling the whole body, *y*-shaped.

Host—*Pseudotropius garua*, Day.

3. **Bucephalopsis magnum,** n. sp.

(Figs. 8—9)

Host—*Pangasius buchanani*, Cuv. and Val.

Habitat—Large intestine.

Locality—Allahabad.

Description :—Only half a dozen specimens of this species were obtained from one siluroid fish named above, on the 13th of April, 1927.

This parasite is the biggest of the Indian species recorded here, and probably also largest of all known species of the genus. It is flesh-coloured in life, and cylindrical in appearance. Like other forms the body exhibits considerable movements of expansion and contraction when placed in salt solution.

In proportion to the body, the anterior sucker is relatively small and comparatively more ventrally placed than in other species of the genus. The vitellarian follicles also are relatively much smaller, and rounded in form. They are separated from one another and extend, from in front of the anterior border of the intestine, to some distance behind the anterior sucker. The pharynx is prominent and situated on the equatorial line and leads through a muscular œsophagus into the capacious, wide intestine. The ovary is nearly of the same size as the pharynx. It lies near the equatorial line, to the right side of the intestine. The shell gland is close to its postero-internal angle; and all the parts of the female genitalia, in the vianity of the shell gland, are clearly visible in entire mounts owing to great transparency of the parasite (Fig. 8). The uterus takes a very distinctive course in this form as compared with the preceding and succeeding species. On the right side of the body, it hardly extends forwards ahead of the ovary. Its main coils lie along the left side and are confined mainly to the posterior half of the body. Only in one of the three mounted specimens (Fig. 8, ut), one loop extends forwards a little beyond the intestinal border. Another noteworthy feature is that the uterus crosses over from left to right and *vice versa*, through the gap between the posterior testis and the cirrus sac. The metraterm is distinct, though narrow. A cluster of gland cells embraces the metraterm in continuation with those that surround the genital sinus.

The testes are both rounded and bigger than the ovary. In one specimen the posterior one is about as broad as the latter, and the anterior still bigger. They lie internal to the ovary, either both to

the right of the median axis, or on opposite sides of it. The vasa deferentia are quite distinct, as in other forms, and the cirrus pouch presents the characteristic features of the genus. The seminal vesicle appears doubled up on itself (Fig. 9, sv). The genital atrium is surrounded with thick set gland cells, and encloses a big, recurved genital tongue. The genital aperture is nearly subterminal and surrounded by a feebly developed sphincter muscle.

The nervous system is clearly visible in some mounts. The principal nerve ganglia lie behind the anterior sucker and are connected together by a transverse band. Small nerves are given off from the ganglia in front, and larger ones behind (Fig. 8, n).

The excretory bladder is of the same form as in *B. garuai* the species described before.

Relationship.—This species also is readily distinguished from the other known species by its peculiar *y*-shaped excretory bladder, the large size of its body, the oblongish outline of the mounted specimens, and the characteristic position and disposition of the uterine coils. In the nature of its excretory bladder, it resembles the second species of the genus described here; but it differs from it markedly in the following features. *B. garuai* is a much smaller form, and has a very different body shape. The vitellaria in *B. garuai* are bilobed and comparatively much larger than in this form. The uterine coils in *B. garuai* have a much longer extent, reaching to near the anterior extremity both in the right as well as the left field; but, in this species, in spite of a much larger body, the uterine coils lie mostly in the posterior half of body and principally on the left side. The relative size of the suckers and also the position of the ovary in the body are very different in the two species, besides other minor differences. Therefore this form is designated as *Bucephalopsis magnum* n. sp.

Specific diagnosis.—With characters of the genus. In balsam mounts, body ovo-oblongish, broadly rounded at both extremities, of large size; length 8·0—10·0; greatest breadth about middle, 4·2—4·8; anterior sucker 0·30—0·40 behind anterior end, 0·84 in dia.; vitellaria from level of pharynx to some distance behind anterior sucker, midway between median line and side of body; follicles small, round separate from one another, size 0·126×0·126—0·134×0·11, number 13—16 on right, 17—18 on left; pharynx conspicuous, in middle of body, 0·46—0·5 in dia.; œsophagus short; intestine very wide, broadly oval, backwardly directed, 1·6 long, 0·9 broad; ovary globular or pear-shaped, on right side of intestine, near equatorial line, 0·38 in dia.; testes large, rounded, anterior to right of median line 0·9—1·0 in

dia.; posterior, either on median line or slightly to left of it, smaller than anterior, 0·75—0·84 in dia.; cirrus sac less than one-fourth as long as body,

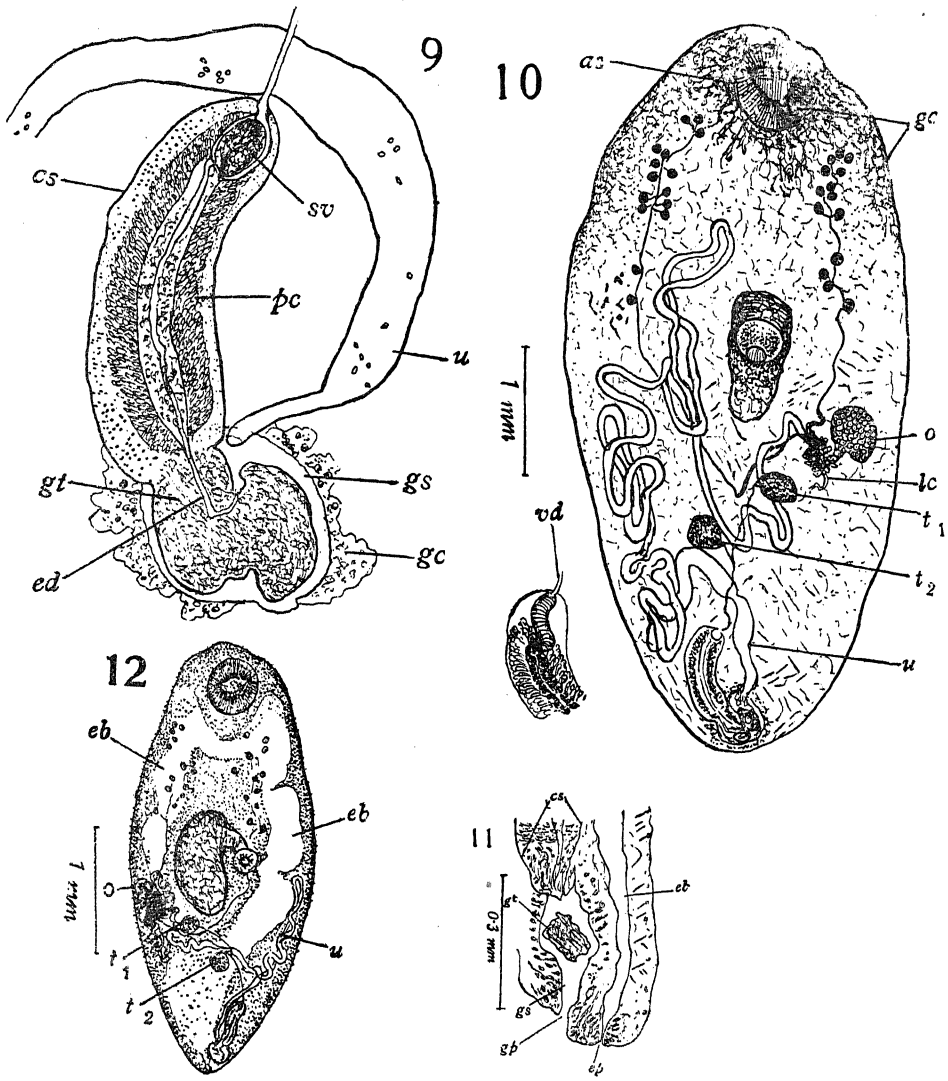

Figs. 9—12. Figs. 8, 10 and 12 are drawn on the same scale, for convenience of comparison.

F. 9. Enlarged sketch of cirrus sac and genital sinus a of preparation of *Bucephalopsi magnum*, n. sp.

F. 10. Dorsal view of *Bucephalopsis confusus*, n. sp.

F. 11. V. S. through genital and excretory pores of same species.

F. 12. Ventral view of *Bucephalopsis minimus*, n. sp.

1·4—1·6×0·3—0·45; uterus nearly confined to posterior half of body, coils mainly on left, cross from left to right and *vice versa* between hind testis and cirrus sac; genital atrium 0·42—0·5 in dia., both metraterm and genital sinus surrounded by numerous gland cells; genital pore subterminal; excretory bladder *y*-shaped, eggs 0·026—0·028×0·0167—0·028.

Host—*Pangasius buchanani*, Cuv. and Val.

4. **Bucephalopsis confusus**, n. sp.

(Figs. 10—11)

Host—*Pangasius buchanani* and *Silundia gangetica*, Cuv. and Val.

Habitat—Terminal part of small intestine and rectum.

Locality—Allahabad.

Description.—In 1927 numerous specimens, 200 to 300, were obtained by me from each of the two siluroid fishes of the first species named above, and a lesser number from one of the three fishes of the second kind. At first sight, this trematode appeared similar to the larger one described as *B. magnum*, the third species of this communication, and also to a much smaller form obtained by another siluloid fish, *Pseudotropius garua*, which is hereafter described as the fifth new species of the genus. But, on closer examination of a large number of preparations, the form proved very different from both of them.

This parasite also is pinkish or flesh-coloured, in the living condition, and semitransparent. The shape of the body, on fixation under gentle pressure, assumes an outline varying from oval, in fully developed individuals, to spindle-shaped in younger ones. But, in all cases, the posterior end is narrower than the anterior, and the broadest part of the body is in the region of the intestine. The individuals exhibit great variation in the relative position of the reproductive glands and their sizes. In quite a number of preparations examined, the ovary, the shell gland, and the anterior testis lie along an oblique line—the posterior testis being internal to this line. In others, the four organs occur on the arc of a wide circle, or the ovary and shell gland are situated on a line, which forms a very acute angle with the line passing through the two testes. As for the size of the principal reproductive glands, in some the female and the male glands are nearly of the same dimensions; but, in the majority of forms the ovary is larger than the testes,—a character quite different from that of the preceding species *B. magnum*, in which the case is the reverse. The cirrus sac is comparatively short, more internal and curved than in other allied Indian species.

The spines over the body are very minute and visible with difficulty under the high power of the Microscope. They are more concentrated anteriorly, but occur throughout. The body is of medium size; and the anterior sucker is subterminal with a wide cavity of 0·38 in diameter. Numerous gland cells surround the sucker and run laterally. The pharynx is subglobular and has a small mouth opening—only 0·07 wide—communicating with a short, ventro-dorsally arched œsophagus. The intestine is as usual saccular, and runs antero-posteriorly.

The ovary lies just behind the equatorial line, in most specimens, and has a rounded outline. It lies on the right side of the body, nearer the lateral margin than the intestinal border of the same side. The Laurer's canal is visible in entire mounts (Fig. 10, lc). The uterine convolutions also mark out this species from the preceding form. In the latter, *B. magnum*, the uterus, after its origin, runs outside the anterior testis and crosses over to the opposite side, behind the posterior testis; but in this species it lies along the inner border of the anterior testis and passes to the left side, in the space between the two testes. Further, its coils of the left side do not lie outside the vitellarian field of the corresponding side, but mostly internal to it. The follicles aresm all, rounded, separated from one another, and the vitelline ducts as distinct as in other species.

The testes are never larger than the ovaries as in *B. magnum*. In outline they vary from oval to roundish. The anterior lies 0·42—0·5 behind the intestine, and the posterior midway between the intestine and the cirrus sac. The cirrus sac is sickle-shaped, of uniform thickness, and extends inwards from 0·85 to 1·1 ahead of the posterior extremity. The seminal vesicle is not well defined and the vas deferens, on entering the cirrus sac, appears distinctly muscular and swollen as shown in the side sketch in Fig. 10. No other species presented this feature. Other parts within the cirrus sac are as characteristic of the genus. Numerous unicellular glands surround the atrium which opens to the outside by a subterminal aperture. The excretory pore is terminal and opens to the outside separately from the genital atrium (Fig. 11, ep.).

Relationship.—This species is intermediate in size between the preceding and the succeeding ones, and like them differs from the known members of the genus in the characteristic form and extent of the *y*-shaped excretory bladder. Besides other characters it differs from *B. magnum* and other species to follow in its numerous gland cells round the anterior sucker, in the relative position of the ovary and the pharynx, and the relative size of the ovary and the testes. It further differs

from the related species in the nature, extent, and disposition of its uterine coils and, above all, in its sickle-shaped cirrus sac, the muscular vas deferens inside it, and the separate excretory and genital apertures. It is therefore new to science and given the name of *Bucephalopsis confusus* n. sp.

Specific diagnosis. With characters of the genus. Body spiny, thick, cylindrical in life; oval, on fixation under pressure; in balsam mounts length 4·0—6·5; greatest breadth 0·5—0·71; anterior sucker 0·67 in dia., with a wide cavity; pharynx distinct, near middle of body, 0·3 in dia.; œsophagus short, 0·1—0·15 long; intestine antero-posteriorly directed, in third sixth of body, 0·88×0·4; ovary rounded, right-sided, nearer body margin than intestinal wall, larger than or nearly equal to testes, behind equatorial line or just touching it, 0·336—0·46×0·306—0·40; uterine coils few, mostly on left, to midway between pharynx and sucker, internal to vitellaria: vitellaria from level of anterior border of pharynx to level of posterior border of sucker; follicles small, rounded, 13—15 on right, 17 or 18 on left, 0·08 in dia., or 0·1×0·075; testes, variable in shape, usually smaller than ovary, anterior to right of median line 0·25—0·38×0·26—0·27; posterior to left of median line, 0·25—0·294×0·21—0·294; cirrus sac curved, one-sixth as long as body; 0·67—0·84×0·21—0·25; seminal vesicle indistinct, vas deferens inside cirrus sac with thicker muscular walls; gland cells numerous, round anterior sucker and genital atrium; genital pore subterminal or ventral 0·12—0·18 ahead of posterior end; excretory bladder large *y*-shaped, pore terminal separate from the genital aperture; eggs yellowish 0·0199—0·0239×0·0146—0·0159.

Host—*Pangasius buchanani and Silundia gangetica* Cuv. and Val.

5. **Bucephalopsis minimus,** n. sp.

(Fig. 12)

Host *Pseudotropius garua*, Day.

Habitat—Large intestine.

Locality—Allahabad.

Description.—This form was found mixed up with the second new species, mentioned in this paper, as *B. garuai*. n. sp. But it differs from it pronouncedly in many important features. For example, it has a much smaller body, of very different form, as is apparent by a comparison of Figs. 5 and 12 which are drawn nearly on the same scale. The new species is further distinguished from *B. garuai* n. sp. in the more backward position of the ovary, in the rounded, smaller vitelline follicles, as compared

with the larger bilobed ones of the latter, and in the extent and disposition of the uterine coils. In its feebly spiny body and general topography it resembles the preceding species, *B. confusus* n. sp., and differs from *B. magnum* n. sp. But it is easily differentiated from *B. confusus* n. sp. also, by its smaller size, by the relatively different sizes of the male and female gonads, and by its still smaller and nearly straight cirrus sac. This species is further distinguishable from *B. confusus* n. sp., and other forms of the genus, by the more backward extension of the posteriorly directed arm of its excretory bladder. In fact, the excretory bladder in this Gasterostome reaches its extreme condition and well-nigh assumes the form of an inverted J, instead of being *y*-shaped. In the specimen sketched in Fig. 12, the excretory bladder (eb), has its descending arm visible up to the level of the hinder margin of the intestine; but in other preparations it extends further backwards. Thus, the parasite is clearly different from those previously described, and also from other known forms. It is designated as *Bucephalopsis minimus* n. sp. by virtue of its small size.

Specific diagnosis.—With characters of the genus: small-sized; in balsam mounts; body-like thick spindle, anterior end broader than posterior; cuticular spines feeble; length 3·0—3·36, greatest breadth, about middle, 1·2—1·47; vitelline follicles minute 0·0588 in dia., or 0·059× 0·042, from pharynx to near hinder margin of sucker; pharynx, on equatorial line, 0·21—0·25 in dia.; intestine sac-like, 0·75 long; ovary, smaller than testes, right-sided, posterior to pharynx, 0·168×0·126; shell gland variable in position, either behind or in front of ovary; testes ovoidal, larger than ovary; anterior 0·277×0·142 near anterior limit of posterior third of body; posterior, more behind, 0·21×0·168; cirrus sac, nearly straight, very small, one-eighth to one-ninth as long as body, 0·378×0·126; genital tongue broad, triangular; excretory bladder *y*-shaped, with very long descending arm; excretory pore subterminal separate from genital aperture; eggs 0·226—0·0239×0·0133—0·0145.

Host—*Pseudotropius garua*, Day.

Discussion of the Indian Species of the genus Bucephalopsis.

In the diagnostic Table of *Bucephalopsis* species, given by Eckmann, 1933 (pp. 104-105) are included 8 completely known species. They are *B. haimeana* (Lacaze-Duthiers, 1854), *B. exilis* Nicoll, 1915, *B. pusilla* (Stafford, 1905), *B. arcuata* (Linton, 1900), *B. elongata* Ozaki 1928, *B. triglae* Van Beneden 1870, *B. gracilicens* (Rudolphi, 1819), and *B. lata* Ozaki, 1928. All the five Indian species described here are readily distinguished from these. The first one, *i.e.*, *B. fusiformis* n. sp. only, has a

straight, tubular, excretory bladder like them, the other four have a very different type of characteristic *y*-shaped excretory bladder, and thus stand apart from *B. fusiformis* n. sp., and all other known species, in a group by themselves. It is therefore worthwhile to consider whether, on the basis of this important character, the new species, *B. garuai*, *B. magnum*, *B. confusus*, and *B. minimus*, should be separated into a new subgenus, within the existing genus *Bucephalopsis*, or placed in a new genus. For the present, I adhere to the former view, and intend to take up this point, in a later communication when dealing with other forms, and the relationships of the various genera of the Family Bucephalidæ.

Thus, there remains only *B. fusiformis* n. sp. to be distinguished from forms possessed of a more or less similar excretory bladder. Of these *B. haimeana* has the vitellaria arranged in circular groups, and *B. lata* has a rhomboid or rounded body. They are therefore readily differentiated from the allied Indian form. In the other known forms the ovary lies close to the anterior testis, a condition very different from that of *B. fusiformis* n. sp. in which the ovary is situated far ahead of the anterior testis. Other characteristic differences have been already discussed in the descriptions of the various species.

GENUS BUCEPHALUS

1. **Bucephalus tridentacularia**, n. sp.

(Fig. 19. a and b)

Host—*Aoria aoria* = *Macrones aoria*, Day, and *Aoria seenghala* = *Macrones seenghala*, Day.

Habitat—Small intestine, hinder region.

Locality—Allahabad.

Description.—During the years 1927—1932, of the three fishes examined of the species aoria, only one was infected with this parasite. But out of seven fishes of the species seenghala, three harboured this trematode. The number of specimens collected from a single host varied from 6 to 50 in one case. As the fishes reached me long after they were caught; in each infected one, a number of worms were found dead or nearly so. Still sufficient well preserved examples exist with me.

The body is rather slender and covered with minute spines. It is divisible into a narrower anterior and a somewhat broader posterior part. The colour of the worm is whitish when alive. The anterior sucker is distinct and presents the unique characteristic of the genus in its tentacles

which number eight in this species. Each of these tentacles is shaped like a trident or an arrow-head with two shorter, lateral processes on opposite sides of the main stem. These tentacles appear to arise from muscular ridges along the wall of the sucker and are capable of considerable expansion and contraction in the living parasite. Some of them when retracted completely become indistinguishable. The pharynx is subglobular and leads through a short œsophagus into the dilated bulb-like intestine directed forwards, in most of the examples It lies in the hinder part of the second third of the body.

The ovary is rounded or pear-shaped and is situated along the right marginal field, in advance of the intestine. Between it and the large oval testis occur the compact shell glands. The vitellaria occupy the lateral fields . and extend, from in front of ovary or intestine, to midway between the latter and the anterior sucker. The follicles are rounded and vary in number from 14—20 on each side. Unlike the members of the genus *Bucephalopsis*, the vitelline ducts are not distinct in entire mounts. The uterus, after its origin, runs backwards: passing the anterior testis along its dorsal aspect, it crosses over to the left side, between the pharynx and the cirrus sac. It then forms rather thick, sinuous, ascending and descending loops in the mid-vitellarial field, and runs along the left side of the cirrus sac before it opens into the genital atrium. The eggs are tinted, light yellow, and fill the whole of the uterus.

The two testes are nearly of the same size and form. They lie in a line with the ovary equidistant from the outer margin of the body. The anterior testis occurs alongside the intestine and pharynx, close behind the ovary; but the posterior one (F. 13. t_2) is situated far behind, in the last quarter of the body. In specimens not quite expanded, like the one sketched in Fig. 13, it reaches the posterior level of the genital sinus. The cirrus sac extends forwards to the pharyngeal region. It encloses a conspicuous seminal vesicle and presents the usual characteristic features of the genus. The genital sinus is rounded, occupied by the genital tongue and opens ventrally, a short distance ahead of the terminal end.

The excretory bladder is a straight, elongated, tubular structure extending forwards to some distance behind the anterior sucker (Fig. 13, eb). It opens to the outside by a small terminal aperture, round which appear to exist some cellular elements.

Relationship.—Of the hitherto recorded species of the genus, *Bucephalus,* the form described by Linton, 1910, as *Bucephalus* sp. has probably four tentacles while *B. gorgon*, Linton has 18 tentacles. The

rest, *B. polymorphus* Baer 1827, *B. elegans* Woodhead 1930 and *B. uranoscopi* Yamaguti 1934, have seven tentacles each. Thus the species above described differs from all of them in having eight tentacles. Further, the tentacles of *B. carangis* and *B. polymorphus* are provided with a single lateral process. It is only in *B. elegans* and *B. uranoscopi*, that a double lateral process exists like that of the form under discussion. Of these the Japanese form, *B. uranoscopi*, based on a single specimen which, through the generosity of Dr. Yamaguti to whom I again express my deep gratitude, is before me for comparison. It is readily distinguished from its Indian relative by its much larger size and attenuated body-shape, by its larger vitelline follicles, by its smaller eggs, and the relatively smaller reach of its cirrus sac inwards. In fact it appears that the specimen has its anterior end unnaturally elongated, probably owing to the parasite having died before fixation, as I have noticed to happen in a form to be described hereafter. In the nature of the tentacular-processes also the two species differ from one another. This only leaves us *B. elegans* which appears to resemble the species under discussion rather closely. But, in the former, the two processes of the tentacles (Woodhead, 1930) are on the same side and unequal in length, whereas in the latter, they are of equal length and placed on opposite sides of the tentacle. Besides this, Van Cleave and Müller, 1934, after having examined a number of examples of the species *elegans* from Oneida lake fishes are of the opinion that "these structures seem to be indicative of senescence," because in their specimens from rock bass, which Woodhead acknowledged to belong to the species *B. elegans*, only traces of seven papillae were detected and in some even these could not be traced. Their figure 7, Plate 28 (1934) shows no lateral processes. *B. elegans* is further distinguished from the new species by its smaller size, and the comparatively more forward position of the pharynx and the posterior testis. For these reasons, the species described above is certainly new to science, and is named *Bucephalus tridentacularia* n. sp., because of its tentacles shaped somewhat like a trident.

Specific diagnosis.—With characters of the genus. In balsam mounts, body elongate, anteriorly narrower, length 1·07—1·75; greatest breadth, in region of pharynx, 0·38—0·46; anterior sucker prominent, 0·125 in dia., subterminal, with eight arrowhead-like tentacles having 2 lateral processes on opposite sides of the main stem, 0·026 long, 0·013—0·016 broad; pharynx 0·08—0·11 in dia., at one-third length of body from hinder end; intestinal sac anteriorly directed, 0·16—0·38 long, reaching middle of body; ovary 0·15 in dia., globular, right-sided, just ahead of equatorial line or

beside intestinal sac; uterine coils in mid-vitellarial field, between posterior testis and anterior level of vitellaria; vitelline follicles minute 0·018—0·02 in dia., from front margin of intestine or ovary to midway between intestine and anterior sucker, number 14—20 on each side; testes oval, larger than ovary, anterior behind ovary, 0·14—0·2 × 0·12—0·16; posterior far behind, to right of cirrus sac, 0·13—0·19 × 0·15—0·18; cirrus pouch large, on left side, 0·29—0·53 long, 0·07—0·12 broad; genital pore ventral, 0·05—0·15 from posterior end; eggs light yellow, 0·0189—0·020 × 0·013—0·015; excretory bladder elongated, broadly tubular, pore postero-terminal.

Host—*Aoria aoria*, Day and *Aoria seenghala*, Day.

2. **Bucephalus aoria**, n. sp

(Figs. 14 and 15)

Host—*Aoria aoria*, Day = *Macrones aoria*, Day.

Habitat—Small intestine.

Locality—Allahabad.

Description.—In two of the fishes of the above-named species, a few examples of a gasterostomum, different from the one just described as *B. tridentucularia*, were met with. The majority of them were dead before they could be fixed, and some had died within the host before it was dissected. In the latter, the anterior third of the body had got drawn out into a delicate, long, neck-like portion. They were therefore but poorly preserved. The tentacles in them are, however, more clearly seen (F. 15, ten.) than in comparatively better preserved individuals.

The worms are small, elongated in form, with the body slightly thicker about its middle. Their size varies from 0·8—1·0 in length and from 0·25—0·27 in maximum width, in the unpreserved state. On fixation the length is somewhat reduced (0·5—0·6). The anterior sucker is ventrally faced and measures 0·118—0·14 in diameter (Fig. 14). It bears along its latero-dorsal margin a number of short processes or fimbriae, somewhat like those of *B. gorgon* Linton 1905, but the tentacles in the Indian species are much smaller than those in the American form. In numbers the tentacles appear to vary from 14 to 22 in different individuals examined; but, owing to insufficient material I am not quite certain of their exact number. In other respects also the new species differs from *B. gorgon*, the only representative of the genus with 18 tentacles. Dr. Linton has very kindly promised to send me his slides of this and other American forms described by him, but as he is at present away from his head-quarters, they are likely to reach me not earlier than May next.

They will therefore be taken into consideration in a subsequent part of this communication

The pharynx is round, with a diameter 0'6, and is situated behind the middle of the body; the œsophagus is short and leads into the sac-like intestine directed anteriorly or dorso-laterally. The intestine measures 0'125 in length and 0'05 to 0'067 in breadth in life.

The ovary is rounded (Fig. 14, o) and lies about the middle length of the body, towards the right side. Its diameter varies from 0'06 to 0'08. The vitelline follicles are arranged in two compact masses, one on each side of the body, from level of anterior margin of ovary to midway between it and the sucker. They are minute, 0'01 to 0'014 in diameter, and vary from 16 to 20 in number on each side. The testes are nearly ovoidal or somewhat triangular in outline, and nearly as big as the ovary. In position, however, they vary somewhat. The anterior, in all

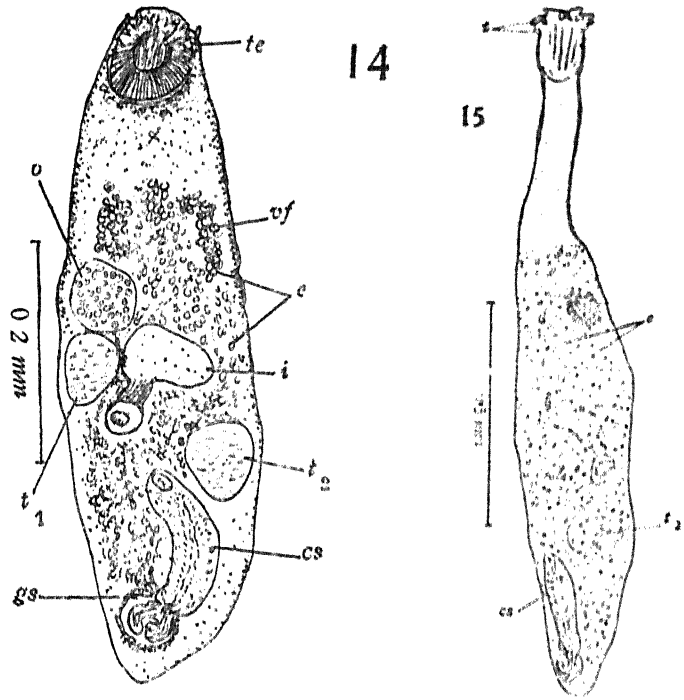

Bucephalus aoria, n. sp. Figs. 14 and 15.

Fig. 14. Ventral view.

Fig. 15. Dorsal view of an elongated specimen, poorly preserved.

specimens examined, follows closely behind the female gonad, and measures 0'06 × 0'04. The posterior lies, in some preparations, on the same

side as the anterior and is separated from it by a distance nearly equal to half its length. But in some mounts, the posterior testis occurs on the opposite of the body, with the pharynx intervening between it and the anterior. This condition does not appear to be a normal feature. It measures 0·05—0·08 × 0·04—0·06. The cirrus sac is nearly equal to one-fourth the length of the body, and encloses within it a small seminal vesicle and other parts characteristic of the genus. The genital sinus is large, with the bifid muscular tongue inside, and is surrounded by a narrow circle of unicellular glands. The genital pore is subterminal. The eggs are light yellow in colour and 0·012—0·016 × 0·0106—0·011 in size.

The excretory bladder was not seen.

Thus, the form is provisionally described as a new species, as I consider it distinct from *B. gorgon*, but I reserve my final opinion, pending the arrival of the American material.

The specific diagnosis also is not given, but will be furnished when better preserved material is available.

References

Braun, M. 1879—1893. *Klassen und Ordn. des Thier-Reichs*, pp. 912-913.

Eckmann, F. 1932. *Zeitsch. f. Parasitenk.*, **5**, 94—111.

Lacaze-Duthiers 1854. *Ann. d. Sc. Nat.*, Paris, 4 ser., **1**, 294-302.

Lebour, M. V. 1908. *Northumberland Sea Fisheries Report* for 1907.

Linton, E. 1901. *Bull. U. S. Fish. Com.* for 1899. **19**, 407-492.

„ „ 1904 (1905). *Bull. Bur. Fisheries, Washington*, **24**, 321-428.

„ „ 1910. *Papers from the Tortugas Lab. Carnegie Inst. Washington*, (Pub. No. 133), **4**, 11-98

Luhe, M. 1909. *Die Susswasserfauna Deutschlands*, 217.

Nicoll, W. 1914. *Parasitol.* **3**, 322—359.

„ W. 1924. *Parasitol.* **16**, 127.

Ozaki, Y. 1924. *Dobutsu Gaku Zasshi*, **36**, 173—201.

„ „ 1928. *Jap. Jour. Zool.*, **2**, 35-60.

Van cleave, H.J. and Mueller, J. F. 1934 *Roos. Wild Life Ann.*, **3**, 161—334.

Woodhead, A. E. 1929. *Trans. Amer. Micros. Soc.*, **48**, (3), 256—275.

„ „ 1930. *Ibid*, **49**, (1); 1-17.

Yamaguti, S. 1934. *Jap. Jour. Zool.*, **5**, 249—541.

In the above and in the following a dot is used to denote a differentiation with regard to time and a dash to denote a differentiation with regard to χ.

The Energy-Momentum Identity

There is an identity which has to be satisfied by the energy tensor

$$T_\mu^\nu = (\rho + p)\, g_{\mu\sigma}\, v^\nu v^\sigma - p g_\mu^\nu \qquad (10)$$

when the line-element is of the form (4). For such a form

$T_2^3 = T_3^2 = T_2^4 = T_4^2 = T_3^4 = T_4^3 = T_1^3 = T_3^1 = T_2^1 = T_2^1 = 0$ giving

$v^2 = v^3 = 0$. Since v^i is a unit vector satisfying

$$1 = -\mathrm{R}^2\,(v^1)^2 + S^2(v^4)^2 \qquad (11)$$

$$T_1^1 = -\mathrm{R}^2\,(\rho + p)(v^1)^2 - p \qquad (12)$$

$$T_2^2 = -p \qquad (13)$$

$$T_3^3 = -p \qquad (14)$$

$$T_4^4 = -(\rho + p)\, S^2\,(v^4)^2 \qquad (15)$$

$$T_1^4 = -(\rho + p)\, \mathrm{R}^2\,(v^1)(v^4) \qquad (16)$$

we have on eliminating (v^1) and (v^4), $\rho + p$ and p from (11), (12), (13), (14), (15), and (16)

$$S^2(T_1^4)^2 + \mathrm{R}^2\,(T_2^2 - T_1^1)\,(T_2^2 - T_1^1) = 0 \qquad (17)^*$$

The last result is similar to the result obtained by Walker[2] for an isotropic line-element. The identity (17) has to be satisfied by the components of the energy momentum tensor given above. The differential

* Several solutions of the equation (17) have been given by V. V. Narlikar and Moghe in two papers, *Phil. Mag.* Dec. 1935 p. 1104; *M. N. R. A. S.*, 1935 Supp. p. 735.

equation obtained by substitutions in (17). We will call this the equation of state for the condensation.

The Solution of the Equation of State

In order to solve the differential equation of state we make further the assumption that $R = R(t)$ and $R_1 = R(t)T(\chi)$. If also $S = 1$ the differential equation becomes.

$$(T'^2 - T\,T'')\ \sin^2\chi + (T' - 1) = 0 \qquad (18)$$

This may be easily solved by using the substitution $T\sin\chi = u$ which transforms (18) into

$$u\,u'' = u'^2 + 1 \qquad (19)$$

The only solutions of (19) which gives a distribution of matter free from singularities are the particular solutions $T = 1$ and $T = \cos\chi$: the former gives the non-state universe while the latter does not seem to be of any practical interest.

The hypothesis $S = 1$ is of no interest for the problem that we have proposed to solve since S has to be to the first order of approximation the gravitational potential of the spherical condensation. We have however given thought to the hypothesis $S \neq 1$ in order to investigate whether there are any new solutions of interest.

Taking $R = R(t)$, $T = 1$; and $S = S(\chi, t)$ the differential equation of state is obtained in the form

$$\dot{R}^2 \cdot SS_{11}\,[2R\ddot{R} - 2\dot{R}^2 - 2R\dot{R}\dot{S}/S]/S_1^2 + S^2S_{11}\,[S_{11}(1 - y^2) - 2S_1y + 2S^2/S_1^2] = 0. \quad (20)$$

Where $y = \cos\chi$ and $S_1 = dS/dy$, $S_{11} = d^2S/dy^2$. A solution of this seems to be available in series. Let us assume

$$S = a_0 + a_1y + a_2y^2 + \ldots + a_n\,y^n + \qquad (21)$$

Where a_0, a_1,...etc. are all functions of time. In view of the form of the static solution we may take $a_2 > a_1$. There is no loss of generality in taking a_0 a constant. Assuming that the series (21) is convergent we obtain the coefficients a_2, a_3...etc. in terms of a^0 and

a_1. The boundary conditions fix a_o and a_1 as in the static case. Of the first few terms we will give only a_2 and a_3, the rest, which are more complicated, may be obtained similarly.

$$a_2 = -\frac{(a_o^2 + \dot{R}^2 - R\ddot{R}) \pm \sqrt{\left[(a_o^2 + \dot{R}^2 - R\ddot{R})^2 - 4\dot{R}^2 a_1^2\right]}}{2a_o} \tag{22}$$

$$a_3 = -\frac{a_2\left[\dot{R}\dot{a}_1 + a_1(5\dot{R}^2 - R\ddot{R})\right] + 2a_o a_1 a_2 (a_o + a_2)}{3\left[a_o^2(a_o + a_2) + a_o(\dot{R}^2 - R\ddot{R}) + a_o^2 a_2\right]} \tag{23}$$

a_o and a_1 must be so chosen that

$$\left(a_o^2 + \dot{R}^2 - R\ddot{R}\right)^2 > 4\dot{R}^2 a_1^2 \tag{24}$$

If the two terms separated by the inequality sign become equal a_3 becomes infinite and the solution in series is not valid. The interpretation is that R, $\dot{R}$ and $\ddot{R}$ control the arbitraries a_o and a_1 in this manner.

We should like to express our most sincere thanks to Prof. V. V. Narlikar for suggesting the problem and helping us to work it out.

References.

1. R. C. Tolman: *Relativity, Thermo & Cosmo* p. 247, (1934).
2. A. G. Walker: *Q. J. Maths* (Oxford Series) **6**, 42, 89.

A NOTE ON A GENERAL LINE-ELEMENT

By V. V. Narlikar and D. N. Moghe

Benares Hindu University, Benares

Received November 5, 1935

For a line-element containing no cross-terms some relations are found to exist between the expressions for T_1^1, T_2^2, T_3^3, T_4^4. The equilibrium of a particle in the observer's frame is considered, and an expansion of space is shown to be a necessary and sufficient condition for the first order stability of a particle, at any point, in a world with no cross-terms.

Dingle[1] has recently calculated the three-index symbols and components of the energy momentum tensor for the line-element

$$dS^2 = -Adx_1^2 - Bdx_2^2 - Cdx_3^2 + Ddx_4^2 \ldots\ldots\ldots\ldots \quad (1)$$

Where A, B, C, D are all functions of x_1, x_2, x_3 and x_4. A few properties of (1) deserve attention. The expression for T_4^4, show that

$$-KT_4^4 = -K\rho = f\left(A,\ B,\ C,\ D,\ \frac{d}{dx_1},\ \frac{d}{dx_2},\ \frac{d}{dx_3},\ i\frac{d}{dx_4}\right) \ldots (2)$$

Where f does not contain the second derivative with respect to time of A, B, C, D; and, in fact, only the quadratic terms in $\frac{dA}{dx_4}$, $\frac{dB}{dx_4}$, $\frac{dC}{dx_4}$ being involved in (2), (2) may be treated as the equation of local energy. In the non-static special universe (2) takes the form

$$-K\rho + \frac{3}{R^2} + \frac{3\dot{R}^2}{R^2} - \lambda \quad (3)$$

Converting (3) into a Hamiltonian we can get the two equations of the non-static universe from the Hamiltonian. Taking (2) as a Hamiltonian, however, we do not get the other equations for the components of the energy momentum tensor. It is interesting, however, to note that the equations for the pressure can be obtained by performing certain operations

upon (2). If S (a,b) stands for the operation of substituting a for b and b for a

$$-KT_1^1 = Kp_1 = S(A,D)\, S\left(\frac{d}{dx_1}, i\frac{d}{dx_4}\right) f \quad \ldots\ldots\ldots \quad (4)$$

$$-KT_2^2 = Kp_2 = S(B,D)\, S\left(\frac{d}{dx_2}, i\frac{d}{dx_4}\right) f \quad \ldots\ldots\ldots \quad (5)$$

$$-KT_3^3 = Kp_3 = S(C,D)\, S\left(\frac{d}{dx_3}, i\frac{d}{dx_4}\right) f \quad \ldots\ldots\ldots \quad (6)$$

Another interesting property of (1) may be noted. The three equations of the geodesics whith $x_4 = t$ as the independent variable may be written down in the form

$$\frac{d^2x_\alpha}{dt^2} - \left\{ \mu\ \nu,\ 4 \right\} \frac{dx_\mu}{dt} \cdot \frac{dx_\nu}{dt} \cdot \frac{dx_\alpha}{dt} + \left\{ \mu\ \nu,\ \alpha \right\} \frac{dx_\mu}{dt} \cdot \frac{dx_\nu}{dt} = 0 \qquad (7)$$

$\alpha = 1, 2, 3.$

It is clear from (7) that every point of the space (1) is a point of equilibrium if

$$\left\{ 44,\ \alpha \right\} = 0 \quad , \quad \alpha = 1, 2, 3. \qquad (8)$$

By this it is meant that a material particle placed anywhere at rest in the coordinate system in space (1) will remain permanently so. This means that D must be a function of time. In that case D can be absorbed in the time coordinate and hence it is perfectly general to assume $D = 1$.

Eddington has already remarked that the actual space of the universe may be very irregular—not spherical at all. For such a universe we may consider the line-element

$$ds^2 = -Adx_1^2 - Bdx_2^2 - Cdx_3^2 + dx_4^2 \quad , \qquad (9)$$

every point of space of which is shown to be a possible position of equilibrium.*

*Use is made here of the general method proposed by Prof. V. V. Narlikar for the discussion of stability in a paper communicated to the Royal Astronomical Society; now in the press for the Jan. number of the *M. N. R. A. S.*

For a small motion about a position of equilibrium the geodesics give the equations

$$\frac{d^2x_1}{dt^2} + \frac{d}{dt}\left(\log A\right)\frac{dx_1}{dt} = 0 \qquad (10)$$

$$\frac{d^2x_2}{dt^2} + \frac{d}{dt}\left(\log B\right)\frac{dx_2}{dt} = 0 \qquad (11)$$

$$\frac{d^2x_3}{dt^2} + \frac{d}{dt}\left(\log C\right)\frac{dx_3}{dt} = 0 \qquad (12)$$

For stability it is necessary and sufficient that

$$\frac{d\ (\log A)}{dt}, \quad \frac{d\ (\log B)}{dt}, \quad \frac{d\ (\log C)}{dt}$$

should be positive. It is presumed here that so long as the small motions continue

$$\frac{d\ (\log A)}{dt}, \quad \frac{d\ (\log B)}{dt}, \quad \frac{d\ (\log C)}{dt}$$

vary very slowly.

Applying the above result to the non-static spherical space we get Narlikar's result, that every position of equilibrium in the expanding universe is one of stable equilibrium.

References.

1. R. C. Tolman: *Rel. Thermos. & cosmo* (1934) p. 254.

NITROGEN FIXATION AND AZOTOBACTER COUNT ON THE APPLICATION OF MOLASSES AND SUGARS TO THE SOIL IN FIELDS. PART I.

By N. R. Dhar and E. V. Seshacharyulu

Chemistry Department, Allahabad University

Received January 10, 1936

1. Azotobacter numbers do increase in abundance and reach a maximum where they remain more or less stationary and help the fixation of atmospheric nitrogen when molasses or sugars are added to soil.
2. No correlation or direct proportionality between the Azotobacter numbers and the nitrogen fixed is observed.
3. In the control plot Azotobacter numbers remain more or less stationary.
4. Nitrogen fixation in the tropical soils is not mainly a bacterial process but is aided by photochemical and induced or catalytic oxidations going on simultaneously.
5. Not only the available nitrogen but also the total nitrogen of the soil increases considerably on the application of molasses.
6. Moisture content of the molassed plots is always greater than the control.

In publications from this laboratory it has been shown by Dhar, Mukerji and Kar [1], Dhar and Mukerji [2] that nitrogen fixation takes place on the addition of energy-rich substances like sugars (canesugar and glucose) or molasses to the soil. They have shown that the fixation of nitrogen not only takes place in ordinary soils but also in sterilised soils on the addition of energy-rich materials, when exposed to sunlight. Dhar and Mukerji were able to fix atmospheric nitrogen by the induced oxidation of glucose and canesugar in presence of ferrous hydroxide by passing air that has been previously passed through concentrated sulphuric acid and ferrous sulphate in sulphuric acid, which not only removes atmospheric ammonia and nitric nitrogen but also kills all bacteria. From the results of their experiments, the above authors have concluded that nitrogen fixation in tropical soils is not only a bacterial process but due also to the photochemical and induced oxidations going on side by side since

soil contains oxides of metals like iron, manganese, titanium etc. and is exposed to sun light for several hours daily.

According to the bacterial theory the nitrogen fixation is due to the non-symbiotic organisms such as Clostridium and Azotobacter, which are partially responsible for the fertility of soils leaving apart the symbiotic bacteria leguminosæ. Clostridium works more or less under anaerobic conditions and thus it seems probable that the nitrogen obtained from the air by this organism does not add any considerable quantity to the soil supply under aerobic conditions. The other organism namely, Azotobacter is present in abundance in all tropical soils. This organism is aerobic and is mainly responsible for the non-symbiotic fixation of nitrogen from air. Many workers have shown that Azotobacter in culture media fixes atmospheric nitrogen on the addition of energy-rich substances like carbohydrates and increase in numbers with increase of fixation of nitrogen. But so far no body has been been definite about the nitrogen fixation in field conditions due to Azotobacter. The researches of Dhar and Mukerji have established definitely for the first time that nitrogen fixation can take place in natural conditions in fields when sugars or molasses are added.

No quantitative work has been done either in cultures or in soil under natural conditions to obtain a relation between the actual increase in the Azotobacter numbers and the fixation of atmospheric nitrogen on the addition of energy-rich substances like carbohydrates or the salts of organic acids. The present investigation was, therefore, undertaken by the authors to determine how the Azotobacter in soils under natural conditions will be affected by the application of molasses, which contains about 60% of carbohydrates and whether there is any correlation between the Azotobacter numbers and the amount of fixation of atmospheric nitrogen. Another aim of the present work is to ascertain whether the fixation of atmospheric nitrogen in tropical soils is mainly a bacterial process or due also to other agencies namely photochemical and induced or catalytic oxidations.

Different amounts of molasses 10 and 30 kilograms were added to two equal plots of land of area 144 sq. ft. in the University grounds and a third plot of equal area was kept as control without the addition of

molasses. The Azotobacter count and the nitrogen estimations (ammoniacal, nitric and total nitrogen) of all the three plots were made before the addition of molasses. The plots were dug up twice a month and the same amount of water was added to the three plots at the same time. At regular intervals, the Azotobacter count and the nitrogen estimations of the plots were done. The soil in all the experiments was taken approximately from depths varying from one to nine inches, the surface layer being rejected at all times. Soil was never taken from definite places in the plots but always a random sampling was made from 40 to 50 places in each plot for examination and analysis. Azotobacter counts were made by the plate method using Beijerinck's mannite medium to which 2% agar was added to obtain the solid medium.

Experimental

The general procedure adopted for determining the number of Azotobacter per 1 gram of dry soil was as follows:—

Samples of soil from the same plot were well mixed to ensure uniformity in composition and then sieved. The fine soil so obtained was spread out uniformly and a final random sampling was ensured by picking samples from different places of the spread out layer and throughly mixing them.

Samples from individual plots were treated separately as above. The final samples were used both for bacterial counts and nitrogen estimations.

Beijerinck's medium was used in these experiments.

Tap water	1000 c. c.
Mannite	20 gms.
$K_2 H PO_4$	0·2 gm.

To this were added 20 gms. of agar and sterilised at 20 pounds pressure for 15 minutes to prepare the solid media for plating purposes,

All glass vessels including petri dishes, test-tubes and pipettes were sterilised in a hot air oven at a temperature of 160° for 2 to 3 hours.

0·1 gm. of the mixed soil finally obtained was carefully weighed out into a sterile boiling test-tube, 10 c. c. of autoclaved tap water added, and the tube well shaken for 5 to 6 minutes, which time is generally considered to separate the organisms from the soil. The tube was then allowed to stand for half a minute. A series of sterile dilution tubes with 9 c. c. of autoclaved tap water were taken and 1 c. c. of supernatant liquid from the original tube was transferred by a sterile 1 c. c. pipette with proper precautions to the first dilution tube and the mixture well shaken. Further dilutions were carried out in the same way up to a limit which was found out by experience until 1 c. c. of the mixture in the last dilution tube when plated allowed a growth of 40 to 300 colonies. Platings were done by transferring 1 c.c. from the final and intermediate dilution tubes to sterile petri dishes and pouring 8 to 10 c.c. of melted media and shaking the petri dishes in the usual way until the media was set to ensure an even distribution of the colonies.

The plates were incubated at 30 - 31° for three days and counted on a proper counting chamber illuminated by an artificial light with the help of a lens 2½ inches in diameter and of 4 inches focal length. Only plates containing 40 - 300 colonies were counted and an average of 4 plates was taken.

The Azotobacter content of each sample of soil was counted as above separately for three times and the final average of 12 counts obtained.

The types of colonies included in the count were pale raised rounded colonies, round raised concentric and semitransparent with denser whitish centres and deep white and greyish colonies elliptical to spindle-shaped and milky white raised colonies.

The correctness of the selection of Azotobacter colonies was invariably tested before commencing the counts by morphological examinations of the organisms of various types of colonies.

The moisture content of the soil under examination was also simultaneously determined by heating 1 gm. of soil in an air oven at 100° for 1 hour and noting the loss in weight.

From the figures obtained above the Azotobacter content of 1 gram of dry soil was finally calculated.

Chemical Analysis

The ammoniacal nitrogen in the soil was determined in the following way. 50 grams of soil which was dried in a steam oven were treated with 5 grams of pure potassium chloride and 5 grams of pure magnesium oxide and about 100 c.c. of water and distilled for six hours on a water-bath. At the same time a current of air purified by passing through a solution of ferrous sulphate in sulphuric acid was aspirated. The ammonia was absorbed in two conical flasks containing standard solutions of sulphuric acid. The ammonia that was obtained was determined colorimetrically by nesslerization in a Duboscq Colorimeter.

The nitric nitrogen of the soil was estimated by treating the soil from which ammonia has been removed by the previous procedure with 1 gm. of Devarda's alloy free from ammonia and nitrate and 25 c. c. of 1% sodium hydroxide solution and left over night for the reduction of nitrite and nitrate to ammonia. When the reduction was complete the ammonia set free was estimated as in the first stage.

The total nitrogen was estimated according to the method of Robinson, McLean and Williams[3] by heating 5 gms. of well dried and powdered soil with 20 c. c. pure concentrated sulphuric acid, 5 gms fused potassium sulphate and a few crystals of copper sulphate for four hours. The ammonium sulphate thus formed was estimated as before.

In the estimation of nitrogen the same soil sample used for bacterial determination was utilized.

The following results have been obtained:—

Molasses applied to the plots on 22-10-1935.

Control plot

Date	Ammoniacal Nitrogen %	Nitric Nitrogen %	Available Nitrogen %	Total Nitrogen %	Moisture content %	Number of Azotobacter in millions per 1 gram of dry soil.
22-10-1935					1.8	2.3
26-10-35	0.00124	0.00304	0.00428	0.082	3.28	2.3
30-10-35					2.5	2.4
3-11-35	0.0013	0.00304	0.00434	0.08	1.8	2.0
7-11-35					3.1	2.3
11-11-35	0.001216	0.003	0.004216	0.0792	3.0	2.7
15-11-35	0.001216	0.003	0.004216	0.0792	2.5	2.3
22-11-35	0.001216	0.003	0.004216	0.0792	3.1	2.5
30-11-35	0.001216	0.003	0.004216	0.0792	2.9	2.3
7-12-35	0.001216	0.003	0.004216	0.0792	2.2	2.6
18-12-35	0.001216	0.003	0.004216	0.0792	5.7	2.8
29-12-35	0.001216	0.003	0.004216	0.0792	4.8	2.5
18-1-36	0.001216	0.003	0.004216	0.0792	2.8	2.1

Control plot

Date	Ammoniacal Nitrogen %	Nitric Nitrogen %	Available Nitrogen %	Total Nitrogen %	Moisture content %	Number of Azotobacter in millions per 1 gram of dry soil.
5-2-36	0.001216	0.003	0.004216	0.0792	2.2	2.6
12-3-36	0.0012	0.00288	0.00408	0.078	4.24	1:3

Plot containing 10 Kilograms of Molasses

Date	Ammoniacal Nitrogen %	Nitric Nitrogen %	Available Nitrogen %	Total Nitrogen %	Moisture content %	Number of Azotobacter in millions per 1 gram of dry soil
22-10-1935					1.7	5.1
26-10-35	0.00155	0.003398	0.004948	0.088	4.3	5.2
30-10-35					4.0	8.8
3-11-35	0.0024	0.003424	0.005824	0.0884	3.3	17.9
7-11-35					3.9	16.7
11-11-35	0.002846	0.003648	0.006494	0.0912	3.86	17.7
15-11-35	0.002904	0.003688	0.006592	0.0912	3.5	16.4
22-11-35	0.003048	0.003904	0.006952	0.0932	4.56	16.8

Plot containing 10 Kilograms of molasses

Date	Ammoniacal Nitrogen %	Nitric Nitrogen %	Available Nitrogen %	Total Nitrogen %	Moisture content %	Number of Azotobacter in millions per 1 gram of dry soil
30-11-35	0.002874	0.003952	0.006826	0.0932	3.1	17.2
7-12-35	0.00284	0.004	0.00684	0.0932	2.85	17.8
18-12-35	0.00284	0.004	0.00684	0.0932	6.8	22.2
29-12-35	0.002824	0.004	0.006824	0.0922	5.2	20.4
18-1-36	0.0028	0.00392	0.00672	0.0922	3.1	21.0
5-2-36	0.0028	0.00392	0.00672	0.0922	3.0	22.6
12-3-36	0.0024	0.00369	0.00609	0.0912	5.3	10.7

Plot containing 30 Kilograms of molasses

Date	Ammoniacal Nitrogen %	Nitric Nitrogen %	Available Nitrogen %	Total Nitrogen %	Moisture content %	Number of Azotobacter in millions per 1 gram of dry soil
22-10-1935					1.2	6.4
26-10-35	0.002208	0.00396	0.006168	0.0953	5.4	6.6
30-10-35					4.3	6.8

Plot containing 30 Kilograms of molasses

Date	Ammoniacal Nitrogen %	Nitric Nitrogen %	Available Nitrogen %	Total Nitrogen %	Moisture content %	Number of Azotobacter in millions per 1 gram of dry soil
3-11 35	0.002472	0.00399	0.006462	0.0953	3.8	4.7
7-11-35					4.2	7.2
11-11-35	0.002664	0.004048	0.006712	0.0966	4.3	57.7
15-11-35	0.002728	0.004048	0.006776	0.0966	4.0	5830.0
22-11-35	0.0028	0.004048	0.006848	0.0966	5.4	5960.0
30-11-35	0.002904	0.004048	0.006952	0.0976	4.3	5040.0
7-12-35	0.003048	0.004096	0.007144	0.1	4.1	25600.0
18-12-35	0.003728	0.004096	0.007824	0.1024	8.2	27600.0
29-12-35	0.003904	0.0042	0.008104	0.1036	6.5	27500.0
18-1-36	0.0042	0.0043	0.0085	0.1076	4.3	22600.0
5-2-36	0.00448	0.00442	0.0089	0.1076	4.1	25400.0
12-3-36	0.003904	0.00464	0.00854	0.1036	8.0	1410.0

Discussion

From the foregoing results, it is clear that Azotobacter numbers in the soil increase in abundance on the application of molasses and reach a maximum value where they remain more or less stationary. It can also be concluded from the results that the rate at which they developed is not in proportion to the nitrogen fixed. Another interesting fact that we observe from the results is that whenever there was an increased fixation of ammoniacal nitrogen there was almost a steadiness in the bacterial numbers. This fact leads us to the conclusion that fixation of atmospheric nitrogen is not mainly bacterial but being aided by other agencies. If the process of fixation were mainly a bacterial one there should always be an increase in the numbers of Azotobacter with increase of fixation. Moreover, in the case of the plot containing 30 Kilograms of molasses we observe that there was a slight decrease in the Azotobacter numbers compared to the blank in the outset, when there was a considerable increase in the ammoniacal nitrogen. This indicates that the fixation of nitrogen is not entirely a bacterial process. These facts go together to show that there is no real correlation between the Azotobacter numbers and soil nitrogen increase. The Azotobacter do develop abundantly on the addition of molasses to the soil and thus help in the nitrogen fixation besides the photochemical and induced or catalytic oxidations going on simultaneously. Another important fact is that not only the available nitrogen but also the total nitrogen of the soil increases considerably by the application of molasses. Also it can be seen from the results that the moisture content of the molassed plots is greater than the control one. No appreciable change either in the Azotobacter numbers or nitrogen content of the control plot is observed. It is well-known that not only carbohydrates but glycerol, sodium tartrate, sodium succinate, calcium lactate, sodium citrate, sodium propionate, calcium butyrate and potassium oxalate have been utilised as energy sources (compare Lohnis and Pillai [4]) for the fixation of atmospheric nitrogen in culture media. It has been emphasised in the publications of this laboratory that all these substances are oxidised photochemically or by induction or by bacteria with liberation of energy. It is apparent, therefore, that nitrogen fixation is possible when an energy source is availaible by the oxidation of different types of organic substances.

Further work is in progress to see whether the fixation of atmospheric nitrogen in tropical soils is mainly a bacterial one or due also to the photochemical and other agencies.

We are greatly indebted to Captain D. N. Chakravarti, I. M. S. for his kind help in the bacteriological work.

References

1. Dhar, Mukerji and Kar, *Proc. Acad. Sc. U. P.*, **4**, 175, 1934
2. Dhar and Mukerji, *Ibid*, **4**, 330; **5**, 61, 1935.
3. Robinson, Mc. Lean and Williams, *Journ. Agri. Sc.*, **19**, 315, 1929
4. Lohnis and Pillai, *Central. Bakt.*, II, 20, 781, I908

ON THE RECONSTRUCTION OF THE MASS-DEFECT CURVE AND THE STABILITY OF BERYLLIUM ISOTOPE Be_4^8.

By N. K. Saha, Allahabad

Communicated by Prof. M. N. Saha

Received January 6, 1936.

§1. Introduction.

The mass-defect curve for the nuclei He^4, Be^8, C^{12},...Si^{28}... forming the series X_{2n}^{4n} is constructed on the 'new mass-scale' with the help of transmutation data and the few new mass-data of Bethe. The new curve reveals the following interesting points: (1) The nuclei of the light elements of this series are more stable than one would suppose from Aston's old mass-defect curve; (2) The most stable nucleus of this series is Ne_{10}^{20} (having the number of α-particles, $N_\alpha = 5$), and nuclei heavier than this become more and more unstable. This may explain the important fact that the nuclei of this series do not occur beyond Ca_{20}^{40} ($N_\alpha = 10$); (3) From the position of Be^8 on the new curve the mass-defect of this nucleus is found to be almost zero. This raises the important question of stability of Be^8-nucleus and its possible connection with the origin of helium deposits observed by Lord Rayleigh in the mineral beryl. The question is fully discussed from all available mass-data of Be_4^8.

Recent works of Bethe[1] and of Rutherford, Oliphant and Kempton[2] have resulted in the detection of a small error (~ 1 in 3000) in the mass-ratio of He^4: O^{16}, and this has led ultimately to a revision of the whole mass-scale of isotopes. An important consequence of this development is that the old mass-defect curve of isotopes drawn mostly according to the data of Aston and Bainbridge requires reconstruction. It is the purpose of the present paper to carry out this programme for isotopes of the type X_{2n}^{4n} which may be supposed to be built up entirely of 1, 2, 3,....α-particles. The masses of He_2^4, C_6^{12} and O_8^{16} of this series are known from Bethe's works. It will be shown here that the masses of other members of this series Ne_{10}^{20}, Mg_{12}^{24} and Si_{14}^{28} can be calculated from existing data (§2), while there is no data at present with the aid of which it is posible to calculate the exact masses of S_{16}^{32}, A_{18}^{36}, and Ca_{20}^{40}. After this element we do not get any with an isotope having

the formula X_{2n}^{4n}, so that the presumption is when $n>10$, such nuclei become unstable. The mass-defect curve for this series of isotopes, when redrawn according to the new values, reveals several points of interest. These are discussed in §3. The position of the isotope Be_4^5 on the mass-detect curve is of special interest with reference to the stability of this isotope, whose presence is suspected but which has not yet been detected by mass-spectrograph. Moreover Lord Rayleigh[3] has observed large quantities of helium deposits in the mineral beryl. The origin of helium in this mineral containing beryllium has so far been a complete mystery, though it is believed to be connected in some way to the stability of the isotopes of Be. This adds a further importance to the exact position of Be^8 on the mass-defect curve. The question has been fully discussed from a review of all available data (§4) regarding the mass of Be^8.

§2. Calculation of the Masses of Ne_{10}^{20}, Mg_{12}^{24}, Si_{14}^{28} from Transmutation Data.

For calculating the accurate masses of isotopes two alternative methods are available: (1) To determine from a critical examination of the original methods of comparing the mass-spectra of each isotope, what correction, in terms of that for He_2^4 (taken to be $+4x$), should be applied to the old mass-value of any isotope; (2) To select suitable reactions of nuclear transformation experimentally observed, and from the few known mass-data on the new scale to compute the unknown mass of an isotope from such reactions. The first one is the method employed by Rutherford, Kempton and Oliphant, and the second is an obvious extension of Bethe's method. In what follows, we shall proceed according to the second method. This method, although capable of yielding results of great accuracy, is in the first place indirect, and secondly the energy evolved in many reactions cannot be known accurately on account of complicated energy distributions of the bombarding and resulting particles, or due to emission of γ-rays. So the proper selection of nuclear reactions is really a matter of some difficulty, specially for slightly heavier nuclei.

(*a*) *Mass of* Ne_{10}^{20}. According to Bethe's calculation, the masses of the X_{2n}^{4n}-type of isotopes are known up to O_8^{16} on the new mass-scale. The mass of Ne_{10}^{20}, the next isotope of this series, may be obtained by using the reaction:

$$Ne_{10}^{20} + n_0^1 = O_8^{17} + He_2^4 + 3{\cdot}9 \text{ MV} \quad \ldots \quad \ldots \quad (1)$$

observed by Harkins, Gans and Newson[4] in which they bombard Neon by means of Po + Be-neutrons, and α-particles are emitted. The energy balance of this disintegration is observed by them to be $-3{\cdot}9.10^6$ eV. Since on the new mass-scale (Bethe), $O^{17} = 17{\cdot}0040$, $He^4 = 4{\cdot}00336$, $n_0^1 = 1{\cdot}0085$, the reaction (1) therefore yields

$$Ne_{10}^{20} = 19{\cdot}9946.$$

Now Kurie[5] has shown that the reaction (1) may be interpreted as consisting of an intermediate product Ne^{21}_{10}, such that

$$Ne^{20} + n^1_0 = Ne^{21} \quad O^{17} + He^4 \quad \ldots \quad \ldots \quad (2)$$

$$Ne^{20} + n^1_0 + E_t = Ne^{21} \quad \ldots \quad \ldots \quad (2a)$$

$$Ne^{21} = O^{17} + He^4 + E \quad \ldots \quad \ldots \quad (2b)$$

where E is the *proper disintegration energy*, E_t is the *threshold energy* of capture of the neutron, that is, the lower limit of neutron-energy at which disintegration begins. From an interpolation of the curve representing the change in kinetic energy in the reaction for different neutron-velocities, Kurie obtains $E = 3{\cdot}9$ MV and $E_t = 7{\cdot}8$ MV. So Ne^{21} may be calculated either from (2a) or (2b). In this way we obtain

$$Ne^{21} = 21{\cdot}0114$$

from (2a), and 21·0115 from (2b).

(*b*) *Mass of* Mg_{12}^{24}. Next we can calculate Na_{11}^{23} and Na_{11}^{24} from Lawrence's data. Lawrence[6] bombarded sodium by deuterons of 2·15 MV energy, and observed α-particles, protons and electrons to be emitted. The following reactions were suggested:—

$$Na_{11}^{23} + H_1^2 = Ne_{10}^{21} + He_2^4 \quad \ldots \quad \ldots \quad (3)$$

$$Na_{11}^{23} + H_1^2 = {}^*Na_{11}^{24} + H^1 \quad \ldots \quad \ldots \quad (4a)$$

$${}^*Na_{11}^{24} = Mg_{12}^{24} + \bar{e} + \gamma\text{-rays} \quad \ldots \quad (4b)$$

In reaction (3), the energies of the deuteron and the α-particle, and the recoil energy of Ne^{21} are respectively 2·15 MV (= 0·0023 mass-units), 7·3 MV (= 0·0078 mass-units) and 0·0017 mass-units. So using $H^2 = 2{\cdot}0142$, we get

$$Na_{11}^{23} = Ne^{21} + He^4 - H^2 - 0{\cdot}0023 + 0{\cdot}0078 + 0{\cdot}0017$$
$$= 23{\cdot}0078,$$

The nucleus ${}^*Na_{11}^{24}$ produced in the reaction (4a) is radioactive and the protons emitted have their ranges distributed over a wide limit from

10 to 49 ± 2 cms (of air). Assuming the proton group of longest range (energy 6·2 MV$\equiv$0·0067 mass-units) to correspond to the $*Na^{24}$ - nucleus in its ground-state, we at once get

$$Na_{11}^{24} = Na^{23} + H^2 - H^1 + 0{\cdot}0023 - 0{\cdot}0067 - 0{\cdot}0006$$
$$= 24{\cdot}0089,$$

0·0006 mass-units being the energy of the recoil nucleus Na^{24}.

From reaction (4b) we can calculate Mg_{12}^{24} which is formed by the disintegration of $*Na^{24}$ with the emission of a negative electron of maximum energy limit 1·2 MV. Strong γ-rays of energy 5·5 MV are emitted in this process. Allowing for these, we can calculate

$$Mg_{12}^{24} = Na^{24} - \bar{e} - 0{\cdot}0013 - 0{\cdot}0059$$
$$= 24{\cdot}0012.$$

(c) *Mass of* Si_{14}^{28}. To obtain the mass of Si_{14}^{28} starting from that of Mg_{12}^{24}, we have to pass through the calculations of the masses of Al_{13}^{27}, and Al_{13}^{28}. Now Al_{13}^{27} is given in terms of Mg_{12}^{24} by the reaction

$$Mg_{12}^{24} + He_2^4 = Al_{13}^{27} + H^1 - 1{\cdot}6 \text{ MV} \quad \ldots \quad (5)$$

observed by Klarmann[7]. This gives

$$Al_{13}^{27} = Mg^{24} + He^4 - H^1 + 0{\cdot}00172$$
$$= 26{\cdot}99820$$

Finally we have the reaction observed by McMillan and Lawrence[8] when Aluminium is bombarded by deuteron:

$$Al_{13}^{27} + H_1^2 = Si_{14}^{28} + n_0^1 \quad (6)$$

$$\begin{cases} Al_{13}^{27} + H_1^2 = *Al_{13}^{28} + H_1^1 & (7a) \\ *Al_{13}^{28} = Si_{14}^{28} + \bar{e} & (7b) \end{cases}$$

$$Al_{13}^{27} + H_1^2 = Mg_{12}^{25} + He_2^4 \quad (8)$$

(7 a, b) represent the main reactions observed. In (7a), allowing for the energy of the deuteron (2·2 MV), the maximum range of the proton groups (63 cms. of air), and the energy of the recoil nucleus Al_{13}^{28}, the energy balance is 5·3 MV. From these data, we can compute Al^{28} as

$$Al_{13}^{28} = Al_{13}^{27} + H^2 - H^1 - 5.3 \text{ MV}$$
$$= 27{\cdot}9987.$$

Finally, we have the maximum energy limit of the β-ray spectrum in (7b) equal to 2 MV, which gives

$$Si_{14}^{28} = Al_{13}^{28} - \bar{e} - 2 \text{ MV}$$

$$= 27{\cdot}996.$$

The masses of isotopes of the type X_{2n}^{4n} calculated above are shown in the following table together with the data already known from Bethe's and others' works. The mass defects $(\Delta m)_a$ are given in mg.

Table 1. *Exact masses of neutral atoms* $(O^{16}=16)$ of X_{2n}^{4n}-type.

Element	Old mass-scale	$-(\Delta m)_a$ in mg	New mass-scale	$-(\Delta m)_a$ in mg
He_2^4 ... a	4·00216	0	4·00336	0
Be_4^8 ... $2a$	...	...	(8·00686 (8·00651	−0·14 } +0·21 }
C_6^{12} ... $3a$	12·0036	2·88	12·0037	6·38
O_8^{16} ... $4a$	16·000	8·6	16·000	13·44
Ne_{10}^{20} ... $5a$	19·9967	11·1	19·9946	22·2
Mg_{12}^{24} ... $6a$	...	—	24·0012	19·0
Si_{14}^{28} ... $7a$	27·9818	33·3	27·996	27·52 ?
S_{16}^{32} ... $8a$	...	—	...	...
A_{18}^{36} ... $9a$	35·976	43·44	...	...
Ca_{20}^{40} ... $10a$	...	...	...	...

The mass-defects in the last column when plotted against N_a, the probable number of a-particles in the nuclei, give us the curve shown in Fig. 1 by full line. The curve in dotted line is the mass-defect curve according to Aston's and Bainbridge's old mass-data.

There is some uncertainty regarding the mass of Be^8 as calculated from transmutation data. Oliphant, Rutherford[2] and others have observed the reaction

$$Be_4^9 + H_1^1 = Be_4^8 + H_1^2 + 0{\cdot}00051 \text{ mass-units} \quad \ldots \quad (9)$$

which yields $Be^8 = 8{\cdot}00686$ using Bethe's mass-values. This gives a positive mass-defect of 0·00014 for Be^8 and makes it just *unstable*. On the other

hand Be^8 is also formed in the reaction

$$B_5^{11} + H_1^1 = Be_4^8 + He_2^4 + 8{\cdot}64 \text{ MV} \quad \ldots \quad (10)$$

which has been observed by Kirchner[9], as well as by Rutherford and others. From this reaction we get $Be_4^8 = 8{\cdot}00651$ using as before Bethe's mass-values. According to this Be^8 has got a negative mass-defect of 0·00021, and it is just *stable*. In our figure (full line) we provisionally plot a zero mass-defect for Be^8 and show the two points corresponding to its slightly negative and slightly positive mass-defects on either side. We shall come to a discussion of this point later on.

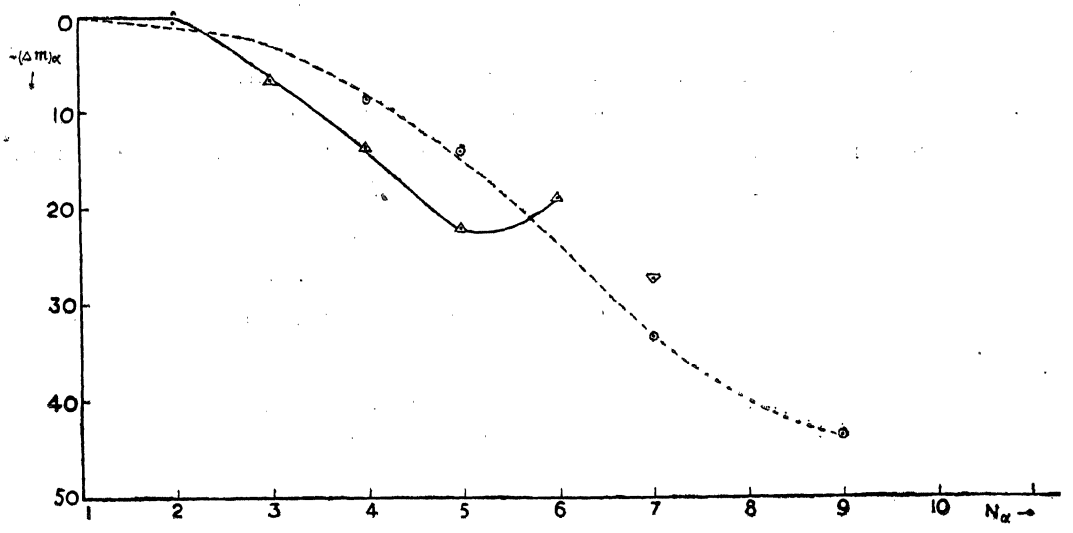

Fig. 1

It will be noticed that all the points lie smoothly on the new mass-defect curve, excepting the last one which corresponds to Si_{14}^{28} The calculation of mass of this isotope from (7) cannot indeed be expected to be accurate, as strong γ-rays are emitted in the reaction (7b) which make the quantitative reaction rather uncertain. We have used this reaction in the absence of any better data.

§ 3. Discussion on the Mass-defect Curve.

The new mass-defect curve shows several points of interest. In the first place the mass defects of very light elements are found in general to be higher than those according to older data (see the dotted curve). This means that their stability is much greater than one would conclude

from Aston's mass-defect curve. Secondly, according to the new curve, the negative mass-defect of isotopes of the X_{2n}^{4n}-series increases rather rapidly with the increase in the number of α-particles (N_α) in the nuclei. But the curve has a minimum somewhere near about $N_\alpha = 5$, that is, for Ne_{10}^{20}, which therefore appears to be the most stable nucleus in the series. The mass-defect then diminishes, indicating that the nuclei with number of α-particles greater than 5 becomes increasingly less stable. This result seems to be significant in view of the well known fact that nuclei of the series X_{2n}^{4n} have not been found, by mass spectrographic methods, to occur beyond C_{20}^{40} (for which $N_\alpha = 10$).

The corresponding mass-defect curve for light elements on the old mass-scale is shown in the same figure by the dotted line. It will be observed that this has a tendency to show an increase in the negative mass-defect of light nuclei right up to $N_\alpha = 10$, and though there is a tendency towards a minimum in the curve beyond this, it is much less pronounced than in the new curve. Thus according to the old curve, nuclei of X_{2n}^{4n}-type should be fairly stable even beyond $C^{40}{}_{20}$, and the non-occurrence of isotopes of this series beyond this cannot be explained.

It may be pointed out here that a similar difficulty exists in the general mass-defect curves for heavy elements drawn according to old data. These curves show generally a minimum near about $N_\alpha = 30$ (Sn^{120}), beyond which they rise rather rapidly. According to these, therefore, many nuclei between Sn^{120} and the radioactive elements, *which are observed to be quite stable*, should really be unstable. Gamow [10] tried to explain this difficulty by assuming that the ordinary mass-defect curve is to be regarded as a composite of a number of smaller curves $f = 0, 1, 2, 3, \ldots\ldots$ according as the number of free electrons in the different groups of nuclei is 0, 1, 2, 3.....Then he was able to show from the intersections of these subsidiary curves that though certain nuclei have got very small mass-defects, the probability of disintegration of these nuclei to pass to more stable nuclei with a transition of electrons or α particles is very small. So stable nuclei may occur among heavy isotopes even with very small mass-defects. But the hypothesis of existence of free electrons in the nuclei has been discarded at present. So this explanation does not hold. It is expected that this difficulty may vanish when the mass-defect curve is

reconstructed on the new mass-scale, as we really find in the case of isotopes of X_{2n}^{4n}–type.

§ 4. Stability of Be^8 and the new Mass-defect Curve.

As has already been mentioned, the mass of the isotope as Be^8 calculated from transmutation data, is to some extent uncertain. The exact mass of this isotope is of great importance for two reasons: (1) Up till now no mass-spectrographic analysis of beryllium has been able to detect this isotope, (2) Lord Rayleigh has observed that helium is found occluded in the mineral beryl, and the proportion of helium in general increases with the geological age of the mineral. It is very probable that the helium gas thus found is due to the spontaneous α–ray disintegration of a radioactive isotope of Be always present in the mineral. One may indeed suppose that this unstable isotope of beryllium is Be^8, which has not really been found by mass-spectrographic analysis to occur in this element under ordinary circumstances. But all attempts by Evans and Henderson,[11] Gans, Harkins and Newson [12] and Libby [13] to detect any radioactivity of ordinary beryllium by using Geiger-Müller counters have ended in failure. The new mass-defect curve does not lead us to any surer ground in this respect, as according to this, the mass–defect of Be^8 may lie between $-0{\cdot}00014$ to $+0{\cdot}00021$, so that it may be either just stable or just unstable. A wider review of all nuclear transmutations where Be^8 is supposed to occur may be useful.

Szilard and Chalmers[14] observed Be emits neutrons under the action of γ-rays. They suggested that one or other of the reactions

$$Be^9+\gamma \rightarrow Be^8+n^1_0\,;\quad Be^9+\gamma \rightarrow 2He_2^4+n^1_0 \qquad \ldots \qquad (11)$$

are possible. From this it appears that the transmutation of Be_4^8 into 2α-particles can easily occur, so that the mass-defect of Be^8 must be very small.

Oliphant, Kempton and Rutherford have observed the following reactions in the transmutation of Boron by protons:

$$B_5^{11}+H_1^1 = Be_4^8+He_2^4+8{\cdot}6\ \text{MV} \quad \ldots \quad \ldots \qquad (12)$$

$$B_5^{11}+H_1^1 = 3He_2^4+8{\cdot}5\ \text{MV} \quad \ldots \quad \ldots \qquad (13)$$

They point out that the difference in energies evolved in the reactions (12) and (13) may be regarded as the binding energy of Be_4^8. This gives the mass of Be^8 less than that of 2α-particles by 0·1 MV, that is,

$$Be_4^8 = 2He_2^4 - 0{\cdot}1\ \text{MV}.$$

This result is independent of all mass-data, and according to it Be^8 should be stable.

Bonner and Brubaker[15] use the reaction

$$Li_3^7 + H_1^2 \rightarrow Be_4^8 + n_0^1 \qquad (14)$$

and from the observed energy of reaction they calculate

$$Be_4^8 \rightarrow 2He^4 + 0{\cdot}3 + 0{\cdot}75 \text{ MV}$$

Crane and Lauritsen[16] have observed emission of γ-rays by bombarding Li with protons, which they ascribe to the reaction

$$Li^7 + H^1 = Be^8 + \epsilon^1 \qquad \ldots \qquad \ldots \qquad (15)$$

where $\epsilon^1 = 16$ MV. Reaction (15) in conjunction with the well-known reaction

$$Li^7 + H^1 = 2He^4 + \epsilon_2 \qquad \ldots \qquad \ldots \qquad (16)$$

where $\epsilon_2 = 17{\cdot}5$ MV, yields

$$Be^8 = 2He^4 + (1{\cdot}5 \pm 0{\cdot}5) \text{ MV}$$

Finally Bernardini and Mando[17] have disintegrated Be by means of γ-rays and have observed a feeble emission of neutrons. On the hypothesis of the formation of Be^8 in this reaction they compute

$$Be^8 \lesssim 2He^4 + 0{\cdot}56 \text{ MV}$$

All these investigations lend evidence to the fact that Be^8 is probably *just unstable*, or if it is stable, it has a very small mass-defect.

One may, therefore, conclude that the helium deposits found in beryl is due to the disintegration of Be_4^8, either in a spontaneous process, or by the action of secondary γ-rays due to cosmic rays found in the atmosphere as suggested by Walke[18].

This, however, does not lead to a final solution of the problem. For the range of α-particles emitted from the supposed disintegration of Be^8, would be very short, and hence its period of decay would be enormously large. So the time necessary for the accumulation of observed amount of helium in beryl would come out on this basis to be much greater than that can be allowed from geological evidences. Further investigations on the radioactivity of Be, will, for these reasons, be highly interesting.

In conclusion, I wish to express my sincere thanks to Professor M. N. Saha F. R. S. for his kind interest and much encouragment in this work.

References

1. Bethe, *Phy. Rev.*, **47** 633, 1935
2. Oliphant, Kempton and Rutherford, *Proc. Roy. Soc.*, **150**, 241, 1935.
3. Rayleigh, *Proc. Roy. Soc.*, **142**, 370, 1933.
4. Harkins, Gans and Newson, *Phy. Rev.*, **44**, 945, 1933.
5. Kurie, *Phy. Rev.*, **47**, 97, 1935.
6. Lawrence, *Phy. Rev.*, **47**, 17, 1935.
7. Klarmann, *Zs. f. Phys*, **87**, 411, 1934.
8. McMillan and Lawrence, *Phy. Rev.*, **47**, 343, 1935.
9. Kirchner, *Naturwiss.*, **22**, 480, 1933.
10. Mott's article in *Handbuch der physik*, **24/1**.
11. Evans and Henderson, *Phy. Rev.*, **44**, 59, 1933.
12. Gans, Harkins and Newson, *Phy. Rev.*, **44**, 512, 1933.
13. Libby, *Phy. Rev.*, **44**, 512, 1933.
14. Szilard and Chalmers, *Nature*, **134**, 437, 1934.
15. Bonner and Brubaker, *Phy. Rev.*, **47**, 973, 1935.
16. Crane and Lauritsen, *Phy. Rev.*, **47**, 420, 1935.
17. Bernardini and Mando, *Phy. Rev.*, **48**, 468, 1935.
18. Walke, *Phy. Rev*, **47**, 969, 1935.

A CRITICAL REVIEW OF THE PRESENT THEORIES OF THE ACTIVE MODIFICATION OF NITROGEN

By M. N. Saha and L. S. Mathur

Physics Department, Allahabad University

Received December 10, 1935

All the existing theories regarding the phenomenon of Active Nitrogen have been criticised in the present paper and the authors have tried to show the inadequacy of each one of them. It is concluded that atomic nitrogen has nothing to do with the active modification and the experiments which establish its presence are not correctly interpreted. It is shown that the long life of the afterglow which is about 5½ hours according to the recent experiments of Lord Rayleigh throws a new complexion on the phenomenon. It is thought that in Active Nitrogen the molecule is raised to some state composed of two ^2D atoms and probably located at 9·77 volts.

The first attempt at a theoretical explanation of the phenomenon of Active Nitrogen was made by the senior author and Dr. N. K. Sur[1] of this laboratory in 1926; they thought that ordinary unexcited molecules of Nitrogen are excited by a discharge to an energy which they estimated to be about 8·5 volts. This excited molecule was supposed to have a very long life and when it collides with a foreign molecule or an atom, then it transfers this energy to the second particle by collisions of the second type. The second molecule or atom is thereby excited to emit its spectrum or become chemically reactive. In this way they attempted to explain many of the results obtained by E.P. Lewis[2], Fowler and Strutt[3].

At the time when this suggestion was made our knowledge of the energy levels of the Nitrogen atom and the molecule was practically non-existent and this suggestion stimulated an extraordinary amount of activity on the subject. All these works gave rise to further theories or modifications of Saha and Sur's theory. In view of these works, and the great advance in our knowledge of the spectrum of the N atom and the molecule[4] it is possible now to take a critical review of these theories.

Birge[5] held that the energy of the metastable molecule was not 8·5 volts as then considered by Saha and Sur but 11·4 volts, a value which is now known to be rather wide off the mark. The next theory was that of Sponer[6] and is now known as the *triple collision theory*. In this it is supposed that by the discharge, the Nitrogen molecule is split up into free atoms. The afterglow is produced when two atoms recombine and the energy of recombination is delivered over to a third molecule which happens to be present at the point of collision. This hypothesis explains to some extent the long life of the afterglow as well as the experimentally observed fact that the decay of the afterglow is not a monomolecular, but either a bi- or tri-molecular reaction. The basis of Sponer's assumption was that the *energy of dissociation of the normal Nitrogen molecule into two* ^4S *atoms is 9·5 volts* a value which was favoured by the knowledge of the molecular spectrum of N_2 available up to that time. It has now been found that this value is too high, for Herzberg[7] has proved that the heat of dissociation of N_2 into two ^4S atoms is 7·34 volts.

In 1929, the above theory was modified by Cario and Kaplan[8] who assumed that Active Nitrogen contains a mixture of metastable molecules of Nitrogen in the A $^3\Sigma$ state, and metastable atoms in ^2P and ^2D states, whose excitation energies are 3·56 and 2·37 volts respectively. It was thought that molecules in A $^3\Sigma$ state are excited to B $^3\Pi$ state with $v' = 10, 11$, and 12 by collisions with ^2P and to the state $v' = 6$ by collision with the metastable atom ^2D. This point is well illustrated in table 1.

From table 1, it will be seen that in the zero vibrational level of the A $^3\Sigma$ metastable state will be raised to the $B^3\Pi$ state with $v = 6$ or 12 by coming in collision with ^2D and ^2P atoms respectively. Thus these bands will be enhanced, as was actually found to be the case in the experimental work of Kichlu and Acharya,[9] Herzberg, Sponer and others.

At the time when this theory was propounded the energy value of the A-level was supposed to be 8·1 volts, so that the energy of the level B_{12} to which the nitrogen molecule was raised by collision with the nitrogen ^2P atom was 11·56 volts, that of the B_6 level which is produced by collision with the ^2D atoms would be 10·48 volts. Now, the energy content of the Nitrogen molecule which by collision of the second type excites atoms to the emission of their characteristic light has been determined with great care by Okubo and Hamada.[10] They find this energy to

Table 1. *Energy in volts of the vibrational levels of the States* $A\ ^3\Sigma'_g$ *and* $B\ ^3\Pi_g$ *of* N_2.

A-level				B-level	
r	V_A in volts	$V_A + {}^2D$ in volts	$V_A + {}^2P$ in volts	r	V_B in volts
0	0·00	2·37	3·56	0	1·18
1	0·18	2·55	3·74	1	1·39
2	0·35	2·72	3·91	2	1·59
3	0·52	2·89	4·08	3	1·70
4	0·68	3·05	4·24	4	1·99
5	0·84	3·21	4·40	5	2·19
6	1·01	3·38	4·57	6	2·38
7	1·16	3·53	4·72	7	2·57
8	1·31	3·68	4·87	8	2·76
9	1·46	3·83	5·02	9	2·94
				10	3·12
				11	3·29
				12	3·46
				13	3·63

be 9·51 volts. The active molecules present in Active modification of Nitrogen in the original theory of Cario and Sponer are

8·1 ($A^3\Sigma$), 10·48 ($B_6{}^3\Pi$) and 11·56 ($B_{12}{}^3\Pi$)

In none of the atomic reactions so carefully observed by Okubo and Hamada special excitation of any line corresponding to any of the above energy values is noticeable.[11]

It is now known from the discovery of Vegard-Kaplan[12] bands that the energy of excitation of A $^3\Sigma$ state is 6·14 volts. When this became known Cario[13] modified his theory. The energy values of the molecular states now come to be 6·14 (A $^3\Sigma$), 9·60 (B_{12} $^3\Pi$), produced by collision with ^2P atoms and (B_6 $^3\Pi$) produced by collision with ^2D atoms. The authors pointed out that the energy of the B_{12} state is just the same which is obtained in the experiments of Okubo and Hamada.

They further pointed out that the metastable atoms $^2P_{\frac{1}{2}}$ would be generated even in the absence of a discharge by impact of two $A^3\Sigma$ molecules as shown below:—

$$N_2\ A\ ^3\Sigma + N_2\ A\ ^3\Sigma = N_2\ ^1\Sigma + 2\ N\ ^2P_{\frac{1}{2}}$$

$$6{\cdot}14 + 6{\cdot}14 = 7{\cdot}34 + 2\ (2{\cdot}37)$$

$$12{\cdot}28 = 12{\cdot}18$$

But ^2D atoms cannot be produced by this process, and the authors suppose that there are more ^2P atoms in the active modification than ^2D atoms.

In support of this theory Cario and Kaplan argue that the presence of atomic nitrogen in the active modification is supported by the experiments of Wrede[14] and Broadway and Jackson.[15] We wish, however, to point out that a critical review of these experiments shows that proper interpretation has not been put on them. A short account of these experiments which is given below will illustrate this point.

Wrede passes through a discharge tube a steady stream of Nitrogen so that the pressure is maintained constant. There are a number of side-tubes and through a diffusion plug inserted in one of these, the gas in the discharge tube is allowed to diffuse to another tube where, if no discharge passes, the pressure would have the same value as in the discharge tube. If the discharge is allowed to pass, the pressure and temperature on the two sides of the diffusion space varies. The change in pressure can only be due to the fact that some of the molecules are broken up by the discharge into atoms and diffuse faster into the other tube where they recombine to form molecules. Let p_o, T_o be the pressure and temperature in the absence of the discharge and p_e, T_e the corresponding quantities when the discharge is passed.

Then it can be shown that the partial pressure of atomic Nitrogen in the discharge tube is given by

$$\frac{p_A}{p_E} = \frac{1 - \frac{p_0}{p_E}\sqrt{T_E}/T_0}{0{\cdot}293}$$

Wrede actually found that about 20 to 30% of atomic nitrogen is produced in the discharge tube under favourable conditions. We accept this result, but wish to remark that the experiment merely proves that, molecules are broken up into atoms in the discharge space. It does not however, prove that free atoms persist in the afterglow space. In fact, recent experiments of Lord Rayleigh,[16] which show that active nitrogen, segregated in a discharge-free space can continue to glow for 5½ hours, absolutely disprove that atomic nitrogen is responsible for active nitrogen phenomena. Any free atom produced in the excited state will die out in course of 10^{-8} sec. and a metastable atom will revert to the normal ^4S state at most in 10^{-1} sec. Free Nitrogen atom in ^4S state cannot remain uncombined for more than a few seconds and even when they combine, the amount of energy set free is too small to produce any of the characteristic reactions. We therefore conclude that production of atomic nitrogen is of course prompted by the same discharge which produces Active Nitrogen phenomenon, but the two phenomena are not connected as cause and effect.

The same remarks apply to the experiments of Broadway and Jackson.[15] They performed Stern and Gerlach's experiment with molecules and atoms from the discharge space and observed the splitting of the beam on a specially sensitised screen. They obtained traces which were interpreted to be due to N $2p^3$ $^2P_{\frac{1}{2}}$ atoms, but this experiment only proves that such atoms are produced in the discharge space. It does not prove that the atoms persist in their free existence when we consider the afterglow space. Hence the presence of $^2P_{\frac{1}{2}}$ atoms on the plate show that atoms are produced in the discharge and have a pretty long life, of the order of 10^{-2} second.

Thus Cario and Kaplan's theory of Active Nitrogen in which the presence of atomic nitrogen plays such a fundamental part cannot be regarded as valid unless atomic nitrogen is found in the real afterglow, quite separate from the discharge space.

Further no atomic lines of N or N^+ have so far been observed in the spectrum of the afterglow. Kichlu and Acharya[9] failed to obtain lines of the Nitrogen atom due to transition N $2p^2$ $(3s\text{-}3p)$, $2p^2$ $(3p\text{-}3d)$ which are at about λ 8200. No attempt has yet been made by any body to obtain in the active modification the resonance lines of Nitrogen $(2p^3 - 2p^2\,3s,\ 2p^2 3d)$ which are in the Schumann region below λ1700. So the presence of atomic nitrogen in the afterglow has not yet been spectroscopically confirmed. The experiment would be difficult to perform for only an absorption experiment with a fluorite spectrograph can decide whether atomic nitrogen in the ^4S, ^2D, and ^2P states is present in the afterglow, or definitely absent.

We therefore conclude that inspite of numerous experiments the presence of atomic nitrogen in any form in the active nitrogen has not yet been established.

Another point which goes against their theory is regarding the dark modification of Nitrogen which Okubo and Hamada[17] have tried to attack. According to Cario and Kaplan's theory when Active Nitrogen is heated or the active gas is allowed to pass through a heated tube the metastable molecules alone survive while the metastable atoms are destroyed. In the absence of the metastable atoms the metastable molecules will no longer be excited to the $B\,^3\Pi$ state to emit the well known α-bands of the afterglow. If this is so, then the total energy-content of the molecule in the "dark modification" should be much less than in the normal activated state. The best way of estimating the energy of the excited molecule is to make them collide with the vapours of such elements whose energy levels are completely known, and which do not chemically react with Active Nitrogen. Okubo and Hamada[17] found that the line of highest excitation even in the case of the so-called dark modification was λ2654·52 $(6s6p\ ^3P—6s8d\ ^3D)$ in the case of Mercury, corresponding to the excitation energy of 9·51 volts.

Okubo and Hamada[11, 18] try to explain the enhancement of certain bands by the application of the Frank-Condon principle. The details of their paper are not available but from a short account of their work which appeared in *Physical Review* before the values of the triplet terms was known, it appears that they consider that by a discharge the Nitrogen molecule has a tendency to be excited to that particular

vibration level of the B or the A state where the normal distance between the atoms (for $X\ ^3\Sigma$, $r_0 = 1{\cdot}09$ A. U.) remains the same for the near-turning point of the Frank-Condon diagram. Thus, there is a concentration of the atoms $A^3\Sigma^{8,11}$ as the details have not been published, it is difficult to form an accurate judgement of the value of this hypothesis.

From the foregoing short review it will appear that the existing theories of molecular structure are quite insufficient to explain the phenomenon. More well-planned experiments are needed to throw light on the subject. Lord Rayleigh's recent work proves that the surface has a strong catalytic action in accelerating the destruction of the glow. He finds that the poisoning action of the walls can be removed by treating the surface with Sulphuric Acid or Meta-phosphoric Acid. The glow then persists for $5\frac{1}{2}$ hours at least. Unfortunately no details have yet been published regarding the spectroscopy of the segregated glow. The total intensity of the light radiated after segregation during the whole period of decay, and the absorption spectrum of the glow should be carefully measured. It has been ascertained that the decay of the glow is either bi- or tri-molecular which proves that the emission of light is provoked by collisions of two bodies or three bodies and Lord Rayleigh prefers the two body collision. It appears to us that the phenomenon can be explained if we suppose that two excited atoms of Nitrogen $N\ ^2D$ or $N\ ^2P$ form an extremely stable state of the molecule in the following way:

$$N\ ^2D + N\ ^2D = N_2\ ^1\Sigma$$

The state produced is such that it does not easily transit to any of the levels A or X being forbidden by two or three selection principles. The energy of this stable state is very nearly 9·77 volts and when this collides with a normal nitrogen molecule it gives its energy to it raising it to the B_{12} or B_{11} state or the B_6 state. These excited molecules then make the transitions according to the Frank-Condon principle giving rise to the especially enhanced bands. When the molecule collides with foreign atoms or foreign molecules it communicates its energy to the latter in exactly the same way by collision of the second type.

Attempts are being made to verify some of the suggestions.

References

1.	Saha, M. N. & Sur, N. K.,	*Phil. Mag.*, **48**, 421, 1924.
2.	Lewis, E. P.	*Astrophys. Jour.*, **12**, 8, 1900.
		Ibid, **20**, 49, 1904.
		Phil. Mag., **25**, 826, 1913.
		Nature., **111**, 529, 1923.
3.	Fowler, A., and Strutt, R. J.	*Proc. Roy. Soc.*, **85**, 219, 1911.
		" " " **85**, 377, 1911.
		" " " **86**, 56, 1911.
		" " " **86**, 105, 1911.
		" " " **86**, 262, 1911.
		" " " **88**, 110, 1912.
		" " " **92**, 438, 1916.
		" " " **93**, 254, 1917.
4.	Mathur, L. S. & Sengupta, P. K.	*Proc. U. P. Acad. Sc.*, **5**, 187, 1935.
5.	Birge, R. T.	*Nature.*, **114**, 642, 1924.
6.	Sponer, H.	*Zeits. f. Phys.*, **34**, 622, 1925.
7.	Herzberg, G. & Sponer, H.	*Zeits. f. Phys. Chem.*, **26**,1,1934.
8.	Cario, G. & Kaplan, J.	*Zeits. f. Phys.*, **58**, 769, 1929.
9.	Kichlu, P. K. & Acharya, D. P.	*Proc. Roy. Soc.*, **103**, 168, 1929.
10.	Okubo, J. & Hamada, H.	*Phil. Mag.*, **5**, 372, 1928.
11.	Okubo, J. & Hamada, H.	*Phy. Rev.*, **42**, 795, 1932.
12.	Kaplan, J.	*Phy. Rev.*, **45**, 675, 1934.
13.	Cario, G.	*Zeits. f. Phys.*, **89**, 523, 1934.
14.	Wrede, E.	*Zeits. f. Phys.*, **54**, 53, 1929.
15.	Broadway & Jackson,	*Proc. Roy. Soc.*, **127**, 678, 1930.
16.	Rayleigh, Lord.	*Proc. Roy. Soc*, **151**, 572, 1935.
17.	Okubo, J. & Hamada, H.	*Phil. Mag.*, **15**, 103, 1933.
18.	Okubo, J. & Hamada, H.	*Astrophys. Jour.*, **77**, 130, 1933.

A NOTE ON THE COLOURING MATTER OF THE FLOWERS OF *LANTANA CAMERA*, LINN.

By Jagraj Behari Lal

Chemistry Department, University of Allahabad

Communicated by Dr. S. Dutt

Received July 26, 1935.

The anthocyanin colouring matter of *Lantana Camera*, Linn (N. O. Verbenaceae) has been isolated following the well-known method of Richard Willstätter in the form of its hydrochloride. (m. p. 195°) The anthocyanin has been named *Camerin* yield 0·026 %.

Lantana camera, Linn (N.O.Verbenaceae) known in Hindustani as *Ghaneri* is a gregarious straggling scandent shrub bearing flowers in small heads which are pretty, pink-orange or lilac, and of many shades in the same plant. It is a native of America and grows wild in many parts of India where it is common in warmer parts including Ceylon. The roots, leaves, and flowers of *Lantana camera* are reputed to be of considerable medicinal value. D. D. Kanger[1] of the Elphinstone college, Bombay has isolated from the leaves and flowers of *Lantana camera* an essential oil whose physical and chemical constants have been worked out. The present author with a view to isolate the colouring matter of the flowers in a pure state and to study its properties undertook the investigation. The flowers have been shown to contain a new anthocyanin which has been named *camerin* after the generic name of the plant.

Experimental

First the fresh flowers (800g.) were extracted repeatedly with boiling alcohol till they were perfectly colourless and the filtered orange alcoholic extract was concentrated on the water bath. The concentrated alcoholic extract on cooling and standing deposited a considerable amount of sticky yellow mass, and the original orange-colour during the course of manipulation turned brownish yellow. The colour change suggested that the

colouring matter of the flowers was an anthocyanin. The concentrated alcoholic extract was repeatedly extracted with light petroleum ether which readily removed a bright yellow colouring matter showing that carotin was present in the flowers.

Isolation of the Anthocyanin:—The anthocyanin present in the flowers has been isolated in a pure state by following the well known method of Richard Willstatter[2]. The fresh flowers of *Lantana Camera* were in instalments of 0·5 kg. extracted in the cold with glacial acetic acid (2·5 litres) in a 3 litre extraction flask which was occasionally shaken to aid the dissolution of the colouring matter. The filtered bluish-violet glacial acetic acid extract was diluted without addition of hydrochloric acid with thrice its volume of ether when the anthocyanin acetate was precipitated in the form of violet-red viscous syrupy mass. By this process anthocyanins are in general separated from tannins as the latter are soluble in ether.[3]

The violet-red mass was separated from the supernatant liquid and dissolved in 0·05 per cent hydrochloric acid (400 c.c.), filtered from the colourless insoluble residue, and the filtrate treated with a solution of lead acetate till no further precipitate came down. The lead salt was filtered at the pump, washed thoroughly with cold water and dissolved in 200 c.c. of glacial acetic acid filtered from the insoluble residue and filtrate diluted with twice its volume of ether, whereby the lead salt of the pigment was precipitated (1·2 g.). The lead salt was then decomposed with 20 per cent methyl alcoholic hydrochloric acid, filtered, and the filtrate precitated by addition of twice its volume of ether, when the anthocyanin chloride separated in reddish-violet flocks. Thus from 6 kilos of the fresh flowers 1·6 gms. of colouring matter of the above purity were obtained. It was purified by redissolving in 1 litre of 20 per cent methyl alcoholic hydrochloric acid and reprecipitating by diluting with 2·5 litres of ether and keeping it in a refrigerator over night. After repeating the process twice 1·3 grams of pure anthocyanin were obtained, which was then finally crystallised from 10 per cent methyl alcoholic hydrochloric acid.

Properties of the Anthocyanin:—It is a dark violet coloured crystalline mass resembling in appearance crystals of potassium permanganate and the air dried product melts at 195° after previous sintering at 180°. In neutral solvents like water, methyl and ethyl alcohols it is slightly soluble to violet-red solutions and in solution it readily isomerises becoming

brownish red and on standing for several hours the colour is completely discharged and colourless pseudo-base separates as a flocculent white mass. In presence of traces of acids it is fairly soluble in methyl and comparatively less so in ethyl alcohol. On addition of a drop of very dilute solution of sodium carbonate the colour becomes violet, then brownish-red, green and finally yellow with excess of the reagent. With caustic soda solution it gives first a green and then a yellow coloration; with alcoholic lead acetate it gives a bluish violet granular precipitate which gradually turns green and after several hours standing yellowish-green due to pseudo-base formation. With ferric-chloride in alcoholic hydrochloric acid solution it gives reddish-green coloration, and with aqueous copper acetate a greenish yellow coloration.

(Found in air dried sample, C = 48·94, 48·76; H 5·73, 5·64; Cl = 3·98 %)

The air-dried *cumerin hydrochloride* contains water of crystallisation which could not be estimated due to insufficiency of material as well as for want of a vacuum dessicator which could be maintained at temperatures other than that of the room. Consequently at present no formula can be assigned to the anthocyanin chloride.

The author wishes to express his best thanks to Dr. S. Dutt, P. R. S., for his kind interest in the work and to the "Kanta Prasad Research Trust" of the Allahabad University for a scholarship which enabled him to undertake the investigation.

References

1. Kirtikar and Basu, *Indian Medicinal Plants*, Part II. p. 985.
2. R. Willstätter and H. Mattosne, *Liebigs Ann. Chem.*, 1915, 08, p. 15–41.
   R. Willstätter and E. H. Zollizer, *Liebigs Ann. Chem.*, 1916, 412. p. 195–216.
3. S. Ionesco. *Compt. rend. Soc. Biol.* 1927, ii, 267.

HYDROGEN ION CONCENTRATION AND TITRATABLE ACIDITY AT DIFFERENT STAGES OF FRUIT RIPENING

By N. L. Pal

Botany Department, University of Allahabad.

Communicated by Dr. S. Ranjan

Received December 2, 1935.

The pH and the titratable acidity of watery solutions of fruits of *Lycopersicum esculentum*, *Psidium Guayava* and *Citrus medica* var. *Limetta* and *Citrus Aurantium* var. *Bidardia* at different stages of ripening were found out. It was found that the actual acidity increased for some time and then decreased in the final stages of ripening. The titratable acidity also increased but this value did not show any fall till the end except in *Lycopersicum*. It did not always correspond with the actual acidity and thus there was no direct relationship between the two.

Organic acids which are specially abundant in fruits are of great importance to the plants. They are important as food reserves and nutrient materials and also helpful in maintaining the pH of the cell sap on which the interactions of various metabolic processes greatly depend. Plant fruits have been very frequently used for physiological studies but their acidity, total and actual, has not been fully worked out.

Haas[1] (1917) working on fruits found that both actual and total acidity greatly vary in different species. He found the actual acidity of juice of pineapple to be 0·000035 N (i.e. having a pH equivalent to this strength of acid when completely dissociated), whereas that of cranberry to be as high as 0·004 N. Similarly, the total acids in apples was 0·071 N, in pineapple 0·0004 N, and in cranberry 0·917 N. There existed no direct relationship between the total and actual acidity in these fruits.

These results were generally supported by works of other authors who worked on various other plant parts employing a wide variety of species.

Thus Atkins[2] (1922) found that there was a wide divergence between the pH of the roots, stems and leaves of the same plants.

Smith and Quirk[3] (1926) working on different parts of *Begonia lucerna* found that the leaves had the pH of 0·9 to 1·36; the top of the shoots pH 1·22 to 2·23 and the base of shoots pH 3·30 to 3·42. The total acidity was in the same sequence, though there was no fixed relationship with the pH.

Martin, Rea and Small[4] (1926) made a great number of estimations of pH of various plants and found that it was constant in some plant parts whereas in others it varied.

Gustafson[5] (1924) estimated the total acid and the H-ion concentration of plant juices of *Zea mais*, *Cucurbita maxima*, *Helianthus sp.* and *Bryophyllum calycinum*. He found that there existed no constant relation between total and actual acidity and that the total acidity was not responsible for the H-ion concentration.

In the present paper an attempt has been made to investigate the changes in the titratable and actual acidity of fruits at different stages of growth which seems to have escaped attention of previous investigators.

The investigations were carried out with four different plants, *Citrus Aurantium* var. *Bidardia*, *Citrus medica* var. *Limetta*, *Psidium Guayava* and *Lycopersicum esculentum*. The procedure was to select fruits of different ages from the same plant and at the same time, and to ascertain the pH and titratable acidity of these fruits. Fruits examined included all stages of growth from very small unripe fruits to fully grown and overripe ones.

The fruits were weighed (after removing the outer covering in cases of *Citrus*-fruits) and then well crushed in a morter, care being taken to remove the seeds of *Citrus* while crushing. As the amount of sap obtained was very small, water to the extent of five times the weight of the fruits was added and a homogeneous solution made. The solution was then centrifuged and the acidity of the clear liquid ascertained.

A point of interest here is that several experiments were performed (the details of which are not given, being of little importance) to find out the change in pH measurements by adding different amounts of water. It was found that addition of water even upto ten times the weight of the fruits did not appreciably change the pH of the solution owing to the high buffer action of the fruit extracts.

The titratable acidity was measured by titrating against standard NaOH of suitable strengths using phenolphthalein as indicator and was expressed as c. c. N/10 NaOH required to neutralise the acid content per gm. of fruit (fresh weight).

The pH was measured by the potentiometric method. Though the atmospheric temperature varied between 23° to 27° C. when these experiments were performed, the calculations of the pH were based upon the average of 25° C. The following table represents the results obtained. Each of the

figures is average of two sets of experiments performed on different days.

Citrus medica.	Size and stage	Green $\frac{1}{4}'' \times \frac{3}{8}''$	Green $\frac{1}{2}''$ dia	Green with slight tinge of yellow at places 1″ dia	Partly green and partly yellow juicy. $1'' \times 1\frac{1}{4}''$	Deep yellow ripe and juicy $1\frac{1}{4}''$ dia.
	pH.	2·77	2·77	2·63	2·63	2·70
	c.c. $\frac{N}{10}$NaOH.	6·76	6·91	6·97	7·12	7·17
Lycopersicum esculentum.	Size and stage	Completely green $\frac{1}{2}''$ dia	Completely green $1'' \times 1\frac{1}{4}''$	Green with slight yellowish tinge. $2\frac{1}{4}'' \times 1\frac{1}{4}'' \times 1''$	Partly greenish yellow and partly red $1\frac{1}{4}'' \times 1\frac{1}{4}'' \times 2''$	Fully red. $1\frac{1}{4}'' \times 1\frac{1}{4}'' \times 1''$
	pH.	4·70	4·50	3·75	3·88	4·00
	c.c. $\frac{N}{10}$NaOH.	0·51	0·46	1·12	1·16	1·03
Psidium Guayava.	Size and stage	Green and very hard 1″ dia.	Green and very hard $1\frac{1}{4}''$ dia.	Green and hard 2″ dia.	Slightly yellow soft. 4″ dia.	Yellow, fully ripe and soft 4″ dia.
	pH.	4·40	4·50	4·40	4·01	3·95
	c.c. $\frac{N}{10}$NaOH.	0·44	0·46	0·46	0·47	0·51
Citrus Aurantium	Size and stage	Green and hard $\frac{1}{2}''$ dia.	Green but less hard $\frac{3}{4}''$ dia.	Green and slightly soft $1\frac{1}{4}''$ dia.	Pale green soft $2\frac{1}{4}''$ dia.	Pale green and softer $2\frac{1}{4}''$ dia.
	pH.	6·02	6·06	6·02	5·88	6·02
	c.c. $\frac{N}{10}$NaOH.	0·17	0·16	0·16	0·16	0·14

Discussion.

For a proper understanding the results obtained are given in a graphical form. The abscissa represents the different stages of fruits and

the ordinate the acidities of the sap solutions. Though all the graphs are drawn to the same scale, in order to compare the titratable acidities and the pH, curves representing these values have been overlapped by suitably changing the origin of one of the scales.

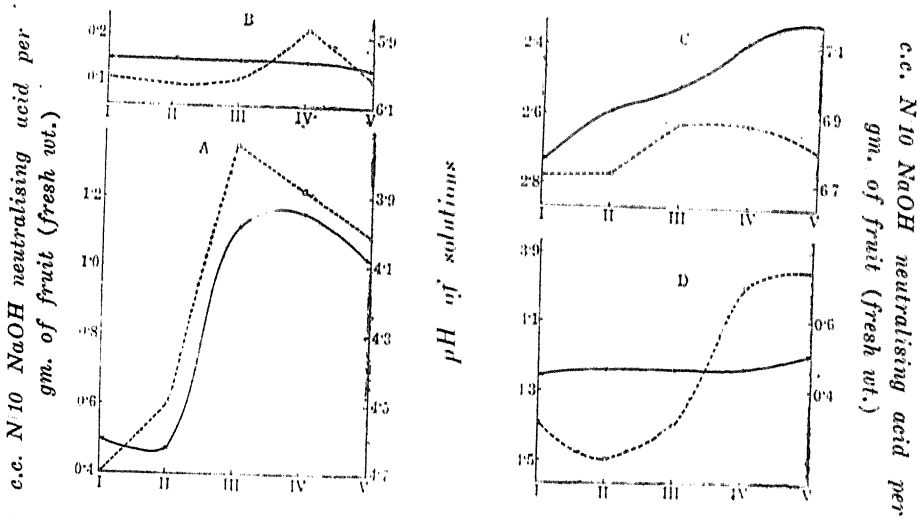

The titratable acidity and pH of fruit solutions at different stages of maturity. Continuous line represents titratable acidity and broken line PH.

A — *Lycopersicum esculentum*; B — *Citrus medica*; C — *Citrus Aurantium*; D — *Psidium guayava*

There are three points of interest in these results. The first is the change in titratable acidities as the fruits ripen. In *Citrus medica* and *Psidium Guayava*, the titratable acidity fairly keeps constant though in the case of the latter there is a tendency for the acidity to rise. But compared to these it goes on rapidly increasing till the end in case of *Citrus Aurantium* while in *Lycopersicum esculentum*, it rapidly rises for some time and then declines in the final stages. Thus the general belief that the acidity of the fruits decreases with increase of age seems to be without any foundation.

The second point of interest is the change in actual acidity (pH). In all cases it rises to a maximum and then slightly falls, except in *Psidium* where probably the last stage examined was not physiologically as ripe as in other cases. The rise, however, is slow in the first stages and in case of *Psidium* it even slightly falls before rapidly rising to the maximum.

A comparison between the titratable and actual acidity curves reveals the difference between the two. In the case of *Lycopersicum* the two curves closely follow each other but in other cases the divergence is evident. Unless the nature of the acids present in the fruits at different stages is fully worked out the exact cause of this divergence is difficult to ascertain. There are two possible causes : (1) Change in the nature or chemistry of the acids by utilisation of the strong ones and replacement of same by a formation of a greater quantity of weak acids. But such a change in the acids of fruits have not yet been demonstrated and this possibility is of little value. (2) The other possibility is an increase of ions responsible for the buffer action. The increase of these ions would automatically change the stronger acids to weaker ones and the actual acidity would fall. This seems to be more probable cause.

Another point of interest is the very wide divergence between the actual acidity and titratable acidity in the different species. The average of all the stages in each is given below. It is, however, to be noted that though the relationship between the two acidities is not constant, the changes in one are accompanied by variations of the same sequence in the other.

	C. medica.	*L. esculentum.*	*P. Guayava.*	*C. Aurantium.*
Actual acidity.	2·70	4·16	4·31	6·00
Titratable acidity.	6·98	0·86	0·47	0·16

My thanks are due to Dr. S. Ranjan for his helpful criticisms and guidance in the progress of this study.

References

1. Haas, A. R., *Bot Gaz.*, **63**, 232. 1917.
2. Atkins, W. R. G., *Agr. Res. Inst. Pusa, Bull,* **136**, 1, 1922.
3. Smith, E. F., and A. J. Quirk, *Phytopath.*, **16**, 491, 1926; *Adv. Sci. Rept.* **94**, 410, 1926.
4. Martin, S. H., M. W. Rea, and J. Small, *British* Assoc.
5. Gustafson, F. G., *Amer. Jour. Bot.*, 11, 365, 1924.

ALKALI SOILS AND THEIR RECLAMATION, PART I

By N. R. Dhar and S. K. Mukerji.

Chemistry Department, Allahabad University.

Received October 24, 1935

(1) Experimental results show that the highly alkaline soils (pH up to 10·8) can be reclaimed by the application of molasses.

(2) The acids present in molasses and produced when applied to soils neutralize the alkali.

(3) The lime present in molasses is rendered soluble by the acids and the soluble calcium salts produced convert the sodium soil of the alkaline fields into a calcium one quickly and deflocculate the alkali soil by forming bigger aggregates and make it more pervious.

(4) The oxidation of the energy rich compounds present in the molasses added to the soil liberates energy which is utilized in the fixation of atmospheric nitrogen and hence the nitrogen content of the alkali soils varying from 0·008 to 0·0025 % increases to 0·05 % as in normal soils.

(5) Alkali Soils are very deficient in micro-organisms due to the high pH values but the addition of molasses causes a great increase of activity and growth of micro-organisms.

Research in Europe and America

Baron Berthollet, one of the greatest luminaries of French Science, who accompanied Napoleon in his Egyptian expedition towards the end of the 18th century was struck by the fact that solid sodium carbonate existed on the banks of the Nile. Being one of the founders of the law of mass action, Berthollet believed that the sodium carbonate was formed by the interaction of sodium chloride obtained by the flooding of the Nile and the calcium carbonate present in the soil. This hypothesis was supported by Hilgard and his colleagues in California, who are pioneers in the reclamation of alkali soils in the United States, and by the workers in the United States Bureau of Soils.

An ingenious explanation of the formation of sodium carbonate was offered by Paul de Mondesir in 1888. He was impressed by the fact that calcium chloride is obtainable in the aqueous extract of a soil

situated near the sea. And he believed that it must have been formed by the action of sodium chloride on the soil. He tried to explain what happened to the sodium, which did not exist in the soluble state. In order to test this point, he treated soil with a solution of sodium chloride in the laboratory and could obtain calcium chloride and an insoluble sodium compound. When calcium chloride is removed by washing, the insoluble sodium compound is easily decomposed by the action of carbonic acid forming sodium bicarbonate and carbonate. By the successive interaction of sodium chloride, water, carbonic acid, and water again, he was able to obtain 100 grams of sodium carbonate from 1 kg. of soil. These experiments can be very readily reproduced and prove, therefore, that the sodium chloride does not react with calcium carbonate as was assumed by Berthollet, but it reacts with the soil forming a sodium adsorption complex and calcium chloride, which can be removed by washing. The sodium adsorption complex can be decomposed by carbonic acid with the formation of sodium bicarbonate and carbonate. The explanation of Paul de Mondesir has been developed and supported by the well-known Russian exponent of soil science, Dr. Gedroiz and is generally accepted.

Principles of Colloid Chemistry were utilized by Gedroiz in his investigations on alkali soils of Russia and their reclamation. Gedroiz observed that the amount of sodium carbonate that could be dissolved by adding water, decreased with successive additions of water. He concluded that the sodium bicarbonate and carbonate existed in the adsorbed state in the soil. When the soil was treated with sodium sulphate or chloride the amount of sodium bicarbonate and carbonate extracted with water increased. When sodium chloride and calcium carbonate were added to soil and extracted with water small amounts of sodium carbonate were obtained. From his experiments Gedroiz concluded that the formation of sodium carbonate in the alkali soil proceeds in three stages–the first is the reaction between the sodium chloride and the soil, the second is the washing away of the soluble product (calcium chloride) and the third is the reaction between the insoluble sodium compound and the carbonate. The simplest explanation is to assume that the sodium chloride reacted with the zeolitic silicates forming a sodium clay, which reacts with the carbonate to form sodium carbonate. This explanation of the formation of the alkaline soils leads us to a method of reclaiming them. Washing away of the carbonate with water is certainly inadequate as long as the clay remains a sodium one. The proper step should be the replacement of sodium

by calcium and this was effected by Hilgard and his associates in California for the reclamation of alkali soils in the Western States of the United States. The alkali soil was treated with gypsum (calcium sulphate) and followed by flooding with water; 12 tons of gypsum per acre of soil was used and this led to the formation of sodium sulphate, which could be washed away and the sodium clay was converted into the calcium one. The gypsum treatment was also adopted in reclaiming large tracts of land in Russia according to the suggestion of Gedroiz and his colleagues.

Powdered sulphur at the rate of 20–30 cwt. per acre has also been used with beneficial results for the reclamation of alkaline soils. By the action of bacteria, chemical catalysts and light, the sulphur is oxidised in the soil forming sulphuric acid, which neutralizes the alkali present in the soil. Ammonium sulphate has also been used, and this reacts with calcium carbonate forming calcium sulphate, which can be washed out by flooding.

The reclamation of Hungarian alkali soils has been carried on by de'Sigmond. The soils containing sodium salts are reclaimed by reducing the evaporation from the surface and by growing lucerne, which requires large amounts of moisture and dries up the soil. In this way the upward movement of the salt is decreased. Press lime, gypsum, farmyard manure etc. have also been used in decreasing the sodium carbonate.

Interesting results have been obtained in the reclamation of the soil spoilt by sea water by Dymond and his colleagues in England. They observed that flooding of land by sea water at first kills the vegetation by the direct action of the salt. When the flood subsided and the rains started, the soils were washed resulting in a partial removal of the salts deposited from the sea water. At this stage the soil was well suited for a good crop yield. But when the soil was further washed by rain, it deteriorated, as the small amounts of salts necessary for the flocculation of the clay particles were removed and the clayey soils did not subside for weeks, and hence cultivation was difficult. Dymond showed that the calcium and magnesium of the soil were displaced by sodium from the salt water. The initial favourable effect was due to the coagulating action of the residual salt, left on the clay. But when the salts were further washed away by rain, the absence of electrolytes caused the soil to be muddy, and flocculation of the clay particles difficult.

Dutch investigators, notably Hissink and his collaborators, from their experience in the Zuider Zee reclamation scheme, are in agreement

with the observations of Dymond and his colleagues. Hissink has stated that the soil left after the sea water has drained away is infertile because it contains sodium clay and in order to make it fertile it must be converted into a calcium clay.

The Dutch investigators have found that the soil in the Zuider Zee area contains a sufficient amount of calcium salts for the conversion of the sodium clay into the calcium one, but the operations takes time, as the calcium in the soil is not in the soluble condition. In the first year after the drainage of the sea water, the soil is sticky, wet and infertile and unsuitable for vegetation. In the second year, the rain water removes a good deal of the salt and the soil dries up appreciably and is suitable for plant growth. But this state of affairs does not last long, and in the third year, practically all the salt is washed out again making the soil sticky and unsatisfactory for cultivation. In the fourth year, the calcium compounds react with the sodium soil converting it into a calcium one ; thus the soil is made suitable for plant growth and at this stage the Dutch farmers begin their cultivation.

It will be evident from the aforesaid that much work has been done in the reclamation of alkali soils and important results obtained in the United States, Russia, Hungary, Holland, England and France.

Research in India

In India experiments were started as early as 1874, by the Irrigation Department for reclaiming alkaline and Usar lands. As no scientist was associated with these researches no definite results were obtained.

"1. The only experiment which can claim to have really reclaimed the Usar land is the application of gypsum. The cost of sufficient gypsum to effect this was very great, about 700 or 800 rupees per acre—and is obviously prohibitive. Even if the cost of gypsum could be reduced to one-half it would still be too expensive if required in the quantity that this land did receive it.

2. The effect of deep and good cultivation coupled with heavy manuring has not been either what is indicated to the unaided eye or what might have been anticipated. The surface foot of soil has been apparently reclaimed but below this the soil is as bad as ever.

3. Scraping of the salts is practically useless.[1] Recently Dr. Dalip Singh and Mr. S. D. Nijhawan[2] have tried to reclaim Kallar (alkaline) soil at Lyallpur, Lalakaku, Montegomary, and Bara farm by the application of a mixture of gypsum and calcium chloride. The pH was 9 before the treatment and it became 8·2 after treatment. They reported that the soil permeability appreciably increases on this treatment after four years and the process of reclamation takes four years, which is also the time required by the application of gypsum or powdered sulphur."

Dr. A. N. Puri is carrying on some experiments in this direction at Lahore. Regarding the success of the work on the reclamation of lands in the United Provinces the following statement of the Director of Agriculture, U. P. is of interest:—

"Usar reclamation experiments were carried on by this Department at Juhi (Cawnpore), and Abbaspur (Unao) without appreciable results and the *Babul* plantations at the places were transferred to the Forest Department. The matter may, therefore, be referred to that Department."

Vast tracts of land in India are alkaline

It is estimated that the total area of *Usar* lands in the United Provinces alone is more than four million acres. Dr. J. A. Voelcker,[3] who examined the extent of alkaline lands in Northern India, stated as follows:—"Enormous areas especially in the plains of Northern India, are thus affected, and in the North-Western Provinces alone, there are between four and five thousand square miles of *Usar* lands". In the Punjab (Lyallpur, Montegomery, and other places), Behar, Mysore, Sind and Bombay, there are vast tracts of such unproductive lands. Naturally the reclamation of these lands is a problem of great importance to India. The salts which make these lands unfit for growing crops, are the carbonate, sulphate and chloride of sodium, sodium carbonate is chiefly responsible for the unproductiveness of such lands, which are generally heavy clay soils and are very often termed *Parti* or waste lands. In Sind and in other parts of the country, normal soils are being converted into alkaline ones by irrigation water. Moreover, there are vast tracts of sea water damaged lands in Bengal, Gujrat, Bombay and Madras Presidencies. Due to various causes the amount of alkaline lands is increasing in India.

Defects of alkali lands.

The chief defects of alkali lands are :—

1. The alkalinity—We have examined several samples of bad *Usar* lands and we find that the pH is as high as 10·8. Neither Azotobacter nor nitrite-formers are observed in cultures obtained with these soils.

2. The amount of calcium compounds is less in these soils than in normal ones.

3. The nitrogen content is small. In several samples examined by us the total nitrogen varied from 0·008 to 0·02%.

4. The soil is highly impermeable to water.

5. The soil particles do not settle readily when shaken with water.

6. The soil lacks bacterial activity.

Molasses and Press mud in the reclamation of alkali soils.

Molasses containing acids, carbohydrates, soluble calcium salts, phosphates, potash etc. can readily remove all these defects of alkaline lands.

Alkaline lands have been successfully reclaimed near Cawnpore, Allahabad and in Mysore by the application of molasses at the rate of one ton per acre and good crops have been grown in these reclaimed areas where no vegetation ever grew.

Our results show that for the reclamation of alkali soils of the dry tracts of Northern India and Mysore molasses can be very usefully applied. It is well known that molasses contains between 60 to 70 per cent of carbohydrates, 4 to 5 % potash, 2 % lime, 0·5 % phosphoric acid, 0·5 % iron and aluminium oxides and 0·5 % combined nitrogen and the rest water. Moreover, molasses is distinctly acidic. Research work carried on in Allahabad, Bangalore, Java, Hawaii, and other sugar-producing countries shows that when molasses is added to the soil, along with carbonic acid, organic acids, like acetic, propionic, butyric, lactic etc. are produced in the early stages in the decomposition and partial oxidation of the carbohydrates present in molasses. Consequently the acids present in molasses and those obtained from the decomposition and partial oxidation can neutralize the alkali of the soils rich in alkali. Moreover, the carbonic acid, which is produced in large amounts from the decomposition and oxidation of the

carbohydrates can convert the sodium carbonate into bicarbonate. Also in the process of the escape of carbonic acid from the molassed soil, the latter is rendered porous and its tilth is improved. The investigations at Allahabad show definitely that the moisture content of the molassed soil is appreciably higher than that of the unmolassed one. The lime, which is added to the soil along with the molasses, is rendered soluble by the organic acids, formed from molasses and is helpful in the conversion of the sodium soil into the calcium one.

The soluble calcium salts are beneficial in the improvement of the soil tilth by their flocculating power on the clay particles. Moreover, in presence of soluble calcium salts, the permeability of the soil is greatly improved. Our results show that molasses is a better reclaiming agent for alkaline lands than either gypsum or powdered sulphur, as there is nitrogen loss from soils when these latter reclaiming agents are added to alkaline soil whilst molasses adds nitrogen. The reclaiming effect of molasses is much quicker than that of gypsum or powdered sulphur, because the acids formed from molasses neutralize the alkali quickly and the soluble calcium salts added with molasses improves the tilth and permeability of the soil. It has been reported that four years are necessary for reclaiming alkaline lands on treatment with gypsum or powdered sulphur but with molasses *four to six months* are quite adequate.

Moreover, as the *Usar* lands contain much less total nitrogen 0·008 to 0·02% as against 0·04 % in normal soils, and as there is nitrogen loss from *Usar* lands on the addition of gypsum or powdered sulphur, it seems improbable that these two substances could be used as reclaiming agents in tropical soils, they may be suitable for the soils of temperate countries as they contain more nitrogen (0·1% total nitrogen).

We have repeatedly observed that the pink colour of phenolphthalein obtained by adding this indicator to *Usar* soil mixed with water is quickly destroyed by adding molasses.

We have carried on comparative experiments on the permeability of water through alkaline soils when treated with gypsum, powdered sulphur and molasses and we have observed that the permeability is increased to a greater extent on the addition of molasses to alkaline soils than with gypsum or powdered sulphur. Moreover, our experiments show that suspensions of alkaline soils in water readily coagulate with

formation of aggregates, which settle very readily on the addition of molasses to the alkaline soil suspensions.

Press mud from sugar factories containing large proportions of carbohydrates and calcium compounds is also very useful in the reclamation of alkali and *Usar* lands. Using one ton of molasses per acre of alkaline land, the Mysore Agricultural Department has been able to grow 1200-1800 lbs of rice per acre of land, where no rice crop could be grown before.

We have carried on comparative experiments in the reclamation of alkali soils by using gypsum, powdered sulphur and molasses.

Experiments in dishes with two samples of Usar soils collected from Phaphamau (Allahabad)

A. 1. 200 gms. soil + 8 gms. gypsum.
2. 200 gms. soil + 8 gms. sulphur.
3. 200 gms. soil + 14 gms. molasses.

} Added and exposed to sunlight in dishes mixed with water.

B. *Exactly similar experiments with another sample of Usar soil. The Alkalinity of the soils after a week was as follows (exposed to sunlight for 33 hours).*

Original soil	A.	contained	0·00663%	Na_2CO_3
,, ,,	B.	,,	0·00504	,,
Soil with gypsum	A.	,,	0·00594	,,
,,	B.	,,	0·00451	,,
Soil with powdered sulphur	A.	,,	0·00583	,,
,,	B.	,,	0·00445	,,
Soil with molasses is acidic	A.	,,	0·00504	[H°]
,,	B.	,,	0·00388	[H°]

After 3 weeks exposed to sunlight for 100 hours

Soil with gypsum	A.	contained	0·0058 %	Na_2CO_3
,,	B.	,,	0·00424	,,
Soil with powdered sulphur	A.	,,	0·0053	,,
,,	B.	,,	0·00397	,,
Soil with molasses is acidic	A.	,,	0·00572	[H°]
,,	B.	,,	0·00437	[H°]

After 5 weeks (exposed to sunlight for 184 hours)

Soil with gypsum	A.	contained	0·00328%	Na_2CO_3
,,	B.	,,	0·00364	,,
Soil with powdered sulphur	A.	,,	0·00291	,,
,,	B.	,,	0·00328	,,
Soil with molasses is acidic.	A.	,,	0·00033	[H^+]
,,	B.	,,	0·00427	[H^+]

The above results show that the acidity of the *Usar* soils treated with molasses and the alkalinity of the soils treated with gypsum and powdered sulphur decreases with time when exposed to light and air in dishes with frequent addition of distilled water.

Ammoniacal, nitric and total nitrogen contents of alkali soils before and after treatment with gypsum, powdered sulphur and molasses and exposed to sunlight.

	NH_3 N	NO_3—N	Total Available N	Total N.
Original soils.				
A.	0·00301%	0·00352%	0·00653%	0·028%
B.	0·00084	0·00096	0·0018	0·0082
Exposed soils for 60 hours to sunlight: analysed on the 28th October 1935				
Soil with 7% molasses containing 60% carbohydrates.				
A.	0·00312	0·0032	0·00632	0·0294
B.	0·00216	0·00096	0·00312	0·0085
Soil with 4% gypsum				
A.	0·00076	0·0032	0·00396	0·0277
B.	0·00014	0·00096	0·0011	0·0077
Soil with 4% Sulphur				
A.	0·00084	0·00344	0·00424	0·028
B.	0·0002	0·00096	0·00116	0·0077
(Added in Proof April 24,1936)				
Exposed to sunlight for 180 hours: analysed on 20-11-35				
Soil with 7% molasses.				
A.	0·00364	0·00342	0·00706	0·0311
B.	0·0042	0·00102	0·00522	0·00921

	NH_3—N	NO_3—N	Total available—N	Total—N
Soil with 4 % gypsum				
A.	0·0004	0·00338	0·00378	0·0262
B.	0·00004	0·000906	0·00094	0·00761
Soil with 4 % powdered Sulphur				
A.	0·00042	0·0033	0·00372	0·0255
B.	0·0001	0·00096	0·00106	0·00758

Alkaline soil from Handia Tehsil, Allahabad.

Started on 2-12-35. analysed 4-1-1936.

Condition	pH.	NH_3—N.	NO_3—N.	Total—N.	Total carbon
Original.	10.8	0·00108%	0·00186%	0·0256%	0·2678%
4 gms molasses per kgm. soil	9·8	0·001472	0·00186	0·0256	0·2878
8 gms " "	9·4	0·00156	0·00186	0·0256	0·415
16 gms " "	8·0	0·00175	0·00136	0·0267	0·6696
32 gms " "	7·0	0·002	0·00186	0·0312	1·338
64 gms " "	5·8	0·00233	0·00184	0·0338	2·431
80 gms " "	5·2	0·00242	0·00175	0·0373	2·81
40 gms gypsum"	1·0	0·001	0·00136	0·0256	0·2678
2 gms.sulphur"	10·6	0·000934	0·00184	0·0256	0·2721
		Analysed on 23-1-36			
4 gms molasses "	9·8	0·001928	0·00187	0·024	0·2761
8 gms " "	9·4	0·001944	0.000187	0·028	0·3821
16 gms " "	8·2	0·001964	0·00186	0·0328	0·5852
32 gms " "	7·0	0·00224	0·00187	0·0334	1·092
64 gms " "	6·4	0·00228	0·00185	0·035	2·132
80 gms " "	5·4	0·00266	0·00184	0·0373	2·511
40 gms gypsum"	8·2	0·000964	0·00187	0·024	0·2678
2 gms sulphur"	10·4	0·000938	0·00184	0·024	0·2721
		Analysed on 13-2-36			
4 gms molasses per kgm. of soil	9·8	0·00196	0·00188	0·0243	0·2721
8 gms " "	9·2	0·00199	0·00188	0·0281	0·3288

Condition	pH.	NH_3—N	NO_3—N	Total—N	Total—carbon
16 gms " "	8	0·002	0·00184	0·0328	0·4892
32 gms " "	7	0·00268	0·00184	0·0344	0·922
64 gms " "	6·6	0·00296	0·00184	0·0365	1·832
80 gms " "	5·8	0·0031	0·00184	0·03925	2·428
40 gm gypsum"	8·2	0·0000946	0·00188	0·0242	0·2622
2 gms sulphur "	10·2	0·00091	0·00184	0·0242	0·2622
Analysed on 28-2-36.					
4 gms molasses per kgm. of soil	9.8	0·00194	0·00184	0·0244	0·2722
8 " "	9·2	0·00196	0·00188	0·028	0·3125
16 " "	7·8	0·0022	0·00186	0·0361	0·4421
32 " "	7	0·0029	0·00184	0·04	0·7259
64 " "	6·4	0·0031	0·00184	0·0422	1·412
80 " "	6	0·0032	0·00184	0·0435	1·9837
40 gms gypsum "	8	0·00096	0·00188	0·0244	0·2684
2. gms sulphur "	10	0·00094	0·00186	0·0244	0·2688
Analysed on 24-3-36					
4 gms molasses "	9·8	0·00096	0·0028	0·0242	0·2731
8 gms " "	9·0	0·00142	0·0028	0·028	0·312
16 " "	7·5	0·00162	0·003	0·035	0·3752
32 " " "	7·0	0·00164	0·00328	0·04	0·3986
64 " " "	6·6	0·00184	0·00348	0·0438	0·4077
80 " " "	6.0	0·00232	0·00372	0·0441	0.6189
40 gms gypsum "	6·0	0·0009	0.00188	0·0231	0·2656
2 gms sulphur "	9·8	0·000882	0·00186	0·0232	0·2632

Alkaline soil from Handia Tahsil, Allahabad, was treated with press mud, containing 44·8% Carbon and 0·583% nitrogen, on the 22nd Jan. 1936.

Analysis on the 3rd Febrary 1936

Original	10·8	0·00108	0·00186	0·0256	0·2678

Condition	pH	NH_3—N	NO_3—N	Total—N	Total carbon
10 gms press mud per kilogm. soil	10·5	0·00092	0·00186	0·035	0·586
20 gms. " "	10·5	0·00121	0·00184	0·0402	0·932
50 gms. " "	10·4	0·00241	0·00186	0·053	1·08
100 gms. " "	1·0	0·0028	0·00186	0·07	2·192
200 gms. " "	9·4	0·0046	0·00184	0·14	4·584
10 gms. " "	10·4	0·00106	0·00186	0·028	0·612
20 gms " "	10·2	0·00106	0·00186	0·0338	0·881
Corresponding dark. 50 gms. " "	10	0·00162	0·0018	0·0437	1·182
100 gms. " "	9·7	0·00186	0·0016	0·056	2·282
200 gms. " "	9·6	0·0024	0·00162	0·08	4·6652

Analysed on the 14th February 1936.

10 gms. " "	10·5	0·00106	0·00186	0·035	0·574
20 gms. " "	10·5	0·00126	0·00186	0·0411	0·8219
50 gms. " "	10·2	0·00232	0·00186	0·0623	0·968
100 gms. " "	9·5	0·0035	0·00186	0·0934	2·095
200 gms. " "	9	0·0056	0·00184	0·1866	4·288
10 gms. " "	10·5	0·001	0·00184	0·0294	0·608
20 gms. " "	10·5	0·00108	0·00184	0·0329	0·8725
Corresponding dark. 50 gms. " "	10·2	0·00176	0·0018	0·0467	1·085
100 gms. " "	9·5	0·00264	0·00162	0·0622	2·212
200 gms. " "	9·2	0·0031	0·00144	0·0998	4·525

Analysed on the 13th. March 1936

10 gm. of press mud per kilogm. soil	10·5	0·00102	0·0012	0·0292	0·3926
20 " "	10·5	0.00108	0·00426	0·0314	0·5042
50 " "	10·2	0·00164	0·00132	0·0609	0·6539
100 " "	9·5	0·0018	0·00214	0·0875	1·2499
200 " "	9·0	0·0035	0·0028	0·1938	2·188

	Condition	pH.	NH_3 N	NO_3 N	Total—N	Total—carbon
Corresponding dark.	10 gms of press mud per kgm. soil	10·5	0·00096	0·00116	0·0292	0·5829
	20 " "	10·5	0·00096	0·00116	0·0323	0·8245
	50 " "	10·2	0·0014	0·0012	0·0472	1·025
	100 " "	9·5	0·00162	0·00122	0·0632	2·186
	200 " "	9·0	0·00186	0·0012	0·0998	4·465

References

1. J. W. Leather, *Investigations on Usar land in U. P.*, p. 37, 1914.
2. Dalip Singh and S. D. Nijhawan, *Indian Agric. Sci.*, **2**, 1, 1932.
3. J. A. Voelcker, *Improvement of Indian Agriculture*, *London*, p. 55, 1893.

STUDIES IN THE RESPIRATION OF MANGO LEAVES (MANGIFERA INDICA)

By N. K. Chatterji

Department of Botany. Allahabad University

Communicated by Dr. S. Ranjan

Received January 8, 1936.

In this paper the ontogenic drift of Mangifera leaves in relation to CO_2 O_2 activity has been traced out.

The CO_2 output as well as the O_2 intake of Mangifera leaves (mango) of various ages have been noted and a correlation has been attempted with the sugar content of these leaves. The differences in the nature of respiration of the two sets of leaves have been attributed to the factor of seasonal periodicity. Stress has been laid on the actual difference of O_2 intake and CO_2 output and a possible explanation of this high oxygen intake has been attempted.

Introduction

In this paper, the ontogenic drift of mangifera leaves in relation to CO_2/O_2 activity has been traced out. These leaves are red when they come out and gradually turn green as they advance towards maturity. The procedure of work has been to start with very young leaves leading on to more mature ones and finally to experiment with old yellow leaves.

New leaves of mangifera come out in two seasons viz. prewinter (from September to November) and post-winter (from January to March) and an attempt has been made to trace the starvation drift of leaves of various ages of both the periods.

The apparatus for the study of respiratory mechanism consists of (i) Leaf-chamber (ii) Aspirator (iii) Haldane's Gas Analysis Apparatus and (iv) Thermostat bath. The whole apparatus in working order is shown in figure 1.

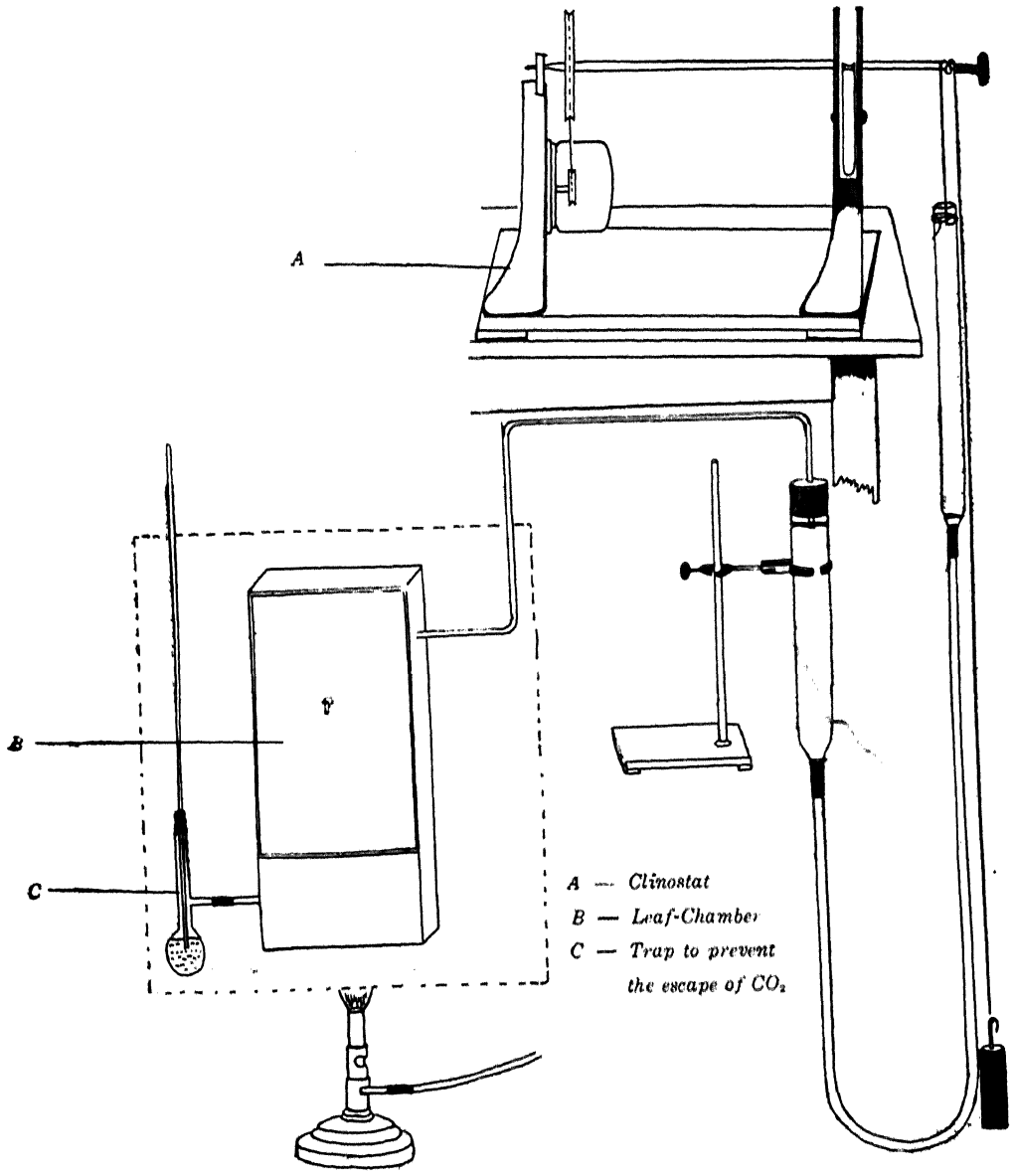

Fig. 1

Method of Experimentation

(i) Leaf-chamber:—A brass leaf-chamber having the dimensions of $9\frac{3}{4}''$ by $4''$ by $1''$ was employed. Inlet and exit tubes were also of brass. To minimise the volume of the chamber melted paraffin was filled in leaving only enough space for the leaf and the petiole (see fig. 1 B.)

The inlet metal tube was connected with a capillary tube which had a water trap at the other end to check the diffusion of the gas outside from the leaf-chamber as shown in fig.1.C.

(ii) Aspirator:—A long graduated glass tube which was fixed by a clamp served as an aspirator. One end of this was attached to another movable glass tube by a pressure rubber tubing. The movable glass tube was worked by a clinostat clock, round the projecting bar of which this tube was attached by a string which was counter-balanced by a weight. The graduated tube and the pressure rubber tubing were filled with mercury and by a gradual lowering of the movable tube the mercury column fell in the graduated tube causing a slow but uniform suction.

Generally 11½ hourly readings were taken when the capillary tube was disconnected from the leaf chamber. The amount of CO_2 and O_2 collected in the graduated tube was then estimated by the well known Haldane's gas apparatus which needs no description.

It would not be out of place to mention here that due to slow suction there is a liability of an increased CO_2 concentration in the leaf-chamber which may bring about a depression in the respiratory process. The researches of Kidd [1] (1914-1915) reveal that there is very little variation in R. Q. up to a concentration of 10%. In the present work, though there may be a slight inhibiting effect of CO_2 concentration, the value of such a procedure exceeds the disadvantages.

(iv) Thermostat bath:—The leaf-chamber was put in the thermostat bath at 34°C. The variation in the temperature did not exceed ± 1°C.

The estimation of O_2 and CO_2 were all reduced to N.T.P. per gm. of leaves (fresh weight) per hour.

Sugar estimation:- For the analysis of sugars a few leaves approximately of the same age with the respiring ones were selected and weighed. After carefully grounding them with sand, a known volume of water was added. The mixture was filtered through a Buchner funnel. Some lead acetate was next added to the solution. The solution was filtered and to the filterate H_2S was passed. To ensure that all lead has been precipitated H_2S was passed a second time. The clear liquid was boiled to remove the excess of H_2S. The volume of the liquid was then carefully noted. This was estimated for sugar by titrating against Pavy's solution (Haas and Hill[2])

Experimental Observations and Discussion of the results

The CO_2 given out by the leaves of various ages and its correlation with the sugarcontent.

The respiration intensities of various ages of leaves at consecutive periods are shown in the form of smooth lines in figure 2.

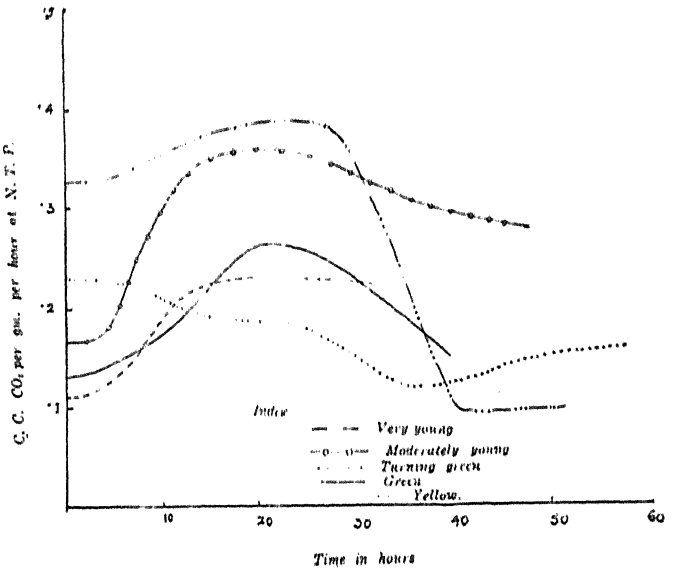

Fig. 2

Practically in all cases except in the yellow leaves, there is at first a tendency, for the respiration rate to go up, but this increased rate never keeps the high level, and within 10 to 20 hours begins to climb down.

Muller Thurgau and Schneider-Orelli[3] (1910) show that a change in temperature has an important bearing on the respiratory process. They say that heating produces an initial increase in respiration intensity which subsequently falls off. Fernandes[4] (1923) also in his work on temperature noticed that raising the temperature to values higher than about 30°C. to 35°C. results in a falling off in respiration rate with time from the initial maximum rate. There is, of course, in all cases an interval of time before this maximum intensity is reached which is known as Time-factor,

Here also the experimental chamber had a higher value than the atmosphere surrounding and the initial rise may be due to higher temperature.

The maximum rate does not keep up the level, but forthwith begins to decline evidently because of depletion of respirable matter.

Sugar estimations of different ages of leaves (Fig. 3) reveal a large excess of the directly respirable sugar in the cells. In the cases of the green leaves, where the amount of sugar is less, iodine test showed that there was a corresponding abundance of starch which was lacking in young and red leaves.

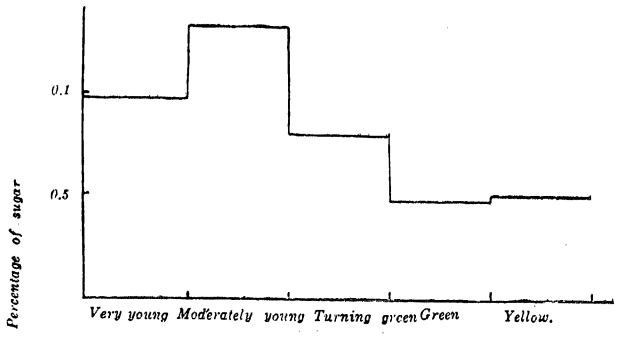

Fig. 3

The sugar concentration starts from the neighbourhood of 1% for the very young red leaves. Thereafter the monosaccharide values fall off in a logarithmic curve to 0·5%. This value is the same for both green and yellow leaves. It may be said, in other words, that the critical concentration of sugars keeps falling off as the leaves approach maturity.

However, interpreting the CO_2 intensities on the basis of sugar values alone, one fails to account for the rise of respiration after a certain hour of experimentation. As a matter of fact there should have been a maximum rate at the very beginning. Clearly then there are some other internal factors which are operating in the mean time.

There is a close parallelism between the maximum rate of respiration and the sugar values of the leaves of various ages. (shown in Fig. 4). The maximum intensity also goes on diminishing with age, and one can conclude the change in respiration of leaves of different ages to be due to the availability of sugar.

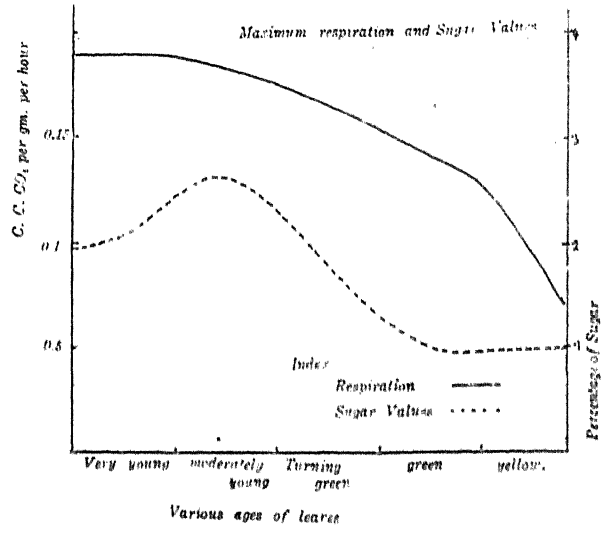

Fig. 4

The maximum respiration rates of each age as shown in figure 4 continue coming down as the leaves progressively proceed towards maturity. The age of the tissue has a marked influence upon the intensity of respiration. Thus Nicolas[5] (1918) noted that the respiratory intensity of young leaves and stems was from three to seven times greater than that of corresponding fully developed organs taken from the older parts of the plants. Bezagu[6] (1919) observed that respiration was relatively weak in young leaves and increased to a maximum at the time the leaf reached its development, after which it decreased as the leaf became older.

Here also the youngest leaves show a decrease in the respiration intensity over the next stage, the reason of which may be attributed to the incomplete growth of the organs concerned.

Kidd, West, and Briggs[7] (1921) also showed that the initial respiratory index of successive leaves decreases with the age of the plant. A similar phenomena is noticed in the present work and the various rates of respiration may be said to be due to the progressive increase in age.

The respiration rates of the Post-winter set are very nearly similar to the curves of the Pre-winter set. The tendency of the leaves in the Post-winter set is to respire more than the leaves in the Pre-winter set.

It has been shown by various workers that the internal factor of seasonal periodicity influences the intensity of respiration. Bonnier and Mangin [8] (1885) working with the perennial plants of temperate climate found that the respiration was greater in spring and showed a slight decrease in summer; a more rapid decrease to a minimum value occurred with the onset of winter, after which the intensity again increased with the return of spring. But at Allahabad the plants grow under tropical climatic conditions; the spring occurs here sometimes in March; summer quickly follows the spring and is very hot and dry. At the end of June the monsoon rains begin and continue until the end of September. After the rainy season, there is a dry autumn followed by winter with low temperature and occasional rains. Thus the general course of respiration will vary according to the season. So a rise in the respiration intensity is noticed in the Post-winter set which is comparatively lower in temperature than the Pre-winter set.

The O_2 intake of the individual records.

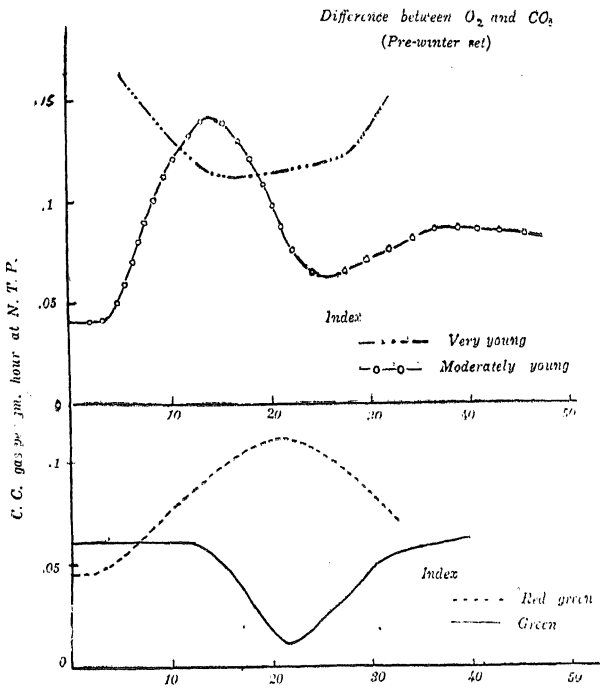

Fig. 5

In the present work along with the CO_2 output of Mangifera leaves of various ages, the O_2 intake have also been undertaken. Stress on the individual O_2 intake has not been given, instead the actual difference between CO_2 output and O_2 intake have been shown and a possible explanation of the high oxygen intake is attempted. The graph showing the O_2 intake of Pre-winter set is given in fig 6.

The nature of the graph of O_2 intake is more or less similar to that of CO_2 output, the difference being only that in all cases the values of O_2 intake is always higher than those of CO_2 output except in few cases e. g. in the case of green leaves, the values of O_2 intake and CO_2 output are the same after 50 hours (Post-winter set). In the case of yellow leaves, however, the values of O_2 intake are sometimes lower than those of CO_2 output.

The difference between O_2 intake and CO_2 output.

Fig. 6 gives graphically the difference between O_2 intake and CO_2 output of the two sets.

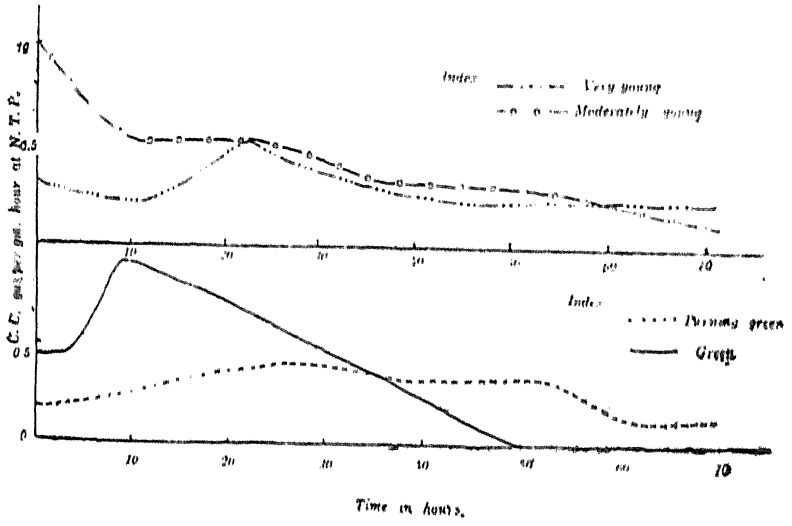

Fig. 6

It is noticed from the graph that with the exception of the young red leaves, the difference starts low, but in about 24 hours it reaches a maximum value and then forthwith begins to decline to a very low value. It may go so low that the difference may become zero in the case of green leaves.

From the simple equation of $C_6H_{12}O_6 + 6O_2 = 6CO_2 + 6H_2O$ + energy, it is clear that in the plant organ where sugar is the substance broken down in respiration, under conditions of a plentiful supply of oxygen, the respiratory quotient should almost invariably be in the neighbourhood of unity. Maquene and Demoussy[9] (1913) investigated the values of respiratory quotient in a number of leaves and have found them to fluctuate between 0·95 and 1·11.

It is clear from the works of many other investigators that the nature of the food reserve in any given organ affects the value of R. Q., but in the case of leaves where carbohydrates are the main substrate for respiration, the R. Q. should approach unity. But in the present work, the respiratory quotient diminishes to a considerable low value such as 0·5. What happens to this extra amount of oxygen ?

Nicolas[10] (1919) working with the leaves which are red when young but turn green later showed that the R. Q. is lower in the red leaves which indicates a greater fixation of oxygen as compared with green ones.

Secondly it may also be possible that the extra amount of oxygen taken in is to a certain extent utilised in the process of development and growth. Cerighelli[11] (1924) reported that respiratory quotient at the beginning of development was always less than unity. Bonnier[12] and Mangin (1885) state that simultaneously with oxygen respiration, there also takes place an independent absorption of oxygen for other purposes (such as formation of organic and carboxylic acids) and this happens in the case of seed germination, vigorous growth and vegetative development.

It may again be possible that sugar is continually being utilized for the formation of some complex substances where additional oxygen may be needed. It has been roughly found in the case of Mangifera leaves that there is a high total acid content in red leaves. If the organic acids are being formed from sugar, it is quite possible that the extra oxygen taken in may be used in the formation of these acids.

In order to ascertain how far acid formation is responsible for higher intake of oxygen, several experiments were afterwards performed on the injection of acids in these leaves. These results which would be published later show a strong possibility of acids being formed from sugar which account for

the high O_2 intake by the plant. This would be dealt with more fully in the above mentioned paper.

The case of the yellow leaves is quite different. It is found that initially the O_2 intake is less than CO_2 output e. g. (−0·07c.c.) it then quickly rises to (+0·04c.c.) and then declines to (+0·01c.c.) and finally to (−0·01c.c.).

It has been noticed in several handcut sections stained with Sudan III that there are oil globules in the yellow leaves while iodine test showed no starch. Thus the previous explanation of oxidation of sugar into organic acid, however, does not hold good in case of yellow leaves. There is not much sugar and starch present in these leaves and therefore the question of oxidation to acid does not arise; moreover, originally the difference of CO_2 and O_2 is negative i.e. CO_2 output is greater than O_2 intake. The appearance of oil in these leaves has a special bearing on this point. This low O_2 intake may be directly due to the formation of such oily substances from sugar. As all fats have a lower oxygen content, it is but natural that when sugars are converted into fats O_2 will be given off.

Pal (1934) [13] has shown that in Spirogyra, the conversion of carbohydrates to fats takes place only in light and the reverse process of transformation of fat to carbohydrates begins to take place as soon as the plants are placed in darn.

The experiment with yellow leaf shows that there is possibility of his scheme holding good in case of higher plants also. When the leaf was cut, it had already been in light and the conversion of sugar to fat had probably proceeded for sometime. At this stage the leaf must have taken in very little O_2 in comparison to CO_2 given out. However, when it was placed in dark, the intake of O_2 began to rise and in 15 hours it rose from −0·07 to +0·04. This shows that the reverse process of conversion of fat to sugar takes place. However, as the quantity of fat got depleted the O_2 intake fell to +0·01 c.c.

Now, comparing the two sets it is found that the differences between CO_2 and O_2 values, in the case of Post-winter set are less than those of Pre-winter set. The variation in the nature of the curves of the two sets may be due to climatic conditions of the two seasons.

The differences of O_2 intake and CO_2 output in the Post-winter set after attaining a maximum value do not rise for a second time except in the case

of the yellow leaves. The secondary rises in these cases may be attributed to the oxidation of some other substances requiring a larger amount of O_2 after certain hours.

Jonesco [14] (1921) finds that plants lose anthocyanins in the dark. He concludes that the anthocyanins are utilised in the nutrition of plants when in darkness. It has also been found here in many cases that after a few days' respiration the red leaves turned to a pale green colour.

Works of Wager, Jorgensen and Kidd [15] (1917) and Osterhout [16] (1918) show that chlorophyll also gets oxidised to formaldehyde in certain cases. These require a higher amount of oxygen for their oxidation and thus fixes up a greater quantity of O_2. The secondary rise is thus concluded to be the results of such reactions.

My thanks are due to Dr. S. Ranjan, for helpful suggestions and criticisms in preparation of this work.

Conclusions

Summarising the result of CO_2 output it is found

(i) That there is always a "S" shaped rise after a time in the rate of respiration which varies in intensity with the age of the leaves.

(ii) That the high rate of respiration seldom remains at that pitch for any length of time, but it declines.

(iii) That the rise may be due to the higher temperature of the experimental chamber.

Summarising the relation of oxygen taken in during respiration the following points are worth noticing :—

(i) The O_2 intake is always greater than the CO_2 output except in yellow leaves where it falls below CO_2 in some cases.

(ii) The difference between O_2 intake and CO_2 output starts low, but afterwards reaches a maximum and then forthwith declines to a small value. It may go so low that the difference may become zero as in the case of green leaves.

(iii) The secondary rises in the O_2 intake may be due to the oxidation of other substances requiring a larger amount of oxygen.

References

1. Kidd, F., *Proc. Roy. Soc.*, B **89**, 136, 1915.
2. Haas, P. and Hill, T. G., *Chemistry of Plant products* Vol. I and II, London, 1928.
3. Muller Thergau, H., and Schneider Orelli, *Flora*, **101**, 309, 1910.
4. Fernandes, D. S., *Rec. Trav. Bot. Neerlandais*, **20**, 107, 1923.
5. Nicolas, G. M. G., *Rev. Gen. Bot*, **30**, 209, 1918.
6. Bezagu, M., *Compt. Rend. Acad. Sci. Paris*, **169**, 701, 1919.
7. Kidd, F., West, C., and Briggs, C. E., *Proc. Roy. Soc.*, B **92**, 368, 1921.
8. Bonnier, G. and Mangin, L., *Ann. des Sci. nat. Bot.*, VII, 315, 1885.
9. Maqune, L. and Demoussy, E., *Comp. Rend. Acad. Sci. Paris*, CLVI, 1912 and 1913.
10. Nicolas, M. G., *Rev. Gen. Bot.*, 1919.
11. Cerighelli, R., *Compt. Rend. Acad. Sci. Paris*, **178**, 645, 1924.
12. Bonnier, G., and Mangin, L., *Ann. Sci. Nat. Ser.*, **6**, 293, 1884 and **18**, 364, 1886.
13. Pal, N. L., *New. Phyto.*, **33**, 241, 1934.
14. Jonesco, S., *Compt. Rend. Acad. Sci. Paris*, **172**, 1311, 1921.
15. Jorgensen, I. and Kidd, F., *Proc. Roy. Soc.*, B **89**, 342, 1917.
16. Osterhout, W. J. V., *Jour. Gen. Physiol.*, 1, 171, 1918.

STUDY OF IONOSPHERE AT ALLAHABAD

By G. R. Toshniwal, B. D. Pant, R. R. Bajpai and B. K. Verma

Physical Laboratory, Allahabad University, Allahabad.

Received January 8, 1936

Observations for November and December 1935, show that 75 meter waves are usually reflected from the F-region. Sporadic E reflections have, however, been observed on several nights. The noon ionization of the E region has been measured during the winter solistice period and found to be about 2×10^5 electrons per c.c. Both the group retardation as well as the stratification splitting has been observed, the former rather rarely. Long retardation echoes show the possibility of existence of ionized regions above the F-region. Complex echoes consisting of several peaks rapidly fading in and out have been seen several times. There seems to be no connection between the magnetic disturbances and the complex echoes. Observations for the reflection coefficient have been taken for the two rays, and values of reflection coefficient greater than unity have been observed. The results find a satisfactory explanation on the hypothesis of undulatory structure of the ionosphere together with the possibility of echo reception from direction other than vertical. Measurement of reflection coefficient late in the night shows that both the rays are absorbed in the reflecting region, a view contrary to those held by the English workers. The desirability of taking more observations in collaboration by several stations is pointed out.

Introduction

Though a lot of work has been done on the study of the Ionosphere, and a large amount of data has been collected for higher latitudes, very little work has been done in the tropics. So far no account has come to our notice about the measurement of reflection coefficient, and in fact very little is known about the ionization of the various regions for the tropical countries. The present paper deals with the measurement of reflection coefficient, the ionization of the E-layer, and the general structure of the ionosphere.

Ionization of the E-layer

It has already been reported to the Academy[1] that a peculiar anomaly exists in the determination of the ionization of the E-layer viz., the curve

showing the relationship between the time of the day and the critical frequency showed two maxima, one at 0800 and the other at 1900 and a minima at 1500 Indian Standard Time (5½ hours ahead of Greewich Mean Time). This was explained to be due to considerable absorption during the day in the D-region, which made real determination of the critical frequency impossible. The power of the transmitting equipment has now been increased and the ionization of the E-region has been measured during the winter solistice period.

The principle of the method for finding out the ionization of any particular region has already been given earlier[2]. It is in fact only necessary to find out that frequency which just penetrates the E-layer and echoes reflected from the next higher region are visible. Let us call this frequency f_E, then the number of electrons per cubic centimeter can be determined from the formula

$$N = \frac{m}{e^2}\frac{\pi}{}f_E^{\,2} = 1{\cdot}24 \times 10^{-8} f_E^{\,2} \qquad (1)$$

where, following Darwin[3], the Lorentz polarization term has been put equal to zero.

In order to avoid the tuning of the antenna circuit a special five wire antenna was erected.[4] These wires were $\frac{3}{4}\lambda$ for λ equal to 45, 55, 75, 90 and 110 meters, and the earthing system was a combination of an earth screen and a buried earth plate. The system though showed resonance at several wavelengths, possessed good transmitting qualities for the entire spectrum of frequencies used during the present investigations.

The critical frequency f_E for the E-region came out to be 4·5 Mc./sec. and 4·0 Mc./sec. on the 23rd and 24th Dec. respectively. The corresponding values of the number of electrons per cubic centimeter comes out from the formula (1) as 2×10^5 and $2{\cdot}5 \times 10^5$ respectively. The value of f_E at Slough[5] (England) and at Washington[6] (U.S.A.) has been found to be 2·6 Mc./sec. and 2·8 Mc./sec respectively.

Equivalent Height

Observations for the variations of equivalent height at constant frequency (4·0 Mc./sec.) were taken visually and were also supplemented by photographic records. They reveal interesting results which are summarized here.

The magneto-ionic theory demands that an electromagnetic wave travelling in an ionized medium will be usually split up into two components known as the ordinary ray and the extraordinary ray, and as has been pointed out by Appleton and Builder[7] we can differentiate between two types of splitting, viz., (1) 'group retardation splitting' and (2) 'stratification splitting'. The former type of splitting is visible when the transmitted frequency is a little above the critical penetration frequency of the region just lower than the one from which reflection is being observed, while the stratification splitting is easily seen when the transmitted frequency is little below the penetration frequency of the layer from which the reflections are being observed. In this type of splitting, as is well known, the ordinary component lags behind the extraordinary component, while in the case of the group retardation splitting the extraordinary ray—since it has a lesser velocity in an ionized medium than the ordinary ray—lags behind the ordinary ray. Thus we see that the two types of splitting are opposed to each other.

The stratification splitting is easier to observe and is always seen early in the morning and late in the night, while the group retardation splitting is rarely seen. We have been able to observe this group retardation splitting often in the morning and seldom in the evening. The two magneto-ionic components showing stratification splitting in the early part of the morning used to combine within a few minutes and about 15 to 20 minutes later, the group retardation splitting was at times visible for a short period. The longer delay component in such a case has been found to be always weaker. This phenomenon seems to be due to an increase in the ionization in the lower regions, which reduces the velocity of the extraordinary ray thus producing circumstances favourable for the group retardation splitting. That this phenomenon is definitely due to the 'group retardation splitting' is further confirmed from the fact that any decrease in the transmitted frequency was found to increase the separation between the two rays, while if the splitting was due to stratification the reverse would have been the case.

Variation of Equivalent Height during the course of a day

The 4-megacycle waves were usually reflected from the F-region. Fig. 1. shows the variation of the equivalent height of the F-layer on the 24th Nov. 1935, and is representative of the usual phenomenon observed. The

extraordinary component first appeared at 0608 I. S. T. and was followed by the ordinary ray at 0620. The two rays were superimposed at 0636, after which violent intensity fluctuations took place. A little after the superimposition of the two rays the equivalent height increased a little and seems to be due to decrease in the group velocity due to increased ionization in the lower regions. This increase in the height for a short time has usually been observed. The equivalent height, at noon, was 240 km. and at 1737 it was 210 km. Great intensity fluctuations again started during the sunset period and several multiple echoes were seen (not shown in the curve). There were as many as six multiple echoes at 2120 and there was no intensity relationship between them. The splitting of the magneto-ionic components took place at 2132. The equivalent height then went on increasing, and the ordinary ray disappeared at 2152, while the extraordinary component disappeared at 2213. No reflection was visible till 0613 of 25th Nov.

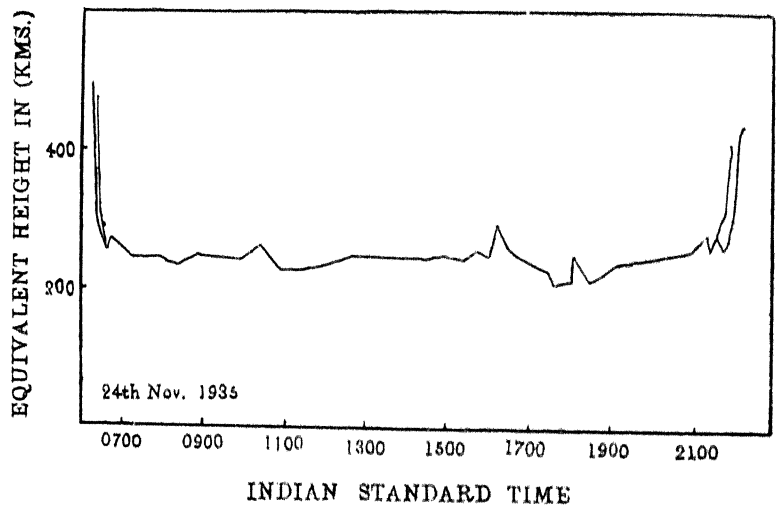

Fig. 1.

Echoes from the E region

During Nov. and Dec. 1935, echoes from the E-region were visible on the 26th and 28th Nov. and 3rd and 4th Dec.

26th. Nov. 1935—Strong multiple E-reflections showing an equivalent height of 115 Km. were visible between 1730 and 1838. At 1829 as many as twelve multiple reflections were visible.

28th Nov. 1935.-Both the E and F-reflections were visible between 2105 and 2115. Suddenly at 2119 all reflections disappeared. At 2123, however, a short-lived reflection showing an equivalent height of 533 km. was seen. At 2125 three echoes showing heights of 330, 362, and 445 kms. were seen which disappeared at 2127.

3rd. Dec. 1935.- Single reflection from E-layer (106 km.) and three multiple reflections from the F-region were simultaneously present at 1953 and 1956, after which only the F-echoes were present. At 2211, single reflection from the E-region (105 km.) and magneto-ionic split echoes from the F-region were visible. The E-echoes disappeared at 2222 I.S.T.

4th. Dec. 1935. Fig 3.—At 2036 the F-echoes suddenly stopped coming and several multiple echoes from E-layer appeared. The equivalent height was about 120 Km. At 2051 the third and the fifth echoes were complex. E-reflections were not visible between 2124 and 2130. E-echoes again appeared at 2130 and finally disappeared at 2316.

Long retardation Echoes and Complex echoes

In addition to the usual multiple echoes, sometimes other echoes appeared showing the presence of some other ionized regions at heights varying from 500 to 800 kms. These can best be seen from figures 3,4,5. The vertical lines on the graph show the presence of complex echoes, where measurements of equivalent heights of individual peaks were not possible.

The echoes would at times become very complex.[8] Any one of the multiple echoes could be complex consisting of several peaks fading rapidly in and out presenting a characteristic 'boiling appearance'. Such a phenomenon is very rare and has been observed by others.

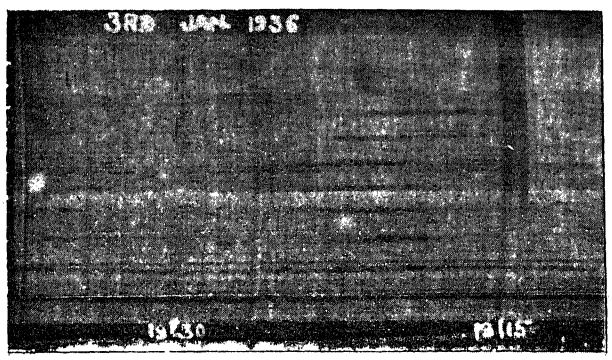

Fig. 2.

Fig. 2-3rd Dec. 1935. shows a small portion of a photographic record of height with time. The beginning of the ground pulse is not shown. Near about 1920 I.S.T. there were as many as 9 multiple reflections. The first black horizontal line represesents the first reflection from the F-region (273 km.) and the rest are multiple echoes. The time scale was not linear and hence the horizontal lines are not equally spaced.

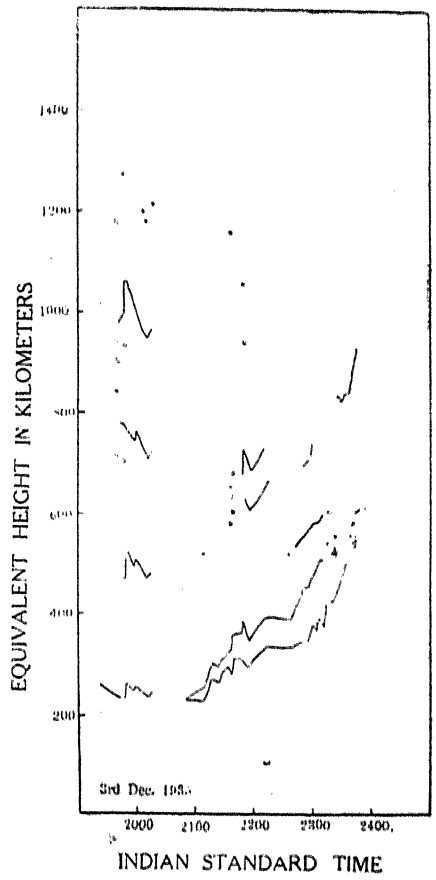

Fig. 3.

Fig. 3.—shows a graph plotted from visual observations taken on the 3rd Dec. At 1940 the first F-echo came from a height of 236 km. but in between the second and the third multiple reflection there was a reflection from height of 659 km. and in between the third and the fourth multiple reflection there was an echo corresponding to a height of 848 kms. Several such echoes were present at various times as will be apparent from the figure.

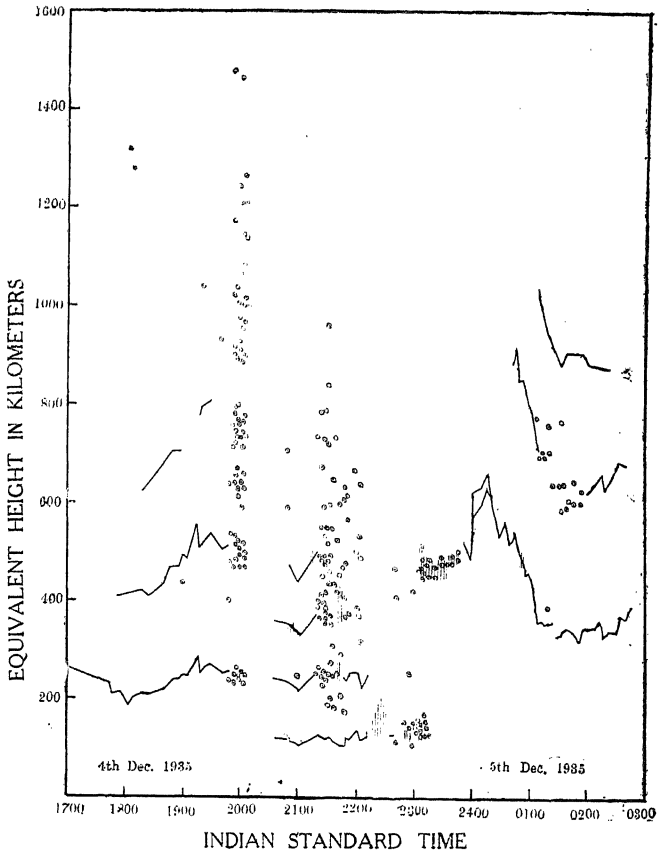

Fig. 4.

Fig. 4—represents the conditions on Dec. 4. Condition of the upper atmosphere seemed to be very much disturbed and several echoes which were definitely not multiples of the F-echo were present. Three multiple E-echoes appeared near about 2036, all of which were complex consisting of many components. At 2051 there were six multiple echoes from the E-region (117 Km.) the first and the third were very complex. The complex echoes were generally very short-lived. At 2142, a little after the disappearance of the E-echoes, echoes corresponding to heights of 250, 417, 522 and 733 kms. were visible. Out of these the second and third were very complex each consisting of three to four components. The complex echoes however vanished at 2148, a little after the appearance of the E-echoes. After 2157 the E echoes became very complex, with a maximum at about 2226. Both the E and F components were complex at

2309. Long delay echoes, which may be reflections from higher ionized region appeared at 0044 as will be apparent from the figure.

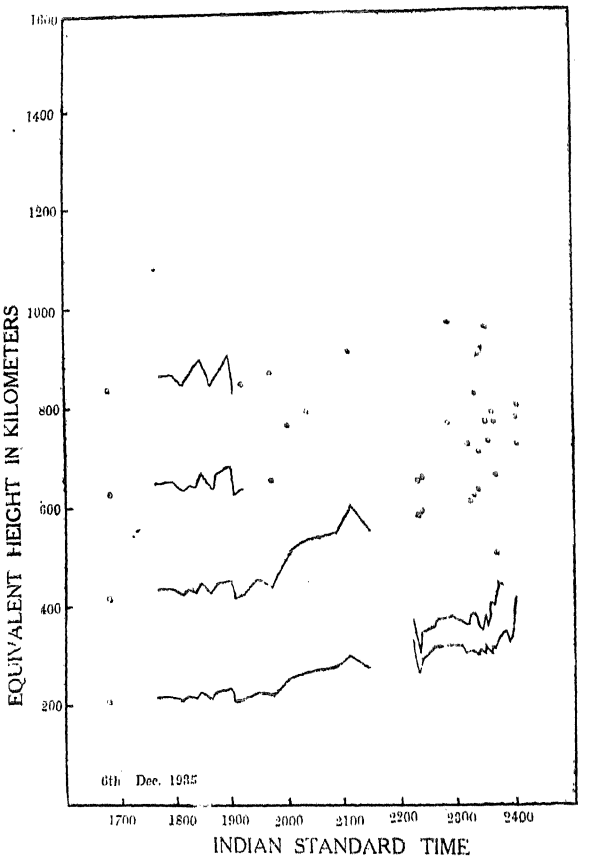

Fig. 5.

Fig. 5.-6th Dec. 1935-The day was not so disturbed as 4th Dec. Several stray long delay echoes were, however, observed between 2300 and 2400. At 2332 three echoes from equivalent heights of 319, 412 and 731 kms. were seen of which the last was very strong and complex. The echoes were last seen at 0001 (802 kms.), but just before disappearing it was a thick composite echo.

Fig. 6.-Dec. 12. 1935–This was also a greatly disturbed day. Long delay echoes from great distances were visible at various times. The complexity of echoes began at 0241 I. S. T., when the fourth, sixth and the eighth echoes were very complex. The complex echoes, however, disappeared at 0244,

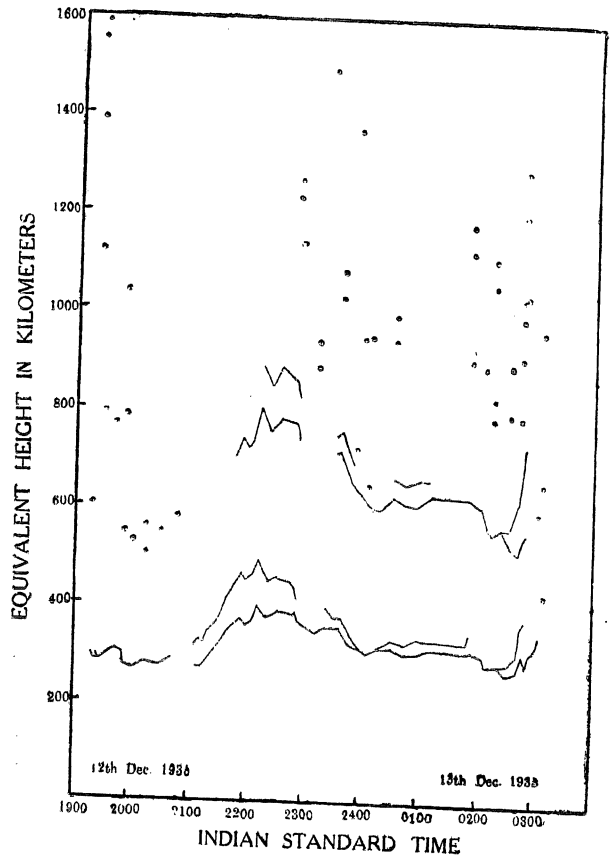

Fig. 6.

Complex echoes were also observed on the 10th December at 2232. Time of disappearance of echoes due to electron limitation during 1935 has been found to be much later in the night than the corresponding period in 1934, and points out to greater ionization in the Ionosphere.

Reflection Coefficient

From Lorentz's theory of absorption we find that the effect of absorption can be expressed in terms of an absorption coefficient κ such that the ratio of the intensity of the emergent wave to that of the incident wave is given by

$$\frac{E}{E_0} = exp.\ [-\int \kappa dh] = \rho \qquad (2)$$

where ρ is the reflection coefficient and h is the thickness of the absorbing layer.

Let F_1 be the amplitude of the first echo reflected from the F layer and F_2 be the amplitude of the second multiple echo. Then,

$$F_1 = \frac{a\rho}{d}$$

and

$$F_2 = \frac{a\rho^2}{2d}$$

if the reflection coefficient for the ground is assumed unity.
Then

$$\rho = \frac{2F_2}{F_1} \tag{3}$$

The apparatus for measurement of the reflection coefficient was placed in the same room in which the transmitter was placed and hence the ground pulse was very strong and it was not possible to compare the amplitudes of the ground pulse and the echo, therefore ρ was usually determined from the formula (3). A linear detector was used for the purpose and the heights of the various echoes as seen on the oscillograph screen were marked on a piece of paper, and ρ determined. Only fairly steady values of the amplitude of the echoes have been used for the determination of ρ.

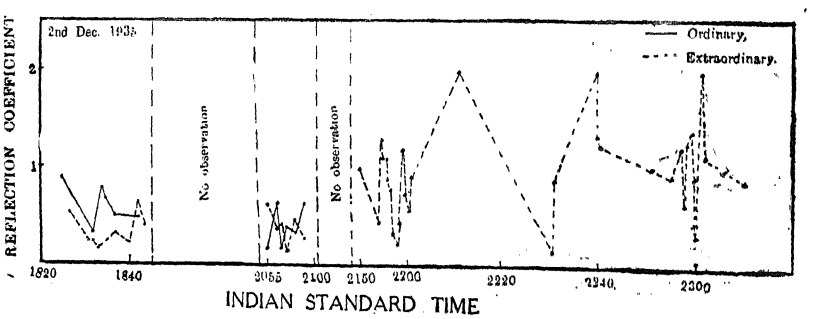

Fig. 7.

Fig. 7.--Represents a typical graph showing reflection coefficient of the two magneto-ionic components on the 2nd Dec. 1935. Between 1822 and 1842 group retardation splitting was visisble. The continuous line represents the ordinary ray (lesser delay component) and the dotted line represents the extraordinary ray (the longer delay component). The ordinary component was always stronger than the extraordinary as is expected from theory since the absorption varies directly as the group path. The graph also shows that the variation of the reflection coefficients for the two

rays are almost always in phase except at one place. At 1850 the two echoes combined after which multiple echoes were seen, the intensities of which were very quickly changing, and hence no observations were possible upto 2055 when stratification splitting set in. The middle portion of the graph has been plotted on a different time scale and shows the intensity relationship of the ordinary and the extaordinary rays. There seems to be no definite relationship between the two rays, since any one of the rays could be stronger than the other. The ordinary ray, however, disappeared at 2101 and hence the rest of the figure shows the variation of reflection coefficient for the extraordinary ray alone. The intensity of the extraordinary ray fluctuated considerably and even steady values for a minute or so which have been measured and represented on the figure show that at times the reflection coefficient was greater than unity. Such results have also been observed by White.[9]

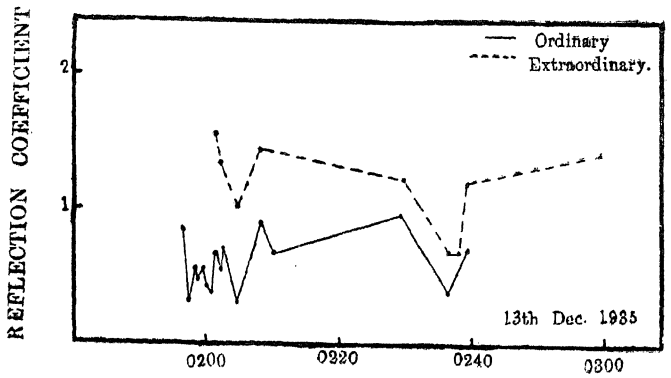

Fig. 8.

Fig. 8. represents conditions late at night on 13th Dec. when both the magneto-ionic components were present and the separation was due to stratification splitting. The curves for the ordinary and the extraordinary reflection coefficients are similar and show that both the rays experience similar absorption. It is expected that after midnight the ionization in the E–layer is extremely small and hence it appears very probable from the nature of the curves that the two components are getting absorbed in the region where reflection occurs.

Conclusions

The observations for the critical frequency of the E-region during the winter solistice shows that the number of electrons per cubic centimeter is about 2×10^5, a figure much higher than those obtained for Washington and Slough. Such a high figure is also expected because of the low latitude of Allahabad, which is 25^0 26'N.

The presence of the echoes from the E–region between 2213 and 2222 on the 3rd Dec., when the F-echoes showed stratification splitting of the magneto-ionic components, seems to be due to 'sporadic reflection' from the E-region, similar to those observed by Kirby and Judson[10].

In order to explain the long retarded echoes to which no known definite ionized regions can be assigned, we have to take into consideration the possibilty of the F+E echoes, and the M-echoes[11]. But unless definite value of the height of the E layer is known at the time the long retarded echoes appear, it is very difficult to make any suggestion for the various long retardation echoes shown in figures 3 to 6. But we see when both the E and F-echoes were present there was no echo which could be called the F+E or the M-echo.

The presence of complex echoes seems to be a mystery. The complex echoes were not visible during Dec. 1934, but in 1935 complex echoes appeared on the 3rd, 4th, 6th, 10th and 12th. The Magnetic characteristic data very kindly supplied to us by the Meteorological Department of the Government of India (for which we thank the Director-General of Observatories) shows that small disturbances were present on the 3rd, 6th, and 12th Dec. while the 4th Dec., when the greatest complexity was observed, is reported to be a quiet day. Therefore the complex echoes do not seem to be connected with the magnetic disturbances.

However, we have to consider the other possibility put forward by one of us[12], that at times the ionized regions may be an undulatory surface with various ledges here and there. The presence of such a structure along with the possibility of arrival of echo from angles other than the vertical can easily account for the complex echoes. If this view of the production of the complex echoes is accepted, we have to search for the agency which can cause such a structure of the ionosphere.

Fig. 7 shows that the reflection coefficients for the two magneto-ionic components seen separated due to the 'group retardation' either

increase or decrease together. This shows that both the extraordinary as well as the ordinary ray are absorbed in the same region situated below the reflecting region. As is expected from the theory we also find that the ordinary ray, which in this case—the group retardation splitting—is the lesser delay component is stronger than the extraordinary ray.

When the ionization in the F region becomes small so that the ordinary ray has ceased to be reflected and the extraordinary alone is present great intensity fluctuations of the echo have been observed and fig. 7 shows that at times the reflection coefficient becomes greater than unity. In addition to the above we have at times seen such a structure of the extraordinary as well as the ordinary ray which shows that they are not single echoes. All the above mentioned phenomena confirm our view already given that there is a great possibility of reflections coming from other parts of the Ionosphere from any direction.

Fig. 8 shows that late at night when the ionization in the E-region is expected to become very small, the reflection coefficient of the ordinary and the extraordinary rays vary in phase with each other. Thus it seems that for the two rays major portion of absorption takes place in the same region, which in our opinion is the reflecting region. This view is against the views of the workers in England[13], and therefore it seems desirable, for confirmation of our view, to measure the reflection coefficient at various frequencies simultaneously. This type of work can best be done by several closely situated stations working in collaboration with each other.

Our hearty thanks are due to Prof. M. N. Saha F. R. S. for the facilities he gave us and also for many useful suggestions throughout the progress of the work.

[*Note added in proof correction May 17, 1936:—*

Later work, after the submission of this paper, shows that complex echoes are due to partial reflection and refraction from strata of ionized regions lying close to the main reflecting layer.

The late disappearance of the echoes during 1935 seems to be connected with the sunspot activity in Dec. 1935. (Nature Feb. 1, p. 183, 1936).]

References

1. Toshniwal and Pant, *Proc. Acad. Sc. U.P.*, **5**, 9, 1935.
2. Toshniwal aud Pant, *loc. cit.*

3. Darwin, *Proc. Roy. Soc.*, A **146**, 17, 1934.
4. White, *Proc. Phy. Soc.*, **46**, 805, 1934.
5. Gilliland, *P.I.R.E.*, **22**, 236, 1934.
6. Appleton and Naismith, *Proc. Roy. Soc.*, A **137**, 37, 1932.
7. Kirby, Berkner and Stuart, *P. I. R. E.*, **22**, 481, 1934.
8. Appleton and Builder, *Proc. Phy. Soc.*, **45**, 805, 1934.
9. Appleton and Builder, *loc. cit.*
   Ratcliffe and White, *Phil. Mag.*, **16**, 15, 1933.
10. White, *Proc. Phy. Soc.*, **46**, 805, 1934.
11. Ratcliffe and White, *loc. cit.*
12. Toshniwal, *Proc. Nat. Inst. Sc. (India)*, **1**, 244, 1935.
13. Farmer and Ratcliffe, *Proc. Roy. Soc.*, A **151**, 370, 1935.

NEW HEMIURIDS (TREMATODA) FROM INDIAN MARINE FISHES.

PART I—"A NEW PARASITE OF THE SUB-FAMILY PROSORCHINAE YAMAGUTI, 1934"

By Har Dayal Srivastava

Offg. Helminthologist,

Imperial Institute of Veterinary Research, Muktesar, India

Communicated by Dr. H. R. Mehra

Received September 14, 1935

A new species of the genus *Prosorchis* Yamaguti, 1934 from the intestine of the fish *Seriolichthys bipinnulatus* from Puri, Bay of Bengal is described. The species differs from the only other known species of the genus in a number of features given at the end of the paper.

Genus *Prosorchis* Yamaguti, 1934

Prosorchis breviformis, n. sp.

Host—*Seriolichthys* bipinnulatus Bleeker.

Habitat—Intestine.

Locality—Puri, Bay of Bengal.

Seven specimens of this interesting trematode were obtained from the intestine of two hosts examined in July, 1935. The worms when alive are light brown in colour and show marked power of contraction and expansion. They can live in normal salt solution for more than six hours. The body is sub-cylindrical, elongated, with a nearly uniform breadth. In permanent mounts it measures 4·5-5·4 mm. in length and 0·75-0·96 mm. in maximum breadth across the acetabular region. It is completely devoid of scales or spines, though unicellular, deeply staining cutaneous gland cells occur in large numbers all over the body.

The oral sucker is situated on the ventral surface behind a roughly triangular, 0·07–0·1 mm. long preoral lip. It is a transversely oval

structure measuring 0·28–0·32 × 0·3–0·35 mm. in size. The acetabulum is spherical, 0·5–0·58 mm. in diameter, about twice the size of oral sucker and is situated at the junction of the first and second thirds of body length. The oral sucker opens posteriorly into a rudimentary prepharynx visible in extended condition only. The pharynx is well developed and oval, measuring 0·12–0·14 mm. across. The extremely small oesophagus bifurcates into two long, sinuous and uniformly broad caeca extending upto the posterior end. At the intestinal bifurcation is given off a small oesophageal diverticulum similar to that present in *Ophiocorchis lobatum* and *O. singularis* Srivastava, 1933.

The excretory bladder is Y-shaped. The main stem is a fairly wide sinuous tube extending from the posterior end to the acetabulum. The stem bifurcates into two lateral cornua just behind the acetabulum which anastomose with each other dorsal to the pharynx. The genital atrium is situated in the median line on the ventral surface in level with the posterior thirds of the oral sucker. It encloses a very small genital papilla on which the ductus hermaphroditicus opens.

The testes, two in number, are small, spherical bodies of 0·2–0·23 mm. diameter, occupying an obliquely tandem position in the intercaecal space about half-way between the intestinal bifurcation and acetabulum. The vesicula seminalis is a small, elongated swollen tube of 0·26–0·35 × 0·1–0·14 mm. size and lying between the testes and intestinal bifurcation. It opens anteriorly into a short, tubular pars prostatica, 0·08–0·09 × 0·015–0·04 mm., surrounded by numerous prostate gland cells. The pars prostatica continues anteriorly into the ductus ejaculatorius which joins the terminal part of the uterus to form the ductus hermaphroditicus.

The ovary is transversely ovoid measuring 0·16–0·23 × 0·2–0·27 mm. in size and situated in the intercaecal space in the first fifth part of the posterior half of body. From its anterior margin is given off a short oviduct which soon receives the ducts from the receptaculum seminis and yolk reservoir before entering the ootype. The receptaculum seminis is a small, spherical structure lying dorso-lateral to the shell gland complex. The Laurer's canal which arises from the receptaculum seminis is a prominent, fairly long and coiled tube ending in a terminal vesicle. The shell gland complex lies immediately in front and partly overlapping the ovary and is nearly two thirds the size of the latter.

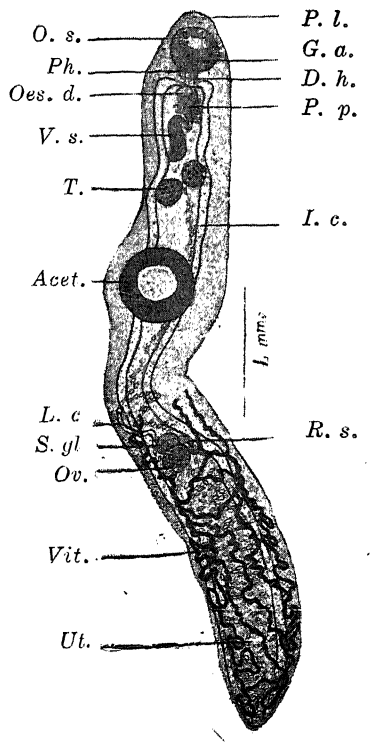

Fig. 1

Prosorchis breviformis n. sp.

Lettering:—*Acet.* Acetabulum, *D. h.* Ductus hermaphroditicus, *G. a.* Genital atrium, *I.c.* Intestinal caecum, *L. c.* Laurer's canal, *O. s.* Oral sucker, *Oes. d.* Oesophageal diverticulum, *Ov.* Ovary, *Ph.* Pharynx, *P. l.* Preoral lobe, *P. p.* Pars prostatica. *Prp.* Prepharynx, *R. s.* Receptaculum seminis, *S. gl.* Shell gland complex, *T.* Testis, *Ut.* Uterus, *V. s.* Vesicula seminalis. *Vit.* Vitellaria.

The vitellaria consist of two to four longitudinal, highly convoluted tubes extending from the ovary to the hinder end. The main tubes give off intricately convoluted secondary branches which anastomose with one another. In a few specimens two or three small secondary branches extend to short distances in front of the ovary. The yolk reservoir is very small and lies dorsal to the ovary.

The uterus in the post-ovarian part extends in short transversely arranged descending and ascending coils which overlap each other. In front of the ovary the ascending part runs in short transverse

coils upto the pharynx where it receives the ductus ejaculatorius to form the ductus hermaphroditicus. The eggs are small, numerous, light yellow in colour and measure 0·033–0·038 × 0·018–0·025 mm. in size.

Prosorchis breviformis, n. sp., differs from the type species of the genus *P. pcenopsis* Yamaguti, 1934, in the shape and much smaller size of body which is uniformly broad with its maximum breadth occurring across the acetabular region, comparatively caudad position of the acetabulum, position of the testes, shell gland complex and receptaculum seminis and the character and disposition of the vitellaria.

I am deeply indebted to Dr. H. R. Mehra for his valuable help and to our Director, Mr. F. Ware, F.R.C.V.S., I.V.S., for facilities and kind encouragement in the work.

References

1. Srivastava, H. D., *Bull. Acad. Scs., U. P*, **3**, 41, 1933
2. Yamaguti, S., *Japan. Journ. Zool. Tokyo*, **5**, 249, 1934

NEW ALLOCREADIDS (TREMATODA) FROM INDIAN MARINE FISHES

PART I—"NEW PARASITES OF THE GENUS *HELICOMETRINA* LINTON, 1910"

By Har Dayal Srivastava,

Offg. Helminthologist,

Imperial Institute Of Veterinary Research, Muktesar, India

Communicated by Dr. H. R. Mehra.

Received September 14, 1935

Two new species of the genus *Helicometrina* Linton obtained from marine fishes at Puri, Bay of Bengal are described. *Helicometrina septorchis* n. sp. is a rare parasite, whereas *Helicometrina orientalis* n. sp. in the frequency of occurence and variety of hosts is second only to *Decemtestis biacetabulata* described in the second part. Diagnosis of the germs *Helicometrina* and key to the species are given.

Not a single trematode is so far known from Indian Marine Fishes. At the suggestion of Dr. H. R. Mehra I visited Puri, a well known town on the coast of the Bay of Bengal, in the summer of 1935 and made an extensive collection of the helminth parasites of marine fishes. In this paper, the first of a long series, is given the account of two new species of *Helicometrina* Linton. The type species of the genus—*H. nimia*—was described by Linton in 1910 from the gut of several marine fishes of the Dry Tortugas. Layman in 1930 described *H. azumae* from *Azuma emmnion* as the second species of the genus, which Manter in 1933 transferred to the genus *Rhagorchis* Manter, 1931, owing to the absence of polar filament in the egg, besides, morphological similarities and host relationships of the two species—*R. odhneri* and *H. azumae*. The second valid species of the genus—*H. parva*—was added by Manter in 1933 from the gut of *Iridio bivitatus*.

I am deeply indebted to my Professor, Dr. H. R. Mehra at whose initiation I undertook a study of the rich and interesting helminth fauna of Indian fishes, besides, morphological and life history studies of helminths of domestic animals, for his ever ungrudging help and valuable suggestions. I am also grateful to our Director, Mr. F. Ware, F. R. C. V. S., I. V. S., for facilities and kind encouragement.

Helicometrina septorchis n. sp.

Host—*Sillago sihama* Gunther.
Habitat—Intestine.
Locality—Puri, Bay of Bengal.

This species represents a rare parasite inhabiting the gut of an Indian marine fish. Only four specimens were obtained from the intestine of one out of a number of hosts examined at Puri in July, 1935. The body is fairly muscular, elongated with broadly rounded off ends and completely devoid of spines or scales of any kind. The living worms are light brown in colour and show moderate power of contraction and expansion. Mature specimens in permanent mounts measure 5·0–5·3 mm. in length and have a uniform breadth of 1·2–1·3 mm. The suckers are fairly muscular and spherical. The subterminal oral sucker, 0·3 mm. in diameter, is smaller than the acetabulum which measures 0·4 mm. across and is situated at the end of the first third of body length. The size ratio between the oral and ventral suckers is as 3 : 4. The prepharynx is rudimentary and is seen only in the extended condition of the worm. It communicates posteriorly with a well developed, ovoid pharynx of 0·17–0·18 × 0·14 mm. size. The oesophagus is a small, straight tube nearly twice the length of the pharynx. The caeca are long and narrow, running posteriorly in a more or less straight course to a little distance in front of the hinder end. The excretory bladder is a straight, uniformly broad, median tube extending from behind the ovary to the posterior end. The excretory pore is terminal.

The male reproductive system consists of seven testes, measuring 0·3—0·35 × 0·35—0·4 mm. in size, spherical or ovoid in shape and arranged in pairs in the intercaecal space in two longitudinal rows, one on either side of the median line. The last unpaired testis lies almost in the median line at about one fifth or sixth of body length from the posterior end. The cirrus sac is moderately long and sinuous, extending

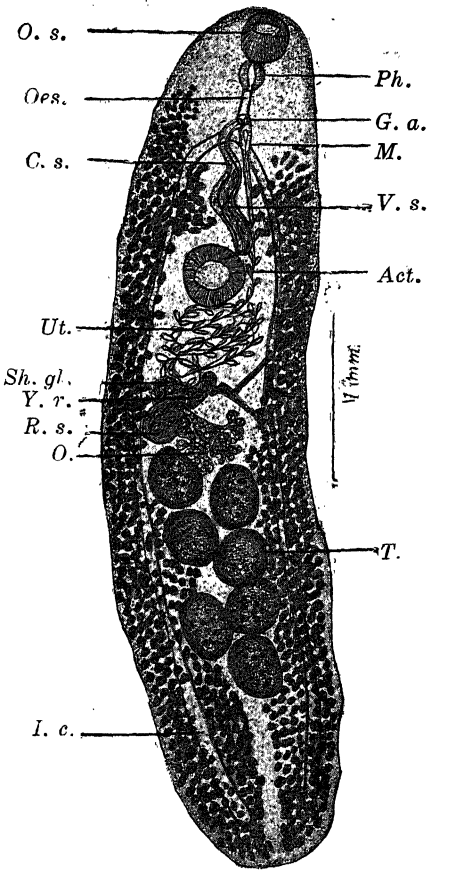

Fig. 1

Helicometrina septorchis n. sp.

Lettering:—*Acet.* Acetabulum; *C.s.* Cirrus sac; *G.a.* Genital atrium; *I.c.* Intestinal caecum; *M.* Metraterm; *O.* Ovary; *Oes.* Oesophagus; *O. s.* Oral sucker; *Ph.* Pharynx; *R. s.* Receptaculum seminis; *Sh.gl.* Shell gland; *T.* Testis; *Ut.* Uterus; *Vit.* Vitellaria; *V. s.* Vesicula seminalis; *Y. r.* Yolk reservoir.

from the middle of the oesophagus to the acetabulum. It encloses a bipartite, uniformly broad vesicula seminalis, a small elongated bulb-shaped pars prostatica surrounded by prostate gland cells, a small ductus ejaculatorius and a knob-like cirrus. The genital atrium is a small, shallow, circular depression on the ventral surface in level with the middle of the oesophagus. The male and the female ducts open separately in the genital atrium.

The ovary is bell-shaped with its lower half profusely lobed. It measures 0·33—0·35 × 0·44—0·46 mm. in size and is situated in the median line about the middle of body close in front of the testes. The receptaculum seminis is a sac shaped structure of 0·25—0·31 × 0·17—0·19 mm. size. It lies in the intercaecal space to the right of the ovary just behind the diffuse shell gland mass. Laurer's canal is present.

The vitellaria are composed of numerous small irregular follicles, extending laterally from the middle of the oesophagus to the posterior end on the right side. On the left they begin from the level of intestinal bifurcation. Behind the testes as well as on their sides and on either side of the cirrus sac the vitelline follicles extend mesially without, however, meeting in the median line. The short transverse vitelline duct of each side is formed by the union of the anterior and posterior vitelline ducts of either side in front of the ovary. The two transverse ducts meet in the median line in front of the ovary to form a conspicuous, roughly triangular yolk reservoir.

The uterus lies in spirally arranged coils in the intercaecal space between the ovary and the acetabulum. The eggs are operculate, oval, golden yellow in colour with very long unipolar filaments which give them the appearance of beads pendent from a supporting cord. The eggs measure 0·062–0·065 × 0·023–0·025 mm. in size, excluding the filament. Terminally the uterus passes into a fairly muscular metraterm of 0·25 × 0·05 mm. size.

Helicometrina septorchis n. sp. differs from the other two species of the genus, i.e., *H. nimia* and *H. parva*, in the shape and much larger size of body, position of the acetabulum, size ratio of suckers, far cephalad position of the genital pore, number and shape of testes, characteristic shape of ovary, disposition of vitellaria and the larger size of the eggs, besides, differences in the size of the various organs.

Helicometrina orientalis, n. sp.

Host—*Scomber micropeditorus* Rüppell.

Habitat— Intestine.

Locality— Puri, Bay of Bengal.

In the frequency of occurrence and variety of hosts this species is second only to *Decemtestis biacetabulata* described in the second part. In the living condition the parasite has a dark brown colour and shows

considerable power of contraction and expansion. It has an elongated, smooth, uniformly broad body with broadly rounded off ends. In permanent mounts the body measures 2·3—3·9 mm. in length and 0·67—1·0 mm. in maximum breadth across the region of the acetabulum. The suckers are small, spherical and feebly muscular. The oral sucker, 0·2–0·28 mm. in diameter, is situated subterminally on the ventral surface. The acetabulum, measuring 0·28–0·38 mm. across, is situated at the junction of the first and second thirds of body length. The size ratio between the oral and ventral suckers is as 3 : 4 or 4 : 5. Prepharynx is rudimentary. The pharynx is well developed and globular and leads posteriorly into a small oesophagus about twice its length. The caeca are straight and narrow and extend up to the posterior end. The excretory bladder is as in the other species. The excretory pore is subterminal.

The testes, nine in number, are spherical or ovoid in shape and measure 0·16–0·3 mm. in diameter. They are usually arranged in two parallel rows, one on each side of the median line in the intercaecal space, extending from behind the ovary to about the posterior sixth of body length. The cirrus sac is club-shaped, extending from the genital atrium to the acetabulum. It encloses a bipartite, uniformly broad vesicula seminalis, a bulb–shaped pars prostatica surrounded by minute prostate gland cells, a small ductus ejaculatorius and cirrus. The cirrus sac opens independently of the female duct in the shallow genital atrium lying on the ventral surface in level with the middle of the oesophagus.

The ovary of 0·25–0·3 × 0·38–0·53 mm. size is a profusely branched structure situated in the median line close in front of the testes about the middle of body. Receptaculum seminis is large, 0·25–0·4 × 0·16–0·27 mm. in size, saccular, preovarian and dextral. Laurer's canal is present. The shell gland complex lies in front of the receptaculum seminis. The configuration of the uterus is of a type characteristic of the genus. Eggs are operculate, yellow in colour with unipolar filaments and measure 0·055–0·062 × 0·023–0·033 mm. in size, without the filament. Vitellaria are as in the other Indian species, except in their anterior extent.

Of all the species of the genus in its affinities *H. orientalis* stands nearest to the type species—*H. nimia*. It resembles the latter in the length of its body and the number of testes but differs from it in the shape of its body, size ratio of its suckers, length of caeca, far cephalad

position of genital pore, shape of testes and size of eggs. In the position of its genital pore *H. orientalis* resembles *H. septorchis* but differs from it principally in the number of testes, besides, marked differences in the size of the various organs.

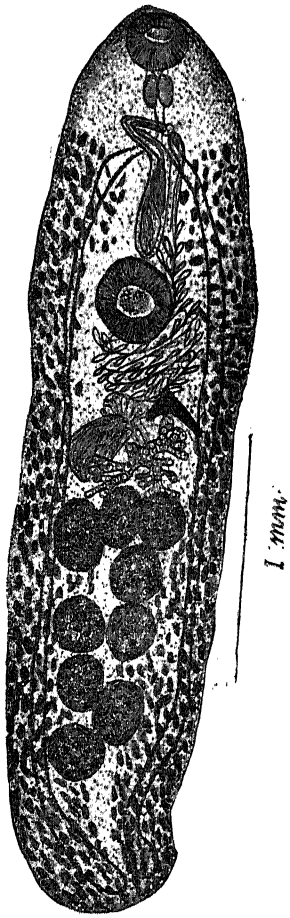

Fig. 2

Helicometrina orientalis, n. sp.

Diagnosis of the genus *Helicometrina* Linton, 1910.

Small to medium sized allocreadiinae with smooth, oval, pyriform or uniformly elongated body; acetabulum larger than oral sucker; prepharynx rudimentary; pharynx small, oval; oesophagus of varying lengths; caeca

narrow extending either upto or almost the hinder end. Genital pore median, either in front or behind the intestinal bifurcation. Testes five to nine in number, entire or lobed, intercaecal, usually arranged in two longitudinal parallel rows in the posterior half of body. Cirrus sac well developed, enclosing a coiled vesicula seminalis, pars prostatica surrounded by prostate gland cells, ductus ejaculatorius and cirrus. Ovary deeply lobed, pretesticular, receptaculum seminis well developed. Vitellaria profusely developed, follicular, extending laterally from any level between pharynx and intestinal bifurcation to hinder end. Uterus spirally coiled between ovary and acetabulum, eggs with unipolar filaments and arranged in a manner so as to appear like beads pendent from a supporting cord. Excretory bladder tubular extending from the ovary to the hinder end. Intestinal parasites of marine fishes.

Key to the species of the genus Helicometrina:—

Genital pore behind intestinal bifurcation ... ...1.
Genital pore in front of intestinal bifurcation ... ...2.

1. Testes nine in number ... ... *H. nimia.*
   Testes five in number ... ... *H. parva.*
2. Testes seven in number ... ... *H. septorchis.*
   Testes nine in number ... ... *H. orientalis.*

References

1. Layman, E. M., *Bull. Pacific Sci. Fishery Res. Sta.*, **3** (6), 1, 1930.
2. Linton, Edvin, *Carnegie Inst. Wash. Pub. No. 133. Papers from the Tortugas Laboratory*, **III**, 15, 1910.
3. Manter, H. W., *Parasit.*, **23**, 396, 1931.
4. Manter, H. W., *Carnegie Inst. Wash. Publ. No. 435 Papers from Tortugas Laboratory*, **XXVIII, XI**, 167, 1933.
5. Srivastava, H.D., *Proc. Nat. Acad. Sci. India* (the present volume).

THE MATHEMATICAL THEORY OF A NEW RELATIVITY

By Shah Muhammad Sulaiman

Chief Justice, High Court, Allahabad

Received April 19, 1936.

Corrigendum

I regret that in the short paragraph No. 11 of Ch. VI sec. II of my theory (Proc. Acad. Sc. U. P. Vol. 5 Part 2 p. 130), dealing with an empirical law which is quite independent and separate from the theory itself, there have been two misprints and one mistake. In the first line, the second term should have the factor $1/r^4$ instead of $1/r^2$. In the seventh line, the correct name should be Freundlich. The last sentence should read: The deflection of light lies between the minimum $2''{\cdot}32$, as shown in Ch. II sec. II (Vol. 4. Part I, pp. 25—6) and the maximum $2''{\cdot}61$, as shown in Ch. VIII sec. VII (Vol. 5 Part 2 pp. 158-9). The spectral shift of light from the edge of the sun is double of Einstein's value.